

CANADIAN THESES ON MICROFICHE

I.S.B.N.

THESES CANADIENNES SUR MICROFICHE



National Library of Canada
Collections Development Branch

Canadian Theses on
Microfiche Service

Ottawa, Canada
K1A 0N4

Bibliothèque nationale du Canada
Direction du développement des collections

Service des thèses canadiennes
sur microfiche

NOTICE

The quality of this microfiche is heavily dependent upon the quality of the original thesis submitted for microfilming. Every effort has been made to ensure the highest quality of reproduction possible.

If pages are missing, contact the university which awarded the degree.

Some pages may have indistinct print, especially if the original pages were typed with a poor typewriter ribbon or if the original document is a photocopy of a poor quality print.

Previously copyrighted material (journals, etc.) published text only, has not been microfilmed.

Reproduction in full or in part of this film is governed by the Canadian Copyright Act, R.S.C. 1970, c.30. Please read the Act for more information.

THIS DISSERTATION
HAS BEEN MICROFILMED
EXACTLY AS RECEIVED

AVIS

La qualité de cette microfiche dépend grandement de la qualité de la thèse soumise au microfilmage. Nous avons tout fait pour assurer une qualité supérieure de reproduction.

Si il manque des pages, veuillez communiquer avec l'université qui a conféré le grade.

La qualité d'impression de certaines pages peut laisser à désirer, surtout si les pages originales ont été dactylographiées à l'aide d'un ruban usé ou si l'université nous a fait parvenir une photocopie de mauvaise qualité.

Les documents qui font déjà l'objet d'un droit d'auteur (articles de revue, examens publiés, etc.) ne sont pas microfilmés.

La reproduction, même partielle, de ce microfilm est soumise à la Loi canadienne sur le droit d'auteur, SRC 1970, c. C-30. Veuillez prendre connaissance des formules d'autorisation qui accompagnent cette thèse.

LA THÈSE A ÉTÉ
MICROFILMÉE TELLE QU'ELLE
NOUS L'AVONS RECUE

Canada

10-315-19359-X



National Library of Canada

Bibliothèque nationale du Canada



Canadian Theses Division

Division des thèses canadiennes

Ottawa, Canada
K1A 0N4

67267

PERMISSION TO MICROFILM — AUTORISATION DE MICROFILMER

• Please print or type — Écrire en lettres moulées ou dactylographier

Full Name of Author — Nom complet de l'auteur

Joy Ann Steele

Date of Birth — Date de naissance

21 November ~~1953~~ 1954

Country of Birth — Lieu de naissance

United States

Permanent Address — Résidence fixe

9946 157 Street
Edmonton, AB
T5E 2T6

Title of Thesis — Titre de la thèse

Membrane Electrophysiological Properties of
Developing Abalone Muscle

University — Université

University of Alberta, Edmonton, AB

Year for which this degree was presented — Année pour laquelle le diplôme fut présenté

1954

Year this degree conferred — Année d'obtention de ce grade

1954

Name of Supervisor — Nom du directeur de thèse

Dr. J. H. Prosser

Permission is hereby granted to the NATIONAL LIBRARY OF CANADA to microfilm this thesis and to lend or sell copies of the film.

L'autorisation est par la présente, accordée à la BIBLIOTHÈQUE NATIONALE DU CANADA de microfilmer cette thèse et de prêter ou de vendre des exemplaires du film.

The author reserves other publication rights and neither the thesis nor extracts therefrom may be printed or otherwise reproduced without the author's written permission.

L'auteur se réserve les autres droits de publication; ni la thèse ni de longs extraits de celle-ci ne doivent être imprimés ou autrement reproduits sans l'autorisation écrite de l'auteur.

Signature

Joy Ann Steele

THE UNIVERSITY OF ALBERTA

MEMBRANE ELECTROPHYSIOLOGICAL PROPERTIES OF DEVELOPING
SKELETAL MUSCLE CELLS

by

Joy A. Steele

A THESIS

SUBMITTED TO THE FACULTY OF GRADUATE STUDIES AND RESEARCH
IN PARTIAL FULFILLMENT OF THE REQUIREMENTS FOR THE DEGREE
OF Doctor of Philosophy

Department of Physiology

EDMONTON, ALBERTA

Fall, 1984

THE UNIVERSITY OF ALBERTA

RELEASE FORM

NAME OF AUTHOR Joy A. Steele
TITLE OF THESIS MEMBRANE ELECTROPHYSIOLOGICAL PROPERTIES
OF DEVELOPING SKELETAL MUSCLE CELLS
DEGREE FOR WHICH THESIS WAS PRESENTED Doctor of Philosophy
YEAR THIS DEGREE GRANTED Fall, 1984

Permission is hereby granted to THE UNIVERSITY OF ALBERTA LIBRARY to reproduce single copies of this thesis and to lend or sell such copies for private, scholarly or scientific research purposes only.

The author reserves other publication rights, and neither the thesis nor extensive extracts from it may be printed or otherwise reproduced without the author's written permission.

(SIGNED) *Joy A. Steele*

PERMANENT ADDRESS:

4416 157 Street

Edmonton, Alberta

114

THE UNIVERSITY OF ALBERTA
FACULTY OF GRADUATE STUDIES AND RESEARCH

The undersigned certify that they have read, and recommend to the Faculty of Graduate Studies and Research, for acceptance, a thesis entitled MEMBRANE ELECTROPHYSIOLOGICAL PROPERTIES OF DEVELOPING SKELETAL MUSCLE CELLS submitted by Joy A. Steele in partial fulfilment of the requirements for the degree of Doctor of Philosophy.

Mark Lynch
.....

Supervisor

A. Kuzinski
.....

T. Gordon
.....

R. Peters
.....

M. Penner
.....

Richard W. ...
.....

External Examiner

Date 4th September 1984
.....

Dedication

To my husband, Gary and to my parents, Ann and Jim

ABSTRACT

Isolated single fibers from the anterior (a.l.d.) and the posterior (p.l.d.) latissimus dorsi muscles of embryonic and young chicks were used to study *in vivo* development of membrane electrical properties. Isolated fibers were obtained by an enzymatic dissociation procedure. Intracellular microelectrode recordings from isolated fibers and from fibers in intact muscles showed that the dissociation procedure did not significantly alter resting membrane potentials, input resistances or membrane time constants. The 14 day embryonic fibers of a.l.d. and p.l.d. did not have a measurable resting conductance to chloride. At hatching, about 70% of the resting conductance in p.l.d. fibers was due to Cl^- . Membrane electrical properties were estimated from the analysis of voltage responses to intracellular injection of rectangular current pulses. At 14 days *in ovo*, membrane resistance (R_m) was approximately $20 \text{ k}\Omega\text{cm}^2$ and membrane capacitance (C_m) was $1-2 \text{ }\mu\text{F}/\text{cm}^2$ for both a.l.d. and p.l.d. The mean membrane length constants (λ) were 1.7 mm for a.l.d. and 1.5 mm for p.l.d. The mean membrane time constants (τ_m) were 35.8 ms for a.l.d. and 25.3 ms for p.l.d. For p.l.d., the values of R_m , τ_m and λ decreased as development proceeded. For a.l.d., there was no change in these values by the time of hatching (21 days). The decreases in the electrical constants for p.l.d. fibers were partly explained by the appearance of a resting conductance to Cl^- during the last week of embryonic development.

Cultures of muscle cells derived from embryonic a.l.d. and p.l.d. muscles did not show fiber type differentiation in culture with respect to resting Cl^- conductance.

Membrane currents were recorded under voltage clamp from chick skeletal muscle with the whole-cell version of the patch clamp technique (Hamill *et al.*, 1981). Muscle cells were grown in tissue culture in the presence of 10^{-8} M colchicine which encouraged formation of spherical muscle cells (myoballs). Membrane Cl^- currents, which underlie a long duration action potential, were studied in detail. Reversal potentials for the steady-state currents varied with Cl^- concentration in a manner predicted by the Nernst equation. Cl^- currents were blocked reversibly by SITS (1.0 mM) and SCN^- (10 mM) and irreversibly by DIDS (10 μM). The currents activated slowly, following a delay, in response to step depolarizations from a negative holding potential. Time constants for activation were obtained by fitting the rising phase of the currents with a single exponential and with another exponential of the opposite polarity to account for the delay. The major time constant was dependent on voltage and decreased from about 200 ms at -30 mV to about 50 ms at 30 mV. The Cl^- currents did not decline during maintained depolarization indicating lack of an inactivation mechanism. Following depolarizing pulses which activated the currents, currents which flowed during repolarization (tail currents) declined slowly and completely. Tail currents were fitted with the sum of two

exponentials. One exponential component had an extremely long time constant on the order of seconds. The kinetics of the tail currents suggested that there must be a long-lived open state from which the channels returned very slowly to the closed state. Since three distinct time constants were found, there must be at least four kinetically distinct states: two closed states and two open states. Instantaneous current-voltage plots were linear indicating that the open channels behaved ohmically. Conductance values could then be calculated. Cl^- conductance showed a sigmoidal dependence on voltage. Conductance was low at potentials more negative than -45 mV, rose steeply between -40 and 0 mV and leveled off above 0 mV. For potentials more negative than -25 mV, conductance changed e-fold for an 8 mV depolarization. Maximal conductance was $1.03 \pm 0.7 \text{ mS/cm}^2$ ($\bar{x} \pm \text{S.D.}$; $n = 14$). Similar Cl^- currents were recorded from muscle cells that had developed *in vivo*, i.e. this Cl^- conductance mechanism is expressed during the course of normal development.

Acknowledgements

Special thanks to Mark Poznansky for providing space, equipment, supplies, etc. and for allowing me to have my freedom. Many thanks to Ed Karpinski for expressing interest in the work and for assistance with the equipment. Also, thanks to Tessa Gordon for getting me interested in skeletal muscle development and to Doug Eaton for the loan of the voltage clamp. Sue Faccio deserves thanks for typing the text of my thesis and Ken Burt's help with the figures is appreciated. Tella Findlay's help with all matter of things is also greatly appreciated. And to all of my companions in 'misery': Don Robertson, Danyanti Bhardwaj, Gary Simatos, Jean Gillespie, Janice Kuster, Glenn Wheeler, Davorka Krizaj Kapljic and Dave Reye, thanks for your friendships. Warm thanks to Sandra Czekanski for terrific company. And thanks to everyone else in the Physiology Department who have been of assistance.

Table of Contents

Chapter	Page
I. ION CHANNELS IN VERTEBRATE SKELETAL MUSCLE	1
A. Ion Channels in Adult Skeletal Muscle	3
Sodium channels	3
Potassium Channels	7
Calcium channels	14
Chloride channels	15
B. Ion Channels in Slow Tonic Fibers	18
Sodium channels	18
Potassium channels	19
Calcium channel	20
Resting conductances	20
C. Ion Channels in Denervated Skeletal Muscle	21
Sodium Channels	21
Resting membrane conductances	23
D. Ion Channels in Skeletal Muscle During in vivo Development	23
Rat muscle	23
Chick muscle	25
E. Ion Channels in Skeletal Muscle During in vitro Development	26
Primary cultures of rat muscle	26
Clonal rat cell line	27
Primary cultures of chick muscle	28
F. Summary and Objectives	29
II. MEMBRANE ELECTRICAL PROPERTIES OF DEVELOPING FAST-TWITCH AND SLOW-TONIC FIBERS OF THE CHICK	32
A. INTRODUCTION	32

B. METHODS	33
Preparation	33
Experimental set-up	36
Data collection and analysis	37
C. RESULTS	39
Isolated fibers	39
Chloride conductance during development	43
Passive cable properties during development	46
D. DISCUSSION	50
III. VOLTAGE- AND TIME-DEPENDENT CHLORIDE CURRENTS IN EMBRYONIC CHICK SKELETAL MUSCLE	55
A. INTRODUCTION	55
B. METHODS	57
Preparation of myoballs	57
Experimental set-up	58
Solutions	64
Liquid junction potentials	67
C. RESULTS	68
Whole-cell patch clamp technique	68
Membrane currents under voltage clamp	82
Membrane currents in isolated myoballs	138
D. DISCUSSION	146
Chloride currents in embryonic chick muscle	146
Comparison with other chloride channels	148
Chloride current kinetics	150
REFERENCES	155

LIST OF TABLES

Table	Page
1. Electrical properties of intact and isolated a.l.d. and p.l.d. fibers.....	44
2. Resting chloride conductance of 14 and 21 day a.l.d. and p.l.d. fibers	45
3. Electrical constants of a.l.d. and p.l.d. fibers during development.....	51
4. External and pipette solutions for whole-cell recording.....	66
5. Effect of test pulse duration on tail current components.....	134

LIST OF FIGURES

Figure	Page
1. Diagram of a.l.d. and p.l.d. muscles.....	34
2. Action potentials elicited from 21 day p.l.d. fibers..	42
3. Resting chloride conductance of cultured muscle.....	47
4. Passive electrical responses of isolated a.l.d. and p.l.d. fibers.....	49
5. Schematic of recording configurations with a suction pipette	61
6. Experimental arrangement for voltage clamp recording..	65
7. Equivalent circuit for pipette and cell membrane.....	70
8. Currents recorded at different stages of whole cell recording.....	71
9. Capacitance current under voltage clamp	74
10. Voltage response under constant current	77
11. Outward membrane currents	81
12. Determination of leakage conductance	83
13. Membrane currents under voltage clamp	86
14. Chloride action potentials.....	87
15. Membrane chloride currents	90
16. Current-voltage relationship of chloride	91

17. Effects of changing external chloride concentrations of membrane currents.....	95
18. Reversal potential as a function of chloride concentrations.....	98
19. Effects of SITS, DIDS and SCN^- on membrane currents..	100
20. Lack of voltage-dependent inactivation.....	103
21. Tail currents.....	104
22. Instantaneous current-voltage plot.....	105
23. Envelope of tails.....	108
24. Conductance as a function of voltage.....	110
25. Current-voltage plot of tail current magnitude.....	113
26. Semilogarithmic plot of conductance as a function of voltage.....	115
27. Semilogarithmic plot of current activation.....	117
28. Delay of activation.....	120
29. Fit of model equation to currents.....	123
30. Time constants of activation versus voltage.....	125
31. Reversal potential of tail currents for different duration test pulses.....	128
32. Semilogarithmic plot of tail currents.....	131
Effect of test pulse duration on tail currents.....	133

34. Semilogarithmic plot of tail current amplitude as a function of test pulse duration.....	135
35. Time constants as a function of voltage.....	136
36. Chloride currents from isolated myoballs.....	139
37. Outward currents from isolated myoballs.....	142
38. Inward and outward currents from isolated myoballs...	143
39. Current-voltage plot of inward and outward currents..	144
40. Single channel events.....	153

LIST OF PLATES

Plate		Page
1	Single isolated posterior latissimus dorsi muscle fibers.....	40
2	Myoball grown in tissue culture.....	59

LIST OF NOTATION AND DEFINITIONS

a.l.d.	anterior latissimus dorsi
p.l.d.	posterior latissimus dorsi
TTX	tetrodotoxin
STX	saxitoxin
SITS	4-acetamino-4'-isothiocyano-2,2'-disulfonic acid stilbene
DIDS	4,4'-diisothiocyano-2,2'-disulfonic acid stilbene
m	Hodgkin-Huxley activation parameter
h	Hodgkin-Huxley inactivation parameter
n	Hodgkin-Huxley activation parameter
V_m	transmembrane potential expressed as potential of intracellular solution with respect that of extracellular solution (mV)
V_o	steady-state deviation of intracellular potential from resting potential recorded at the site of current injection (mV)
V_x	steady-state deviation of intracellular potential from resting potential recorded by an electrode other than the current passing electrode (mV)
x	interelectrode separation (μm)
d	fiber diameter (μm)
λ	membrane length constant (mm)
R_i	input resistance (recorded potential/applied current) ($\text{M}\Omega$)
r_i	intracellular resistance to axial flow of current along fiber (Ω/cm)
r_m	membrane resistance per unit length of fiber (Ωcm)
R_m	membrane resistance (Ωcm^2)
R_i	intracellular resistivity (Ωcm)
λ	membrane time constant (ms)

C_m membrane capacitance ($\mu F/cm^2$)
 G_m membrane conductance (mS/cm^2)
 R_s resistance in series with the cell membrane ($M\Omega$)
Other symbols are defined as they are introduced.

I. ION CHANNELS IN VERTEBRATE SKELETAL MUSCLE

The transmembrane ion movements underlying excitability in skeletal muscle fibers are controlled by voltage- and time-dependent membrane permeabilities. Protein molecules residing in the lipid bilayer appear to be responsible for these membrane properties. They form transmembrane pores which permit ion movements and are referred to as ion channels. Each type of ion channel has characteristic permeability, selectivity and kinetic properties (Armstrong, 1975; Hille, 1976; Neher & Stevens, 1977; Ulbricht, 1977; Armstrong, 1981; Hagiwara & Byerly, 1981).

Electrical excitation in adult skeletal muscle fibers involves voltage- and time-dependent changes of permeabilities to Na^+ and K^+ which allow a transient influx of Na^+ ions followed by an efflux of K^+ ions (Stefani & Chiarandini, 1982). As a result of these ion movements, an action potential is generated. In addition to Na^+ and K^+ channels, a voltage-dependent Ca^{2+} channel has been described in several preparations (Hagiwara & Byerly, 1981; Stefani & Chiarandini, 1982). At the resting membrane potential, Cl^- and additional K^+ channels are primarily responsible for resting membrane conductance (Adrian & Freygang, 1962; Palade & Barchi, 1977). Most of these K^+ channels pass inward current more easily than outward current and are known as inward rectifiers (Adrian, 1969).

Studies of ion channels in adult skeletal muscle have extensively utilized voltage clamp techniques. Since the

membrane permeabilities vary as a function of voltage and time, the ability to control voltage makes it possible to measure ionic currents directly. In addition, membrane voltage can be changed almost instantaneously, permitting separation of capacitative and ionic currents. A recent refinement of voltage clamp techniques has made it feasible to resolve current flowing through individual ion channels (Hamill, Marty, Neher, Sakmann & Sigworth, 1981).

The application of voltage clamp techniques to developing skeletal muscle fibers is technically difficult because of the small size and fragility of embryonic fibers. Most of the information concerning ion channels in developing fibers has been derived from studies of current injection. Several general points can be made however. The excitability properties change during the course of development (Spitzer, 1979). These developmental changes reflect differences in the types of channels that are expressed and differences in the densities of channels in the immature fibers. Other factors, such as differences in intracellular ion concentrations (McArdle, Michelson & D'Alonzo, 1980), may also be involved.

The following sections describe the properties of ion channels present in innervated and denervated adult muscle fibers and in developing muscle fibers.

A. Ion Channels in Adult Skeletal Muscle

Sodium channels

The ionic currents underlying the action potential in skeletal muscle were first described in frog muscle using a three-microelectrode voltage clamp technique (Adrian, Chandler & Hodgkin, 1970a). An early, transient inward current was identified as a Na^+ current. It was blocked by tetrodotoxin (TTX), a specific blocker for Na^+ channels (Narahashi, Moore & Scott, 1964), and reversed at a membrane potential close to the Na^+ equilibrium potential. The time resolution for recording Na^+ currents was greatly improved by the introduction of the double sucrose-gap clamp (Ildefonse & Rougier, 1972) and the vaseline gap method (Hille & Campbell, 1976). The development of current in response to depolarizing voltage steps was sigmoidal in shape. Currents were fit with a Hodgkin-Huxley kinetic model (1952b) where $G_{\text{Na}} = G_{\text{Na}}^{\text{max}} m^3 h$. The conductance to Na^+ ions, G_{Na} , had a maximal value, $G_{\text{Na}}^{\text{max}}$, where nearly all of the channels were open. The third power of m was needed to describe the slow buildup of G following a step depolarization. The physical analogue of such a process is that three particles, voltage sensitive 'gates', must be near a certain area of the membrane at once in order for Na^+ ions to cross. The probability of each gate being there is described by the parameter m . The activation variable, m , increased as potential was made more positive whereas the

inactivation variable, h , decreased.

Na^+ conductance was found to be very voltage dependent. It rose steeply for small depolarizing pulses increasing e-fold for a 3.7 mV depolarization and leveled off above 0 mV. The membrane potential at which the conductance was half activated was around -50 mV and the time constant of activation (τ_m) at 0 mV ranged from 0.5 to 1.25 ms (2-5° C). The Na^+ currents were found to inactivate, i.e. during a maintained depolarization the currents declined. Inactivation was voltage-dependent. The membrane potential for half inactivation was around -70 mV and the time constant of inactivation (τ_h) at 0 mV was about 1.5 ms. The information obtained from the voltage clamp data was used to numerically reconstruct the action potential (Adrian *et al.*, 1970a). Peak Na^+ current density was about 4 mA/cm² and maximal Na^+ conductance was 330 mS/cm².

Na^+ currents recorded from mammalian fast- and slow-twitch muscle fibers have been reported to be similar to those of frog muscle. Only minor modifications of m^3h kinetics were necessary to fit Na^+ currents in rat muscle (Pappone, 1980). The activation curve was shifted 10-15 mV in the hyperpolarizing direction from that found in frog muscle. This shift would increase the likelihood of repetitive action potentials. Rates of activation at potentials more negative than -40 mV were significantly slower in rat than in frog. Values for maximal Na^+ conductance were similar in the two species. In rat, $G_{\text{Na}}^{\text{max}}$ was 120 mS/cm² and

peak Na⁺ current density was 2.5-4.5 mA/cm² (Adrian & Marshall, 1977; Duval & Léoty, 1978; Pappone, 1980). Slight differences between Na⁺ currents in fast- and slow-twitch fibers have been noted (Duval & Léoty, 1980a). Peak Na⁺ current occurred at less negative potentials and the reversal potential was about 7 mV more negative in slow- than in fast-twitch fibers. The difference in the reversal potential is consistent with the finding that the intracellular Na⁺ concentration is higher in slow- than fast-twitch fibers (Sreter & Woo, 1963; Yonemura, 1967; Chutkow, 1973). Also, the density of Na⁺ channels appears to be lower in slow- than in fast-twitch fibers based on differences in saxitoxin (STX) binding capacities (Hansen Bay & Strichartz, 1980).

Selectivity of Na⁺ channels has been studied in frog (Campbell, 1976) and in rat (Pappone, 1980) muscle. The ratio of Na⁺ to K⁺ permeability (P_{Na}/P_K) was 0.048 for frog and 0.045 for rat. Permeability ratios for various cations were very similar to the results obtained by Hille (1975) for Na⁺ channels in frog node to Ranvier. Hille characterized the ionic selectivity of the channels by systematically testing the permeability to an extensive list of small organic and metal cations. He proposed that a 3.1 x 5.1 Å oxygen-lined pore would account for the exclusion of all impermeant cations on simple geometric and chemical grounds.

Based on the density of TTX or saxitoxin (STX) binding sites in frog muscle, which ranged from 175 to 380 sites per μm^2 (Almers & Levison, 1975; Jaimovich, Venosa, Shrager & Horowicz, 1976; Ritchie & Rogart, 1977) and on maximal Na^+ conductances of 50-330 mS/cm^2 (Ildefonse & Roy, 1972; Hille & Campbell, 1976), a single channel conductance of 1.5-15 pS was calculated. This range of values is close to the value of 18 pS determined from single channel records in cultured rat muscle (Sigworth & Neher, 1980).

Evidence has accumulated which indicates that Na^+ channels also reside in the membranes of the transverse tubular system. This system of tubular membranes plays an important role in transmitting the electrical signals of the surface membrane into the central part of the muscle fiber to bring about a nearly synchronous initiation of contraction of myofibrils located at varying depths from the surface. The radial spread of mechanical activation has been reported to have a Q_{10} of 2 which is not easily explained by purely passive propagation of electrical signals along the tubular membranes (González-Serratos, 1971). Spread of mechanical activation was also reported to be less effective in Na^+ deficient or TTX-containing solutions (Constantin, 1970). In addition, reduction of Na^+ concentrations in the lumen of the transverse tubules or application of TTX to block regenerative activity of the tubular membranes has been shown to reduce twitch tension (Bezanilla, Caputo, González Serratos & Venosa, 1972; Caputo & Dipolo, 1973;

Bastian & Nakajima, 1974). Detubulation of muscle fibers (glycerol-induced osmotic shock which interrupts the continuity between surface and tubular membranes) has been shown to reduce TTX binding capacity by about 50% (Jaimovich *et al.*, 1976). Tubular Na^+ currents have been recorded. They appeared as late, slow inward currents under voltage clamp (Hille & Campbell, 1976; Mandrino, 1977). Therefore, voltage-dependent Na^+ currents in the membranes of the transverse tubular system contribute to the spread of depolarization along the tubules and are necessary for full mechanical activation.

Potassium Channels

Several types of K^+ channels have been described in frog skeletal muscle. 1) Delayed rectifier channels give rise to a fast outward current which is responsible for the repolarization phase of the action potential (Adrian *et al.*, 1970b). The currents reach a maximum in about 100 ms at -30 mV (3° C). 2) Slow K^+ channels generate slow currents that reach a maximum in about 3 s at -30 mV (3° C) (Adrian *et al.*, 1970b). 3) The inward rectifier is responsible for a conductance increase when the membrane potential is shifted to more negative levels (Adrian & Freygang, 1962; Adrian *et al.*, 1970b). 4) Ca^{2+} dependent K^+ channels, which open following increases in intracellular Ca^{2+} concentrations, have been postulated to exist in frog muscle (Fink & Lüttgau, 1976; Nicola Ciri Sánchez & Stefani, 1980).

Delayed rectifier: The presence of a clear repolarization phase of the action potential and of delayed currents in detubulated fibers demonstrate that delayed rectifier channels reside in the surface membrane (Gage & Eisenberg, 1969; Nicola Siri *et al.*, 1980). There may also be delayed rectifier channels populating the transverse tubular membranes since the late afterdepolarization following a train of spikes was observed to be slower in larger diameter fibers (Kirsch, Nichols & Nakajima, 1977). The density of K^+ channels has been estimated to be about 14 channels per μm^2 which is 20 times less than that estimated for Na^+ channels (Almers & Levison, 1975).

Tetraethylammonium (TEA) has been shown to block delayed rectification in muscle as it does in nerve (Armstrong, 1975). However, the affinity of the binding sites in muscle was lower by an order of magnitude. TEA shifted the threshold and the activation curve to slightly more negative potentials and also slowed the rate of onset of the currents by about 80% (Stanfield, 1970b).

In frog muscle, the delayed outward K^+ currents could be fit with a Hodgkin-Huxley kinetic model (1952b) using n^4 kinetics, i.e. $G_K = G_K^{max} n^4$. The membrane potential at which activation was half maximal was around -45 mV and the time constant (τ_n) was 5-8 ms at 0 mV. The conductance increased 6 fold for a 3 mV depolarization. Maximal K^+ conductance ranged from 6-23 mS/cm^2 (Adrian *et al.*, 1970a; Stanfield, 1970b; Stanfield, 1975; Almers, 1976). The instantaneous

current-voltage relationship was approximately linear with a mean equilibrium potential of -85 mV. The currents inactivated exponentially with a time constant of $0.5-1$ s at 10 mV (20° C). The steady-state inactivation curve was less steep than that for Na^+ current and the potential for half inactivation was approximately 20 mV more positive (Adrian *et al* 1970a).

Delayed rectifier currents in mammalian muscle have been reported to be similar to those in frog muscle (Pappone, 1980; Beam & Donaldson, 1983a). Current density and time courses were similar in fast and slow twitch fibers of rat. However, slow-twitch fibers exhibited an additional large, slow K^+ current which decayed with a time constant about 10 times longer than that of the delayed current (Duval & Léoty, 1978; 1980a, b).

Slow potassium channels: In frog muscle, tail current measurements suggested the presence of a slowly developing K^+ current that reached a maximum in about 3 s at -30 mV and then slowly inactivated to reach a final steady state level of about one third of the maximum amplitude (Adrian *et al*, 1970b). Slow K^+ currents have been directly recorded after blockade of the delayed rectifier with TEA in intact fibers (Stanfield, 1970a) and in the cut fiber preparation (Almers & Palade, 1981). The time course of the currents could be fitted with a Hodgkin-Huxley model (1952b) with n^2 kinetics and the time constant for activation was about 100 ms at -30 mV (Eaton *et al*, 1981).

the slow currents was about 10° mV more negative than that of the delayed current. This difference has been explained by postulating that the slow K^{+} channel is more selective for K^{+} than the delayed rectifier. Slow K^{+} current density was about one sixth of delayed rectifier current density.

In slow-twitch rat fibers, a prominent slow K^{+} conductance has been reported to be present. In contrast to the findings in frog muscle, the reversal potential for the delayed and slow outward currents was identical in detubulated fibers. In fast-twitch fibers, a much smaller slow component could be inferred from the tail currents. However, this component seemed to be the result of K^{+} accumulation in the lumen of the transverse tubular system as it was absent in detubulated fibers (Duval & Léoty, 1980a, b; Beam & Donaldson, 1983b). Therefore, it appears that fast-twitch muscle has only the fast delayed rectifier while the slow-twitch muscle has an additional slow K^{+} current. The function of the slow K^{+} current is unknown, but its slow kinetics suggest that it may play a role in repetitive activity. Slow-twitch fibers do not show the repetitive firing in response to prolonged depolarization that fast-twitch fibers do (Duval & Léoty, 1980a).

TEA and Zn^{2+} have been reported to block the delayed rectifier while having only a small effect on the slow current (Stanfield, 1975). In mammalian muscle, TEA blocked both currents while 4-aminopyridine blocked only the delayed rectifier (Duval & Léoty, 1980b). Diethylpyrocarbonate, a

histidine reagent, has been reported to selectively block the slow current (cf Stefani & Chiarandini, 1982). The difference in pharmacology between the two currents supports the idea that the slow currents are carried by channels distinct from the delayed rectifier channels.

Inward rectifier The resting conductance of frog muscle shows inward-going or 'anomalous' rectification since it allows K^+ to move in across the membrane more easily than out (Adrian, 1969). Experiments on isolated single muscle fibers (Hodgkin & Horowitz, 1960; Adrian & Freygang, 1962) and on detubulated fibers (Eisenberg & Gage, 1969) strongly suggest that inward rectifier channels reside, for the most part, in the transverse tubular membranes. The channels show voltage- and time-dependent properties. In frog muscle, it has been shown that the conductance is activated by hyperpolarization (Hestrin, 1981; Leech & Stanfield, 1981). The conductance was found to increase e -fold for a 12 mV hyperpolarization. The time constant of activation versus voltage curve and the conductance versus voltage curve were found to shift to more positive voltages when the external K^+ concentration was increased. No appreciable effect of intracellular K^+ concentration was found. Thus, the conductance mechanism depends on voltage and external K^+ concentration (Adrian & Freygang, 1962; Adrian *et al.*, 1970b). Rectification of current flow through this K^+ channel seems to be partly the result of voltage dependent gating (Hestrin, 1981) and partly the result of 'instantaneous' rectification

of the channels since the instantaneous current-voltage relationship has been found to be nonlinear (Leech & Stanfield, 1981). The mechanism underlying rectification in individual channels has not been determined. The inward rectifier in fast- and slow-twitch mammalian fibers has similar properties to the inward rectifier in frog (Duval & Léoty, 1978; 1980a, b). The inward rectifier has been found to be blocked by TEA, Ba^{2+} and Sr^{2+} , but not by Zn^{2+} (Stanfield, 1970a; Standen & Stanfield, 1978).

Inward rectifier currents recorded under normal ionic conditions (low external K^+) have been observed to decline during maintained hyperpolarizing voltage steps. The decline has been demonstrated to be partly the result of K^+ depletion in the lumen of the transverse tubular system and partly the result of a fall in K^+ conductance for extremely large hyperpolarizing pulses (Adrian & Freygang, 1962; Adrian *et al.*, 1970b; Almers, 1972). The fall in conductance for the extreme hyperpolarizing pulses (more negative than -150 mV) was shown to be the result of a potential dependent block by external Na^+ (Standen & Stanfield, 1979).

Noise analysis of inward rectifier currents in frog muscle has given a single channel conductance of about 9 pS (DeCoursey, Dempster & Hutter, 1984). Calculated channel density was 1 channel per μm^2 . Recordings of single channel currents, resulting from blocking and unblocking by Ba^{2+} , in cultured rat muscle have also given a value of about 10 pS for single channel conductance (Ohmori, Yoshida & Hagiwara,

1981).

In summary, two properties of the inward rectifier channels distinguish them from 'normal' delayed rectifier channels. First, conductance of the inward rectifier increases as membrane potential is made more negative. The opposite is true for delayed rectifier channels. Second, conductance of the inward rectifier channels depends on external K^+ concentration while the conductance of the delayed rectifier is independent of K^+ concentration. The molecular mechanism of this peculiar dependence on external K^+ concentration is not understood.

Calcium-dependent potassium channels: Ca^{2+} -dependent K^+ channels have been described in a variety of different cell types (for review, Kostyuk, 1984). The conductance depends on Ca^{2+} and on membrane potential. Studies of single channel events in cultured rat skeletal muscle have shown that elevation of intracellular Ca^{2+} levels increased the frequency and duration of the open state. A similar effect was produced by membrane potential with an e-fold increase in conductance for a 15 mV depolarization (Barrett, Magleby & Pallotta, 1982). Ca^{2+} -dependent K^+ channels from rabbit (Latorre, Vergara & Hidalgo, 1982) and from rat (Moczydlowski & Latorre, 1983) transverse tubular membranes have been studied in planar phospholipid bilayers. It was suggested that the channel requires two bound Ca^{2+} ions for activation and that it is the binding steps which are voltage dependent while the opening and closing of the

K⁺-selective pore is voltage-independent (Vergara, Moczydlowski & Latorre, 1984).

The single channel conductance has been reported to be 300 pS (Barrett *et al.*, 1982; Latorre *et al.*, 1982). The large conductance and the high Ca²⁺ and voltage sensitivity of the channel suggests that it is suited to resist depolarizations of the membrane potential which are accompanied by increases in intracellular Ca²⁺ concentrations. Thus, these channels may be a link between excitation-contraction coupling and membrane repolarization.

Calcium channels

Voltage clamp studies of frog muscle fibers have revealed slow inward currents carried by Ca²⁺ (Sánchez & Stefani, 1978; Almers & Palade, 1981). Currents were abolished by Co²⁺ and Cd²⁺, known blockers of Ca²⁺ channels (Hagiwara & Byerly, 1981), or by removal of external Ca²⁺. Current-voltage relationships showed that currents were evident at -40 mV and reached a maximum at 0 mV. Maximum inward current was 80 μ A/cm² and maximum conductance was 2-5 mS/cm². Ca²⁺ currents could be fit with a Hodgkin-Huxley kinetic model (1952b) using m³ kinetics. The membrane potential at which half-activation occurred was -39 mV and the time constant of activation (τ_m) was 0.11 s at 0 mV. With maintained depolarization, currents declined completely. The time constant of inactivation was 1.1 s at 0 mV. However, it is not entirely clear what mechanisms underlie

'inactivation' of the currents. It could be a voltage-dependent process (Cota, Nicola Siri & Stefani, 1983) or depletion of Ca^{2+} in the lumen of the transverse tubular system (Almers, Fink & Palade, 1981) or perhaps a Ca^{2+} -dependent inactivation as seen in some nerve cells (Kostyuk, 1984).

Ca^{2+} channels have been reported to be located mainly in the tubular membranes (Potreau & Raymond, 1980; Almers *et al.*, 1981). In detubulated fibers, a linear correlation was found between the degree of electrical continuity of the tubular with the surface membranes and the magnitude of the Ca^{2+} currents (Nicola Siri *et al.*, 1980). The functional role of Ca^{2+} channels in muscle is not clear. Skeletal muscle fibers are well known to rely on internal stores of Ca^{2+} for regulating cytoplasmic Ca^{2+} concentrations. During a normal action potential, an insignificant amount of Ca^{2+} would enter the fiber through these channels to directly activate tension (Potreau & Raymond, 1980; Almers & Palade, 1981).

Chloride channels

Cl^- channels make a significant contribution to the resting membrane conductance in avian, amphibian and mammalian muscle fibers. Resting Cl^- conductance has been reported to be (mS/cm^2): 0.2 in frog (Hodgkin & Horowitz, 1959); 0.7 in *Xenopus* (Vaughan, McLarnon & Loo, 1980); 2 in rat (Palade & Barchi, 1977) and about 1 in chicken (Lebeda &

Albuquerque, 1975) muscle fibers. In frog fibers, Cl^- channels appear to be located mainly in the surface membrane (Hodgkin & Horowitz, 1960; Eisenberg & Gage, 1969) while at least 60% of the resting conductance to Cl^- (G_{Cl}) appears to be located in the tubular membranes in mammalian fibers (Palade & Barchi, 1977; Dulhunty, 1979). An obvious advantage to having a large G_{Cl} in the tubular membranes would be that it would shunt the action potential and thus reduce outward K^+ current. This would then reduce the tendency for K^+ to accumulate in the lumen of the transverse tubules. A casual relationship between K^+ accumulation and myotonic activity has been demonstrated in goats with a genetic deficit of G_{Cl} (Adrian & Bryant, 1974). As well, an abnormally low G_{Cl} has been postulated to produce some of the symptoms of myotonia in humans (Bryant & Morales-Aguilera, 1971).

G_{Cl} has been shown to depend markedly on external pH. The conductance has been observed to increase at alkaline pH and to decrease at acid pH. G_{Cl} and pH were related by a sigmoid curve with apparent pKs for the groups controlling G_{Cl} being about 7.0 in frog (Hutter & Warner, 1967; 1972) and 5.5 in mammalian fibers (Palade & Barchi, 1977). In frog fibers, voltage clamp records showed that G_{Cl} decreased as the fiber was hyperpolarized. For example, during a hyperpolarizing pulse of 85 mV from the holding potential, the current decayed with a half-time of 90 ms at pH 7.4. At alkaline pH (9.8), the decay was slower. In contrast, at

pH 5, current increased approximately exponentially throughout the pulse (Warner, 1972). The instantaneous current-voltage relationship was linear in the three pHs tested. However, the steady-state relationship suggested that the current reached a limiting value for large hyperpolarizations. According to Warner (1972), several features of G_{Cl} are consistent with the supposition that Cl^- ions combine with a carrier molecule to an extent determined by the external pH.

The Cl^- conductance in rat (Palade & Barchi, 1977) and in *Xenopus* (Vaughan *et al.*, 1980) muscle has been shown to have similar properties to G_{Cl} in frog muscle. In *Xenopus*, it has been demonstrated that the voltage dependence of G_{Cl} is similar in normally polarized and chronically depolarized fibers. This suggested that G_{Cl} is a function of the difference between resting membrane potential and membrane potential during a test pulse rather than a function of the absolute membrane potential. The findings in *Xenopus* and in rat fibers, have been explained by proposing the existence of aqueous pores for Cl^- (Palade & Barchi, 1977; Vaughan *et al.*, 1980; Loo, McLarnon & Vaughan, 1981). To explain the observed deviation of the current-voltage relationship from that predicted from the constant field equation at alkaline pH, a blocking moiety has been postulated. As the membrane potential becomes more negative, this particle would move to a site that must be occupied by Cl^- to permeate (Vaughan *et al.*, 1980). G_{Cl} in *Xenopus* fibers has been shown to be

blocked by the stilbene derivative, SITS (Vaughan & Fong, 1978).

B. Ion Channels in Slow Tonic Fibers

In addition to twitch fibers, there is another type of fiber in skeletal muscle: slow-tonic fibers. They occur either intermingled with twitch fibers in amphibians and mammals or as a pure slow muscle, the anterior latissimus dorsi, in birds (for review, Hess, 1970; Morgan & Proske, 1984). Slow-tonic fibers have multiple nerve endings, generate a slowly developing tension under repetitive stimulation and give rise to maintained or tonic tension when continuously depolarized with K^+ or cholinergic drugs (Ruffler & Vaughan Williams, 1953b; Hess & Pilar, 1963; Page, 1969). This type of fiber is difficult to study electrophysiologically because the fibers are scarce or have small diameters.

Sodium channels

In frog slow-tonic fibers, activatable Na^+ channels appear to be absent (Burke & Ginsborg, 1956; Gilly & Hui, 1980). However, following denervation, these fibers were capable of generating propagating action potentials which were Na^+ dependent and TTX sensitive (Miledi, Stefani & Steinbach, 1971). In contrast to frog fibers, avian fibers are capable of generating Na^+ -dependent action potentials which are TTX sensitive (Cullen, Harris, Marshall & Ward,

1975). The action potentials were reported to be smaller in amplitude and to have a slower rate of rise than the action potentials in twitch fibers. Mammalian slow-tonic fibers appear to be intermediate between amphibian and avian fibers, as they have been reported to show a graded response to depolarizing pulses. The response was blocked by TTX and disappeared in Na⁺-free solution (Bondi & Chiarandini, 1979; Chiarandini & Stefani, 1979).

Potassium channels

Delayed rectifier: The delayed rectifier has been reported to be present in frog, chicken and rat slow-tonic fibers (Burke & Ginsborg, 1956; Cullen *et al.*, 1975; Bondi & Chiarandini, 1979; Chiarandini & Stefani, 1979). In frog fibers, maximum K⁺ conductance was 0.5 mS/cm² which is about ten times smaller than in twitch fibers. The steady-state conductance versus voltage curve was less steep than in twitch fibers with an e-fold change in conductance for a 15 mV depolarization. Also, the rates of activation were 2-4 times smaller than those of twitch fibers. Whether the delayed rectifier inactivated during maintained depolarization was uncertain (Gilly & Hui, 1980). TEA blocked the delayed rectifier in mammalian and frog slow-tonic fibers (Bondi & Chiarandini, 1979; Gilly & Hui, 1980).

Slow potassium channel: So far, this channel has only been demonstrated in frog slow-tonic fibers (Gilly & Hui, 1980).

Calcium channel

Ca^{2+} channels appear to be present in slow-tonic fibers of the toad (Stefani & Uchitel, 1976). Studies of K^+ and caffeine contractures in the anterior latissimus dorsi of chicks showed that the contractures were partially dependent on external Ca^{2+} , suggesting that these fibers have Ca^{2+} channels (Page, 1969; Huerta & Stefani, 1981).

Resting conductances

Slow-tonic fibers have been reported to have very low resting membrane conductances (mS/cm^2): 0.008 in frog (Stefani & Steinbach, 1969); 0.17 in chicken (Huerta & Stefani, 1981) and 0.25 in rat (Bondi & Chiarandini, 1979). The majority of the resting conductance has been reported to be the result of K^+ since resting conductance to Cl^- was not detectable. Current-voltage relationships have indicated that inward rectifier channels are present in chick and in rat (Chiarandini & Stefani, 1979; Huerta & Stefani, 1981), but not in frog (Stefani & Steinbach, 1969; Gilly & Hui, 1980) slow-tonic fibers. In rat, it has been reported that there is a small resting conductance to Na^+ since Na^+ -free solution hyperpolarized the fibers by 10-15 mV (Bondi & Chiarandini, 1979).

C. Ion Channels in Denervated Skeletal Muscle

Sodium Channels

Denervation of rat skeletal muscle has been reported to cause a shift of activation and inactivation parameters of Na^+ currents by about 10 mV to more negative potentials (Pappone, 1980). The rates of activation and inactivation were not measurably affected. Since the resting membrane potential of denervated rat muscle has been reported to be more depolarized than normal (Redfern & Thesleff, 1971a), the shifts in activation could lead to significant Na^+ current at resting membrane potential. This is supported by the observation that the application of TTX increases the resting membrane potential of denervated, but not innervated fibers (Harris & Thesleff, 1971). The shift in activation may also explain the spontaneous, Na^+ -dependent, oscillations in membrane potential which cause fibrillation in denervated mammalian muscle (Purves & Sakmann, 1974).

The maximum Na^+ conductance in denervated rat muscle has been shown to be similar to that in innervated muscle (Pappone, 1980). This is supported by the observation that saxitoxin (STX) binding capacity was only slightly reduced following denervation (Hansen Bay & Strichartz, 1980). In contrast to this, Barchi & Weigle (1979) have measured a 43% decrease in STX binding to purified sarcolemma of denervated relative to innervated muscle.

It has been reported that the action potential becomes partially resistant to TTX following denervation (Redfern & Thesleff, 1971b; McArdle *et al.*, 1980). In innervated muscle, TTX has been reported to block Na⁺ channels in a manner predicted by the binding of toxin to a single population of channels with a dissociation constant of 5 nM. Following denervation, a second population of Na⁺ channels with a dissociation constant in the micromolar range appeared (Pappone, 1980). This second type of channel was responsible for 25-30% of the total Na⁺ conductance. Thus, it appears that denervation causes, at most, a partial loss of TTX-sensitive Na⁺ channels. It has been reported that denervated frog (Miledi *et al.*, 1971) and chick (Lebeda, Warnick & Albuquerque, 1974) muscle remain normally sensitive to TTX. Therefore, denervation-induced TTX-insensitivity of Na⁺ channels is specific to mammalian muscle.

Interestingly, following denervation of frog slow-tonic muscle, the fibers, which do not normally have Na⁺ channels, acquired a Na⁺-based action potential (Miledi *et al.*, 1971). The amplitude and rate of rise of the action potential was smaller than in twitch fibers and reinnervation with a slow nerve repressed the action potentials. Thus, together with the above results, it appears that the expression of Na⁺ channels is at least partially influenced by innervation.

Resting membrane conductances

Resting membrane resistance has been reported to increase following denervation of fast- and slow-twitch muscle fibers of rats (Albuquerque & McIsaac, 1970; Westgaard, 1975) and of chickens (Lebeda & Albuquerque, 1975). This change has been determined to result from a decrease in resting Cl conductance (Lebeda & Albuquerque, 1975; Lorković & Tomanek, 1977). Interestingly, the increase in membrane resistance in rat muscle could be reversed by direct electrical stimulation of the muscle for 2 weeks beginning on the fifth day following denervation (Westgaard, 1975). For denervated frog muscle (over 1 month), no change in resting Cl conductance was found. But there is a small decrease in resting K conductance (Lebeda & Albuquerque, 1975).

D. Ion Channels and Membrane Properties of Muscle Cells

Neurology

Resting membrane

A complete study of changes in excitability during development of rat muscle has not been done. Action potentials have been recorded from diaphragm muscle of 1-day rat fetuses, although their ionic basis was not studied (Diamond & Milodij, 1962). Recordings of action potentials from diaphragm muscle of the intact rat are available, but they are not suitable for analysis of membrane properties.

TTX-insensitive Na⁺ channels.

A study comparing the action potentials in developing fast- and slow-twitch fibers showed that at 12 days of age there were no differences between the two fiber types (McArdle *et al.*, 1980). The characteristics of the action potential in slow-twitch fibers attained adult values by 18 days, while 50-60 days were required for the fast-twitch fibers. Differences between the two fiber types were apparent by 25 days. A quantitative study suggested that the basis for the differences between the two fiber types and between immature and adult fibers was the result of differences in intracellular Na⁺ concentrations and maximal Na⁺ conductance. Slow-twitch fibers were estimated to have higher intracellular Na⁺ concentrations (29 mM) than fast-twitch (18 mM) and to have a lower Na⁺ conductance (24 versus 34 mS/cm²). Young fibers were estimated to have very high intracellular Na⁺ concentrations (45 mM for fast-twitch and 55 mM for slow twitch). The trend of high to low intracellular Na⁺ concentrations during development was also found for another muscle of the rat (Atwood & Kwan, 1978) and for chick muscle (Barlow & Manery, 1954).

The increase in maximum Na⁺ conductance during development probably reflected an increase in the density of Na⁺ channels. Studies of the number of STX binding sites per unit weight showed an increase from 2 to 21 fmol/mg wet weight from 2 to 25 days of age (Sherman & Catterall, 1982). The appearance of the STX binding sites appeared to occur in

two phases. During the first phase, which was independent of continuing innervation, the STX receptor density increased to 47-57% of the adult level. After day 11, the second phase of development, which was dependent on continuing innervation, gave rise to the adult value of STX receptors.

Chick muscle

The development of excitability in chick muscle has been studied under current clamp (Kano, 1975). At 13 days *in ovo*, most of the fibers gave passive responses to depolarizing pulses, while a small percentage showed afterhyperpolarization, suggesting the presence of delayed rectification. At later stages, the first sign of regenerative activity was a long duration action potential subsequently shown to be produced by an inward Cl^- current (Fukuda, 1974; 1975; Fukuda *et al.*, 1976a, b). By 19 days *in ovo*, a faster spike based on Na^+ was present. Ca^{2+} channels were also inferred to be present from the action of Ba^{2+} on spike duration. Ba^{2+} goes through Ca^{2+} channels (Hagiwara & Byerly, 1981) and blocks K^+ channels. After hatching the Cl^- action potential disappeared.

E. Ion Channels in Skeletal Muscle During *in vitro* Development

Primary cultures of rat muscle

Developmental changes in action potentials have not been studied in primary cultures of rat muscle. However, the ratio of Na⁺ to K⁺ permeability (P_{Na}/P_K) was found to decrease from 0.4 at 3 days to 0.06 at 9 days of culture (Ritchie & Fambrough, 1975). This change in P_{Na}/P_K ratio was probably responsible for the increase in resting membrane potential (-24 to -51 mV) occurring over the same time period. Resting Cl⁻ conductance did not change with time in culture and remained well below adult values.

A novel Cl⁻ channel has been observed with single channel recording techniques (Blatz & Magleby, 1983). The single channel conductance was about 430 pS. The channel was often open at 0 mV. When open, voltage steps from 0 mV to either negative or positive potentials closed the channel after about 1 s. Returning the membrane potential to 0 mV caused the channels to reopen. In several trials, it was found that closed channels opened when the potential was stepped from -60 to 10 mV for a few milliseconds and then back to -60 mV. Once the channels opened, they closed within several seconds. If these channels have similar kinetics in intact cells, then they could possibly contribute to repolarization of the action potential.

Clonal rat cell line

Differentiation of electrical excitability has been studied in a clonal cell line of rat muscle (L6) (Kidokoro, 1973, 1975a, b; Land, Sastre & Podleski, 1973). Myoblasts were electrically excitable and produced small, brief Na^+ action potentials. After fusion, the multinucleate myotubes had overshooting action potentials. The initial spike was the result of Na^+ influx and the plateau of the repolarizing phase was largely the result of Ca^+ influx. These Na^+ channels may have differed from channels found in adult muscle since higher concentrations of TTX and STX were required to block ion fluxes and action potentials (Kidokoro, 1973; Sastre & Podleski, 1976; Lawrence & Catterall, 1981). Current-voltage relationships indicated that delayed rectification was present in myotubes but not in myoblasts. The time course of delayed rectification was thought to be extremely slow as the hyperpolarization following the action potential lasted 4-8 s. The slow kinetics of the delayed rectification may have contributed to the long duration of the action potentials in myotubes (about 100 ms at half height) (Kidokoro, 1973). Inward rectification was present in myotubes and the resting conductance to Cl^- was low (Kidokoro, 1975b). In summary, in this cell line, inward currents were expressed before outward currents.

Primary cultures of chick muscle

The excitability properties of chick skeletal muscle have been shown to change during development in tissue culture. After 2-3 days, inward and delayed rectifier conductances were present (Spector & Prives, 1977). Voltage-dependent Na^+ , Ca^{2+} and Cl^- conductances appeared later, at days 4-5. (Kano, Shimada & Ishikawa, 1972; Kano & Shimada, 1973; Fukuda, 1974; Fukuda *et al.*, 1976a). Cl^- action potentials had extremely long durations (tens of seconds) and could only be elicited if the membrane potential was hyperpolarized below -60 mV or if Cl^- ions were injected intracellularly (Fukuda, 1974; Spector & Prives, 1977).

The rate of rise of the Na^+ action potentials increased from 5 to 30 V/s during 4 to 14 days in culture (Kano & Yamamoto, 1977; Spector & Prives, 1977), but never reached adult values of around 112 V/s (Cullen *et al.*, 1975). The increase in the rate of rise of the action potential appeared to be the result of an increase in the density of Na^+ channels since the binding capacity of TTX to muscle cell homogenates increased during 25 to 100 hours in culture (Frelin, Lombet, Vigne, Romey & Lazdunski, 1981). The authors did not find a change in the affinity for TTX. In another study, the appearance of STX and BTX (batrachotoxin) binding sites were found to follow different time courses (Strichartz, Bar-Sagi & Prives, 1983). These results suggested that the developmental expression of Na^+ channels

was accompanied by a change in the pharmacological properties of the channel.

In cultured chick muscle, another novel channel has been found with single channel recording techniques (Kolb & Schwarze, 1984). This channel was cation selective, but lacked selectivity for one cation over another. The channel appeared to have voltage-dependent gating, but the kinetics were very complex.

F. Summary and Objectives

The surface membranes of mature skeletal muscle fibers are specialized to generate action potentials and to maintain an adequate transmembrane potential. It is now becoming apparent that these electrophysiological properties undergo changes during the course of muscle cell differentiation (Spitzer, 1979; Harvey, 1980). For example, the ionic dependence of the action potential changes during development. Observations such as this raise several questions. What is the exact nature and the time course of the changes in electrophysiological properties which occur during maturation of muscle? Are there changes common to other developing cell types, so that some general rules emerge? By what mechanisms do the changes occur? And do these changes play any role in the growth and maturation of muscle cells?

Muscle cells are attractive for the study of development of electrophysiological properties of membranes since a detailed knowledge about the mature fibers is available.

Furthermore, a great deal of qualitative and quantitative information about membrane electrical properties can be obtained from intracellular microelectrode studies.

Unfortunately, there are technical problems which limit the study of electrical properties of developing muscles. At the embryonic stage of interest, the cells to be studied are generally small in size, making certain electrophysiological experiments extremely difficult, if not impossible, to do. In addition, the fibers are often quite fragile and thus easily and rapidly damaged by microelectrode impalement. Consequently, very few studies and virtually no quantitative work has been done on developing skeletal muscle fibers.

One approach to these problems has been to prepare explant or primary cultures which can facilitate location, identification and experimental manipulation of the cells. Extremely valuable information can be obtained from study of development *in vitro*; however, care should be exercised in generalizing results to *in vivo* development since innervation affects the electrophysiological properties of muscle (for review see, Harris, 1974; Jolesz & Sreter, 1981). For example, it has been demonstrated that denervation of adult muscle leads to several changes: increased membrane resistance (Westgaard, 1975; Lebeda & Albuquerque, 1975; Lorkvić & Tomanek, 1977) and the appearance of TTX-insensitive Na⁺ channels (Pappone, 1980). Clonal cell lines have also been utilized (Kidokoro, 1975a, b), but they may demonstrate abnormal development.

In an effort to study *in vivo* development of vertebrate skeletal muscle, an enzymatic dissociation procedure previously applied to adult rat muscle (Bekoff & Betz, 1977a) was found to be applicable to embryonic chick muscle. The use of isolated single fibers greatly facilitated micro-electrode studies. Membrane electrical properties and resting conductance to Cl^- were studied during embryonic development. Preliminary results on the voltage- and time-dependent ionic currents were also obtained using a single suction pipette voltage clamp. A detailed study of the voltage- and time-dependent Cl^- currents was done on muscle cells grown in tissue culture. The Cl^- currents underlie a long duration action potential and are expressed during the course of normal *in vivo* development. These action potentials appear to be involved in producing contractions (Spector & Prives, 1977).

II. MEMBRANE ELECTRICAL PROPERTIES OF DEVELOPING FAST-TWITCH AND SLOW-TONIC FIBERS OF THE CHICK

A. INTRODUCTION

The electrical properties (resistance, capacitance, time and length constants) of the membranes of skeletal muscle fibers determine their response to electrical stimulation. In birds and amphibians, slow-tonic and fast-twitch fiber types have markedly different membrane electrical properties (Adrian & Peachey, 1965; Fedde, 1969; Stefani & Steinbach, 1969; Gordon, Vrbová & Wilcock, 1981). Slow-tonic fibers receive multiple innervation and do not necessarily conduct action potentials (Ginsborg, 1960a; Ridge, 1971; Cullen *et al.*, 1975; Gilly & Hui, 1980). The initiation of contraction in this fiber type involves the local spread of depolarization from the neuromuscular junctions. Slow-tonic fibers have higher membrane resistances and longer time and length constants than fast-twitch fibers which are singly innervated and rely on propagated action potentials to initiate contraction (Kuffler & Vaughan Williams, 1953a, b).

The membranes of slow-tonic and fast-twitch muscle fibers also differ in regard to resting membrane conductance to Cl^- . Fast fibers have a large resting conductance to Cl^- (Hutter & Noble, 1960; Lebeda & Albuquerque, 1975) while slow fibers do not (Stefani & Steinbach, 1969; Huerta & Stefani, 1981). An abnormally low Cl^- conductance has been found to be partly responsible for the symptoms of myotonia

(Bryant & Morales-Aguilera, 1971; Adrian & Bryant, 1974). This finding supports the idea that the resting Cl^- conductance is important for the stability of the membrane potential, especially during repetitive activity (Hutter & Noble, 1960; Rudel & Senges, 1972).

When do these distinctive properties of fast-twitch and slow-tonic muscle fibers arise during development? I have studied the anterior (a.l.d.) and the posterior (p.l.d.) latissimus dorsi muscles of the chick. A.l.d. is a multiply innervated, slow-tonic muscle and p.l.d. is a focally innervated, fast-twitch muscle (Ginsborg, 1960b). One week prior to hatching, the embryonic fibers of both muscles had high membrane resistances (R_m), long time (τ_m) and length (λ) constants and no detectable resting conductance to Cl^- (G_{Cl}). By the time of hatching, differences between a.l.d. and p.l.d. fibers became clear as a result of decreases in the magnitude of the electrical constants (R_m , τ_m , λ) and the appearance of a substantial G_{Cl} in p.l.d. fibers.

B. METHODS

Preparation

Latissimus dorsi muscles were dissected from white Leghorn chick embryos and young chicks (Figure 1) (Ginsborg, 1960a). The age of the embryo was determined from the number of days of incubation and the date of hatching (21 days) determined the post-hatched age. Single muscle fibers were

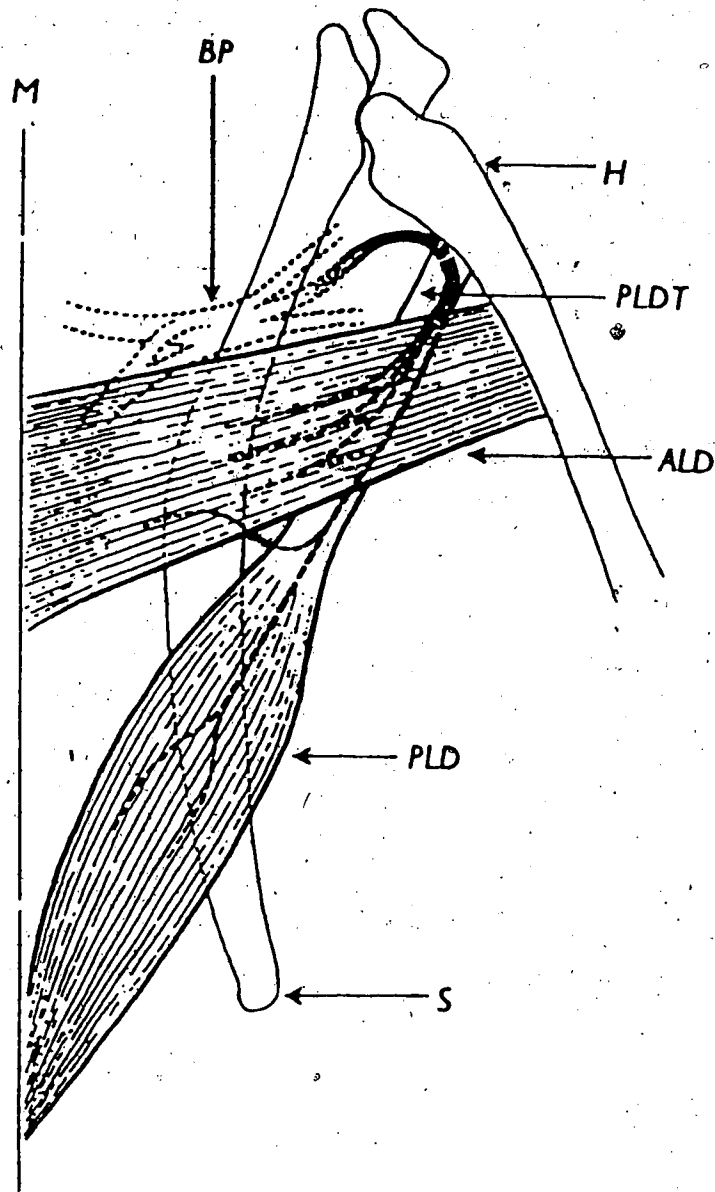


Figure 1. Diagram of a.l.d. and p.l.d. muscles. Dorsal view of the right latissimus dorsi muscle of the chick. ALD - anterior latissimus dorsi; PLD - posterior latissimus dorsi; PLDT - tendon of the p.l.d. muscle; M - midline; H - humerus; S - scapula; BP - brachial plexus. Adapted from Ginsborg (1960b).

isolated using an enzymatic and mechanical dissociation procedure (Bekoff & Betz, 1977a). Loose connective tissue was removed with fine forceps under a binocular dissecting microscope. Muscles were placed in Ca^{2+} -free Eagle's minimum essential medium (MEM; Gibco, Calgary, AB) containing 0.3% collagenase (Sigma Chemical Co., Type I, St. Louis, MO). Muscles were incubated at 37° C in a water-saturated 5% CO_2 atmosphere until the fibers began to dissociate (approximately 1 hour for 14 day embryonic muscles and 2-3 hours for older muscles). After incubation, muscles were rinsed in Eagle's MEM containing 10% horse serum (Flow Labs, Inglewood, CA) and 5% chick embryo extract (CEE). CEE was made by pressing 11 day embryos through a 10 ml syringe. An equal volume of Earle's Balanced Salt Solution (BSS) was added. The composition of Earle's BSS is (gm/l): CaCl_2 , 0.2; KCl , 0.4; NaCl , 0.2; NaHCO_3 , 2.2; MgSO_4 , 0.2; NaH_2PO_4 , 0.14; D-glucose, 1.0. The mixture was allowed to stand for 1 hour at room temperature. It was then centrifuged at 20,000 g for 10 minutes and the supernatant was removed and filtered (0.8 μm). 5 ml aliquots were stored frozen until use. Following the rinsing step, muscles were mechanically dissociated to release single muscle fibers. This was accomplished either by agitation with a jet of solution from a Pasteur pipette or by trituration with a fire polished pipette. The mechanical dissociation step had to be done very gently to avoid damaging the fibers. Isolated fibers were placed in complete medium and kept in 35 mm tissue

culture dishes (Corning) in an incubator. Fibers were used the day they were isolated.

Experimental set-up

Isolated fibers were visualized with phase contrast optics on an inverting microscope (Olympus). Fiber dimensions and interelectrode distances were measured with a calibrated eyepiece micrometer. Solutions were made with glass distilled water and saturated with 95% O₂/5% CO₂. The external solution contained (mM): NaCl, 137; KCl, 5.4; CaCl₂, 1.8; MgCl₂, 0.8; dextrose, 10; HEPES (4-2-hydroxyethyl-1-piperazineethanesulfonic acid), 10. For Cl⁻-free solutions, NaCl was replaced with NaH₂SO₄ and KCl with KH₂SO₄ (Pfaltz & Bauer, Stamford, CT) (Hutter & Noble, 1960) and MgCl₂ with MgSO₄, thereby replacing 98% of the Cl⁻. The pH was adjusted to 7.4. Experiments were done at room temperature.

Conventional techniques for intracellular recording and stimulation were used. Electrodes were conventional glass microelectrodes filled with 3 M KCl (20-60 MΩ). Membrane potentials were recorded using WP Instrument electrometers (models 750 and M4-A). The current passing electrode could be used to record voltage responses simultaneously. The resulting voltage drop across the electrode tip resistance was cancelled by balancing the active bridge circuit before impalement. Current was measured by a current-voltage converter placed in series with the bath ground. Signals were

displayed on a digital oscilloscope (Nicolet Instruments, Series 2090, Madison, WI) and stored on magnetic diskettes. Leakage current from the electrometers was checked frequently and adjusted to as small a value as possible. Digital voltmeters provided constant readout of membrane potential. Current pulse duration and magnitude were controlled with a digital pulse generator (WR Instruments, New Haven, CT).

Data collection and analysis

For estimation of passive cable properties, hyperpolarizing rectangular current pulses were injected intracellularly. The magnitude of the current pulse was adjusted to give no more than a 15 mV response. Input resistances (R_{in}) and membrane time constants (τ_m) were measured at the site of current injection by the current-passing electrode. Membrane length constants (λ) were determined by inserting a voltage-sensing electrode 100-600 μm away (distance limited by field of view) from the current-passing electrode. Additional impalements for recording voltage responses at varying distances from the current-passing electrode were not feasible because of the difficulty in obtaining multiple, stable impalements in the embryonic fibers. Since the current-passing electrode was simultaneously recording voltage, care was taken to minimize any errors from improper bridge balance or coupling. Three different signal paths of

Relatively low resistance electrodes were used and current pulses were as small as possible. Comparison of R_{in} values in Table 2 (voltage measured with a separate electrode) with values in Table 3 (single microelectrode) show no significant differences ($P < 0.1$).

Passive cable properties were calculated from the equations for infinite cables with current injected in the middle of fiber length (Weidmann, 1952; Stefani & Steinbach, 1969). For all reported data, the distance from the current-passing electrode to the end of the fiber, divided by the length constant, was greater than 2, justifying use of the infinite cable equations (Stefani & Steinbach, 1969; Jack, Noble & Tsien, 1975). The length constant (λ) was calculated from $V_x/V_0 = \exp(-x/\lambda)$. V_0 is the steady-state deviation of intracellular potential from resting potential recorded at the site of current injection. V_x is the steady state deviation recorded at a distance, x , from the current passing electrode. Membrane resistance (R_m) was calculated from the following equations: $R_{in} = V_0/I = r_i \lambda / 2$; $r_m = r_i \lambda^2$; $R_m = \pi d r_m$. r_i and r_m are intracellular resistance and membrane resistance per unit length of fiber, respectively. d is fiber diameter. Intracellular resistivity (R_i) was calculated by $R_i = r_i \pi d^2 / 4$. Membrane capacitance (C_m) equals τ_m / R_m . τ_m was taken as 84% of the time needed for the voltage to reach its steady state value.

P values reported in the text are from Student's t test. Data are reported as means \pm S.D.

C. RESULTS

Isolated fibers

Enzymatic dissociation procedures have been used to isolate single fibers from adult skeletal (Bekoff & Betz, 1977a) and smooth muscle (Singer & Walsh, 1980). No effects of enzyme treatment on resting membrane conductances were noted by Betz and Sakmann (1973) and only a slight decrease in resting membrane potential was observed by Bekoff and Betz (1977a).

Single muscle fibers were isolated from latissimus dorsi muscles of embryonic and young chicks. Visual inspection of the dissociated muscles at a magnification of 200x revealed dozens of single muscle fibers that appeared intact as well as fibers that had obviously been damaged. Damaged fibers had 'cytoplasmic blebs' and segments of them had undergone irreversible contracture. Many of the intact fibers settled to the bottom of the dish and adhered lightly to the substrate. They appeared cylindrical in shape and the banded pattern of sarcomeres was visible on fibers from 21 day embryos and older (Plate 1). Isolated fibers remained relaxed in standard external solution. Diameters of the isolated fibers were measured optically (see Table 2); the values compared well with diameters measured

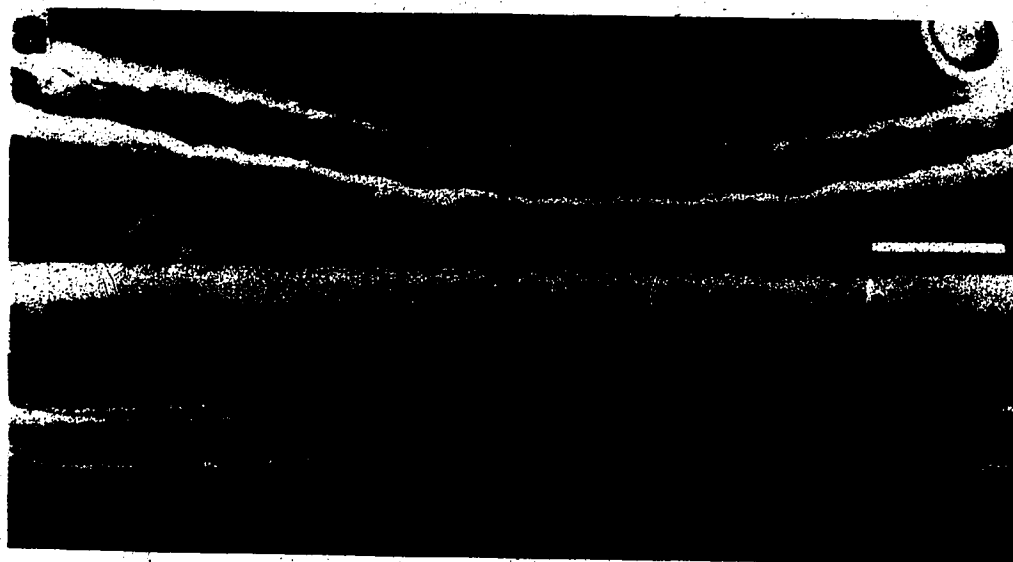


Plate 1. Light microscope photographs of single muscle fibers isolated from 14 A) and 21 B) embryonic posterior latissimus dorsi muscles of the chick. Calibration bar represents 20 μm .

histological sections (Gordon, Purves & Vrbová, 1977).

Action potentials could be elicited by intracellular current injection and were often accompanied by visible contractions (Figure 2). At any one age, the amplitude, rate of rise and duration of spikes were quite variable from fiber to fiber. This variability probably arose because developmental changes in the action potential were occurring and the fibers were not developing synchronously (Kano, 1975).

Fibers that attached to the substrate along most of their length could be maintained in tissue culture for at least one week. During that time, the morphology of the fibers changed. The fibers sent out branches and began to resemble muscle fibers that have developed from myocytes *in vitro*. The cultured fibers exhibited spontaneous contractions and some began to fibrillate after several days in culture. Bekoff and Betz (1977b) reported similar changes for isolated adult rat fibers which had been maintained under tissue culture conditions.

This particular dissociation procedure was suitable for both a.l.d. and p.l.d. muscles dissected from embryos. It was not possible to isolate viable a.l.d. fibers from chicks older than several days primarily because of extensive amounts of connective tissue. The procedure worked well for p.l.d. muscles up to two weeks after hatching. After that age, enzymatic digestion of the extracellular material was fairly complete but the fibers were too long to

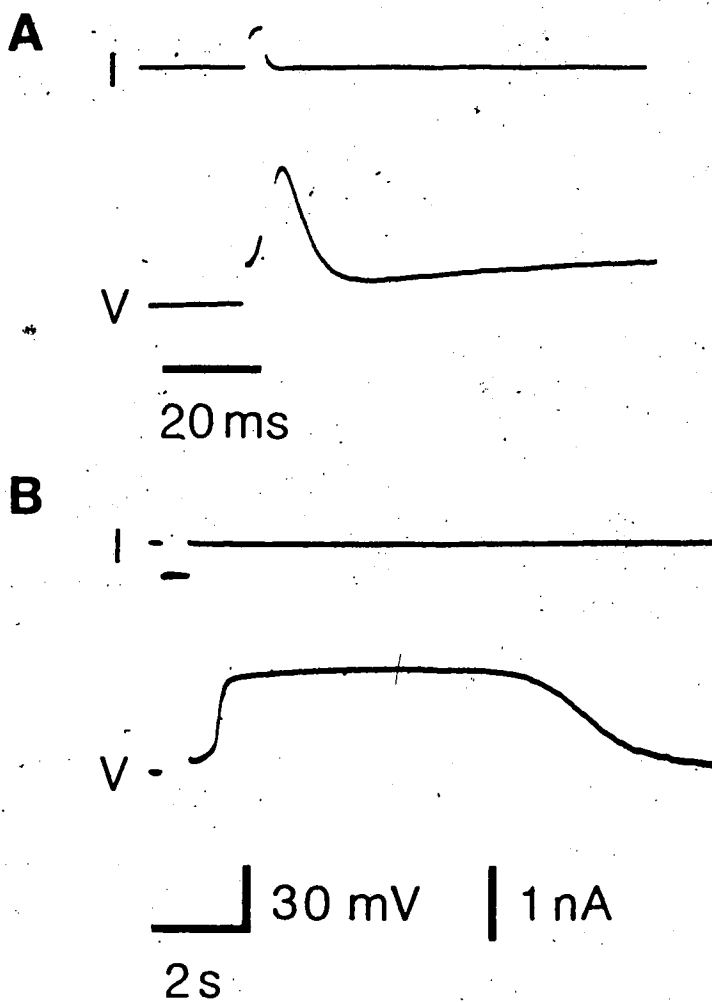


Figure 2. Action potentials elicited by current injection from a 21 day p.l.d. fiber. Resting potentials were -58 (A) and -65 mV (B). Potential at the top of the plateau (B) was -18 mV. Fibers were bathed in normal external solution.

successfully extricate from the network of blood vessels.

To assess the condition of the isolated fibers, values for resting membrane potential (V_m), input resistance (R_{in}) and membrane time constant (τ_m) were obtained and compared to values obtained from fibers in intact muscles. Action potentials were not used as a basis of comparison because of the variability amongst fibers (cf Kano, 1975). Comparison of the values from isolated and 'intact' fibers (Table 1) showed that the dissociation procedure did not have a significant effect on these properties.

Chloride conductance during development

Resting membrane conductance to Cl^- (G_{Cl}) was estimated by measuring R_{in} and τ_m values of single fibers in normal external solution and in a solution in which Cl^- was replaced by an impermeant ion (methylsulphate) (Table 2). No significant differences between the two solutions were found for either p.l.d. or a.l.d. muscles at 14 days or for a.l.d. at 21 days ($P > 0.2$), indicating little or no participation of Cl^- in the resting membrane conductance. For 21 day p.l.d., R_{in} and τ_m were much higher in the Cl^- -free solution, indicating a substantial resting conductance to Cl^- . The contribution of G_{Cl} to the total resting membrane conductance (G_m) was estimated assuming that membrane capacitance (C_m) remained unchanged. Since τ_m is proportional to the inverse of G_m and since G_m is the sum of the conductances to Cl^- and the remaining ions

Table 1. Electrical properties of intact and isolated a.l.d. and p.l.d. fibers. Recordings were made from fibers in intact muscles and from isolated fibers. Muscles were from 21 day embryos. A single micro-electrode was used to simultaneously inject current pulses and record voltage responses. All recordings were made in normal external solution. The number in parenthesis gives the number of fibers.

* $0.1 > P > 0.05$; all other $P > 0.2$

<u>Muscle</u>	<u>Condition</u>	<u>V_m (mV)</u>	<u>R_{in} (MΩ)</u>	<u>τ_m (msec)</u>
p.l.d.	Intact (23)	-64.2 ± 6.8	19.7 ± 6.3	18.3 ± 6.7
	Isolated (36)	$-59.5 \pm 7.2^*$	20.2 ± 9.2	$15.7 \pm 5.5^*$
a.l.d.	Intact (37)	-62.7 ± 6.5	14.7 ± 4.2	30.9 ± 11.0
	Isolated (24)	-61.8 ± 5.9	15.5 ± 5.5	33.7 ± 20.6

Table 2. Resting chloride conductance of 14 and 21 day a.l.d. and p.l.d. fibers. Recordings were made from isolated fibers with one electrode to inject current and another electrode inserted nearby to record voltage responses. Fibers were equilibrated for 30 min to 1 hr in a solution with 98% of Cl^- replaced with CH_3SO_4^- . Fibers were then returned to normal solution and examined. The number in parenthesis is the number of fibers examined.

<u>Muscle</u>	<u>Age (Days)</u>	<u>Solution</u>	<u>R_{in} ($M\Omega$)</u>	<u>τ_m (msec)</u>
p.l.d.	14	Normal (20)	44.2 \pm 22.0	30.2 \pm 13.2
	14	Cl^- free (22)	40.2 \pm 18.4	28.9 \pm 12.1
	21	Normal (31)	18.3 \pm 10.4	15.4 \pm 5.9
	21	Cl^- free (25)	41.5 \pm 11.6	53.9 \pm 7.8
a.l.d.	14	Normal (20)	25.9 \pm 9.2	33.7 \pm 15.2
	14	Cl^- free (21)	22.2 \pm 7.4	28.9 \pm 11.9
	21	Normal (25)	15.0 \pm 4.7	36.0 \pm 13.0
	21	Cl^- free (24)	15.5 \pm 4.8	38.4 \pm 8.4

($G_m = G_{Cl} + G_{ions}$) (Eisenberg & Gage, 1969), it was calculated that G_{Cl} constituted about 70% of the total resting membrane conductance in 21 day p.l.d. fibers. Thus, it was not until the last week of embryonic life that this type-specific property was expressed p.l.d. fibers.

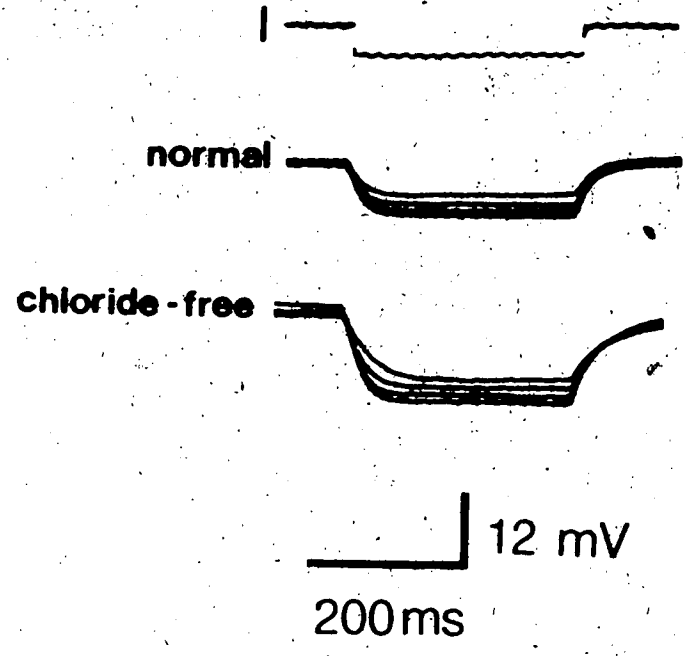
Myotubes were grown in tissue culture (see Methods, Chapter III) from myocytes obtained from 15 day a.l.d. or p.l.d. muscles. Resting G_{Cl} was determined in cultures 5-10 days old. Figure 3 shows the results from a myotube where R_{in} increased from 56 to 80 $M\Omega$ when the solution was changed to Cl^- -free. This was the largest increase observed. In general, R_{in} values only increased 5-20% when the solution was changed to Cl^- -free. For p.l.d. cultures, R_{in} values were $75 \pm 45 M\Omega$ in normal and $90 \pm 49 M\Omega$ ($\bar{x} \pm S.D.$; $n = 11$) in Cl^- -free solution. For a.l.d. cultures, R_{in} values were $60 \pm 25 M\Omega$ in normal and $66 \pm 22 M\Omega$ ($\bar{x} \pm S.D.$; $n = 11$) in Cl^- -free solutions. R_{in} values showed considerable variability and were not significantly different between normal and Cl^- -free solutions for either culture ($P > 0.2$). Thus, fiber type differentiation with respect to this property did not occur in culture.

Passive cable properties during development

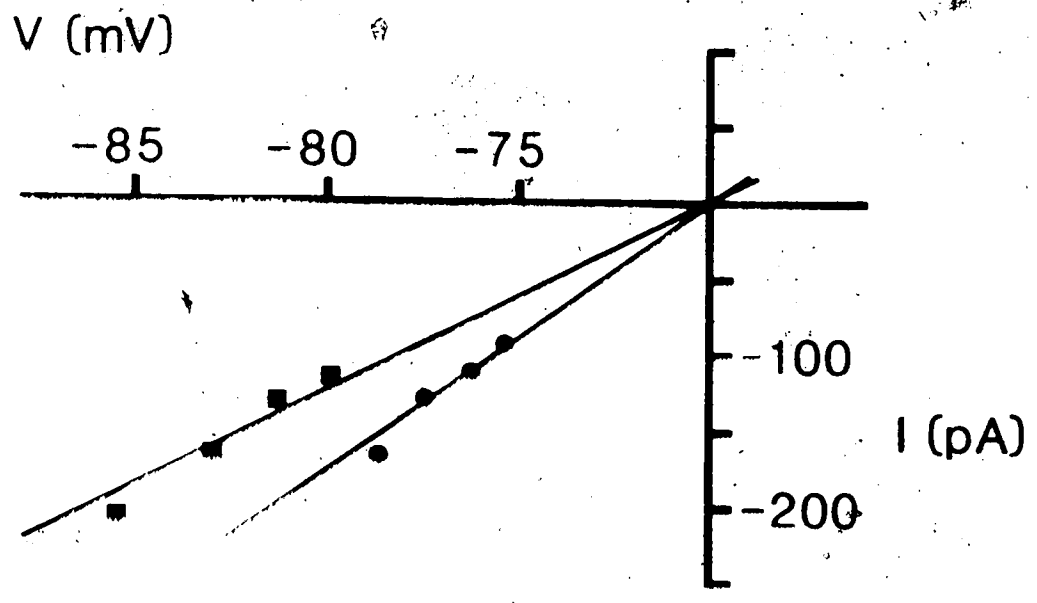
Values for cable properties were obtained by analysing voltage responses to injected current pulses. Voltage was recorded at two separate sites (Figure 4) and only occasionally could two stable impalements be made simultaneously.

Figure 3. Resting chloride conductance of cultured p.l.d. muscle. Myocytes were obtained from 15 day p.l.d. muscles and grown in tissue culture for 5 days. A single micro-electrode was used to inject rectangular current pulses and to record voltage responses (A). Responses were first recorded in normal (149 mM Cl^-) and then in Cl^- -free (3 mM Cl^-) solution while continuously recording from the same myotube. Cl^- was replaced with an impermeant ion, methylsulphate. Current-voltage plots of the data (B) gave an input resistance of 56 $\text{M}\Omega$ in normal solution (circles) and of 80 $\text{M}\Omega$ in Cl^- free solution (squares).

A



B



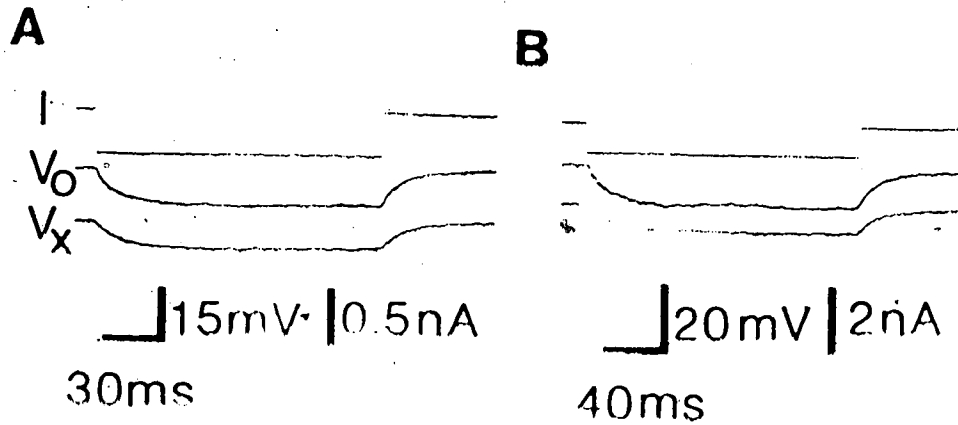


Figure 4. Passive electrical responses of isolated a.l.d. and p.l.d. fibers. Voltage responses were recorded from 21 day p.l.d. (A) and a.l.d. (B) in normal external solution. I is applied current pulse injected in the middle of the fiber length. V_0 is the voltage response recorded by the current injection electrode. V_x is the voltage response recorded by a second electrode 460 μm (A) and 620 μm (B) from the current injection electrode.

The measured and calculated values are presented in Table 3. At the earliest stage studied, 14 days' incubation, the time and length constants for a.l.d. and p.l.d. fibers were long and the means for the two muscles differed only slightly ($P < 0.2$). R_m values were fairly high ($20 \text{ k}\Omega\text{cm}^2$) and the means for the two muscles were not different ($P > 0.1$). C_m values ($1-2 \text{ }\mu\text{F}/\text{cm}^2$) were in line with what would be expected for small diameter fibers (Hodgkin & Nakajima, 1972). As development of p.l.d. proceeded, the values of R_m , τ_m and λ decreased, so that by the time of hatching, differences between a.l.d. and p.l.d. were apparent ($P < 0.001$). For a.l.d. fibers, R_m did not differ at the two ages studied ($P > 0.1$). For p.l.d., R_m decreased further after hatching. A.l.d. fibers were not followed after hatching because the fibers could not be isolated. The values of V_m reported here closely agree with the data of Bennett and Pettigrew (1974) and Kano (1975).

DISCUSSION

Before the mechanisms governing differentiation of muscle fibers into various fiber types can be understood, it is important to know when type-specific properties are expressed during development. Knowledge of the timetable of developmental changes may help to elucidate causal relationships. In the present study of developing fast-twitch (p.l.d.) and slow-twitch (a.l.d.) muscles of the chick, a resting membrane potential was absent in the

Table 3. Electrical constants of a.i.d. and p.a.d. fibers during development. Recordings were made from single fibers the day they were isolated. Rectangular current pulses were injected into the middle of the fiber and the voltage response recorded for the determination of R_i and τ_m . A voltage-sensing electrode was inserted 400-600 μ m away for the determination of λ . Fiber diameters were measured optically, and electrical constants calculated see methods). The number of parenthesis is the number of fibers examined.

Species	Age	λ (μ m)	λ (Ω)	τ_m (μ sec)	mm	λ (Ω/cm)	R_i ($M\Omega/cm$)	λ (μ m)	τ_m (μ F/cm ²)	R_i (Ω/cm)
a.i.d.	1 day	10.8	11.9	5.3	0.2	33	1.2	2.9	1.2	169
			10.7	5.3	0.2	34	4.3	49		
	10 days	11.4	13.8	3.1	0.3	45	2.0	3.3	2.0	103
			17.0	5.8	0.3	56	2.3	55		
			17.1	3.8	0.2	64	1.4	26		
p.a.d.	1 day	11.0	11.7	3.3	0.2	42	1.3	1.3	1.8	45
			11.7	3.3	0.2	48	0.8	45		
	10 days	11.0	11.7	3.3	0.2	48	0.8	1.2	2.5	144
			12.0	3.3	0.2	56	0.3	69		
			13.0	3.3	0.2	97	3.6	30		
12 days	11.0	11.7	3.3	0.2	104	2.5	20.2	1.9	30	
		12.0	3.3	0.2	104	5.7	45			

presumptive fast-twitch muscle at an early stage of development (Table 2). By the time of hatching, the percentage of the total membrane conductance due to Cl^- had reached adult levels. Expression of this property, which is characteristic of adult p.l.d. fibers (Lebeda & Albuquerque, 1975; Huerta & Stefani, 1981), followed the formation of functional end-plates (Gordon, Perry, Tuffery & Vrbová, 1974; Atsumi, 1977). In contrast, G_{Cl} in developing a.l.d. muscles was negligible at both ages studied (Table 2). These results fit well with those of Huerta and Stefani (1981). They found that at three weeks of age, about 70% of the resting conductance of p.l.d. fibers was due to Cl^- , while a.l.d. fibers did not have a measurable G_{Cl} . An increase in the magnitude of G_{Cl} during post-natal development of mammalian fast muscle, but no change for a slow muscle, has been reported by Farbach, Brown and Barchi (1978).

These results raise the possibility that innervation is required for full expression and/or maintenance of G_{Cl} . The contribution of G_{Cl} to the total resting membrane conductance was found to be low (5-20%) for chick muscle cells grown in tissue culture. This appears to be a general finding as G_{Cl} has been found to be low in aneural cultures of rat (Ditchie & Fambrough, 1975), of rat cell line (Kidera, 1976) and of human (Merickel, Gray, Chauvin & Appel, 1981) skeletal muscle. Also, the slight increase in membrane resistance following denervation (Albuquerque & Inseloff, 1968; Westgaard, 1975) has been attributed to a

decrease in G_{Cl} (Camerino & Bryant, 1976). It would be useful to understand the factors controlling expression of G_{Cl} as its magnitude is abnormally low in myotonic muscle (Bryant & Morales-Aguilera, 1971) and in dystrophic mouse muscle (Farnbach *et al.*, 1978).

The lack of clear differences in resting G_{Cl} between muscle cell cultures derived from a.l.d. or p.l.d. muscles suggests that fiber type differentiation does not occur in culture. This conclusion has also been reached from studies of metabolic enzymes, which show type-specific levels of activity, in chick and rat cultures (Askanas, Hee & Milhorat, 1972; Askanas, Shafiq & Milhorat, 1972; Askanas & Hee, 1973). However, slight differences in favor of expression of fiber type in culture have been obtained (Nougués & Bacou, 1977; Bacou & Nougués, 1980). In general though, it appears that the instructional signal(s) directing fiber type differentiation is(are) lacking in the tissue culture environment.

The absolute values obtained for the cable properties of developing slow-tonic (a.l.d.) and fast-twitch (p.l.d.) fibers (Table 3) were higher than previously reported for fibers in intact muscle (Gordon *et al.*, 1977). Since the input resistances and the resting membrane potentials were also much higher, the higher values probably reflect more stable impalements. Also, the method used to estimate the cable properties was more direct than that used by Gordon *et al.* (1977). They calculated the membrane time constant from fiber input

resistances and a mean value of fiber diameter obtained from histological sections.

One week prior to hatching, future slow-tonic and fast-twitch fibers had relatively high membrane resistances, long time and length constants (Table 3) and no detectable resting Cl^- conductance (Table 2). Thus, the properties of the embryonic fibers of both muscles resembled more closely the properties of adult slow-tonic rather than adult fast-twitch (Fedde, 1969; Gordon *et al.*, 1981). By the time of hatching (21 days), R_m , τ_m and λ of p.l.d. fibers, had decreased so that the cable properties of the a.l.d. and p.l.d. fibers were clearly distinguishable. In both fiber types, R_m would be expected to decrease and C_m to increase as the fibers grow in diameter simply because the ratio of transverse tubular to surface membrane is increasing (*cf* Hodgkin & Nakajima, 1972). For the developing p.l.d. fibers, however, the decreases in the electrical constants were mostly attributable to the appearance of a substantial resting conductance to Cl^- during the last week of embryonic development.

III. VOLTAGE- AND TIME-DEPENDENT CHLORIDE CURRENTS IN EMBRYONIC CHICK SKELETAL MUSCLE

A. INTRODUCTION

Membrane chloride conductances have been found in a wide variety of cell types and in a variety of species, ranging from *E. coli* and algae to higher organisms. Utilizing current clamp techniques, Cl^- -dependent action potentials have been observed in certain plant cells (Gaffey Mullins, 1958; Mullins, 1962), in electroplax membranes of some fishes (Bennett, 1961; Hille, Bennett & Grundfest, 1965) and in frog eggs (Ito, 1972). With voltage clamp techniques, Cl^- currents responsible for repolarizing a Na^+ -based action potential have been described in frog eggs (Schlichter, 1983). In *Aplysia* neurones, Cl^- currents activated by hyperpolarization have been observed (Chenoy-Marchais, 1982). Voltage- and time-dependent Cl^- currents have also been described in frog (Hutter & Warner, 1972; Warner, 1972) and in *Xenopus* (Vaughan *et al.*, 1980; Loo *et al.*, 1981) skeletal muscle. With single channel recording techniques, Blatz and Magleby (1983) described a voltage-dependent Cl^- channel with a single channel conductance of 430 pS in cultured rat muscle. The properties of some Cl^- selective channels have been studied by incorporating the channels into planar phospholipid bilayers. Cl^- channels with single channel conductances of 16 and 55 pS have been found in electroplax membranes of *Torpedo* (marine

ray) (White & Miller, 1979, 1981; Hanke & Miller, 1983) and in heart sarcolemma of calves (Coronado & Latorre, 1982), respectively. A voltage-dependent anion-selective channel (VDAC) from mitochondrial outer membrane with a single channel conductance of about 500 pS has been described (Schein, Colombini & Finkelstein, 1976; Colombini, 1979; Doring & Colombini, 1984). Further, ion tracer techniques have been utilized to study a Cl^- transport system in peripheral blood lymphocytes activated by increases in cell volume (Sarkadi, Mach & Rothstein, 1984) and to study a Cl^- permeability system in red blood cells which is mediated by band 3 protein (Cabantchik, Knauf & Rothstein, 1978).

Voltage-dependent anion conductance systems have not been as extensively studied as cation conductance systems. In this chapter, I describe the properties of a time-variant, voltage-dependent Cl^- conductance found in embryonic chick skeletal muscle. The conductance underlies a long duration action potential (Fukuda, 1974; Fukuda *et al.*, 1976a). The action potential can be elicited from the muscle fibers during the last week of embryonic development (Kano, 1975).

Preliminary voltage clamp studies have been done using tissue cultured muscle (Fukuda, 1975; Fukuda *et al.*, 1976b). In the present study, the surface membrane of small diameter myoballs was voltage-clamped with a single suction pipette (Hamill *et al.*, 1981). The data showed that the Cl^- currents activated slowly in response to depolarizing voltage steps

and did not inactivate during maintained depolarization. Upon repolarization to negative holding potentials, the currents recovered extremely slowly from activation. Cl^- currents were blocked by stilbene derivatives which are known to block other Cl^- conductances (Knauf & Rothstein, 1971; Vaughan & Fong, 1978). The Cl^- currents were also found in muscle cells that had developed *in vivo*, showing that this Cl^- conductance is indeed expressed during the course of normal development.

B. METHODS

Preparation of myoballs

Small diameter (10-20 μm) myoballs (spherical muscle cells) were grown in tissue culture. Under sterile conditions, pectoral muscles were removed from 11 day white Leghorn chick embryos and placed in Earle's balanced salt solution (BSS). The muscle was minced into small fragments (1 mm) and then triturated with a fire-polished Pasteur pipette to release single cells. The solution was left to stand for 5-10 minutes to allow debris to settle. The top layer was removed and filtered through lens paper. The cells were gently centrifuged in a clinical centrifuge and resuspended in BSS. This was repeated three times, and after the last centrifugation the cells were resuspended in complete media. Complete media consisted of: Eagle's minimum essential media (MEM), 10% horse serum (Flow Labs,

Inglewood, CA), 5% chick embryo extract (see Methods, Chapter II), penicillin (100 U/ml) and gentamycin (200 μ g/ml). Cell density was determined with a hemocytometer. Cells were plated at 0.8×10^6 cells/ml in 35 mm Corning tissue culture dishes. Plates were placed in a water-saturated 95% O₂/5% CO₂ atmosphere and maintained at 37°C. On day two of culture, the media was changed to one containing 10^{-8} M colchicine (Sigma, Type II, St. Louis, MO). Colchicine encouraged the muscle cells to form spherical myoballs (Plate 2), but did not appear to have any detrimental effects on membrane or cellular properties (Fukuda *et al.*, 1976a). Media was changed every three days.

Myoballs were also obtained from muscle fibers that had developed *in vivo*. Isolated fibers were dissociated from intercostal muscles of 14-21 day embryos according to the procedure outlined in Chapter II (Methods). These muscles were used because the fibers are only several millimeters in length. Isolated fibers often broke into small lengths with more rigorous trituration. Fragmented fibers often sealed and after several hours of incubation spontaneously formed myoballs of various diameters (20-70 μ m).

Experimental set-up

Membrane currents were recorded under voltage clamp with the whole-cell recording technique of Hamill *et al.* (1981). Briefly, suction was applied to a wide-tipped micropipette to establish a tight seal, in the giga-ohm range,

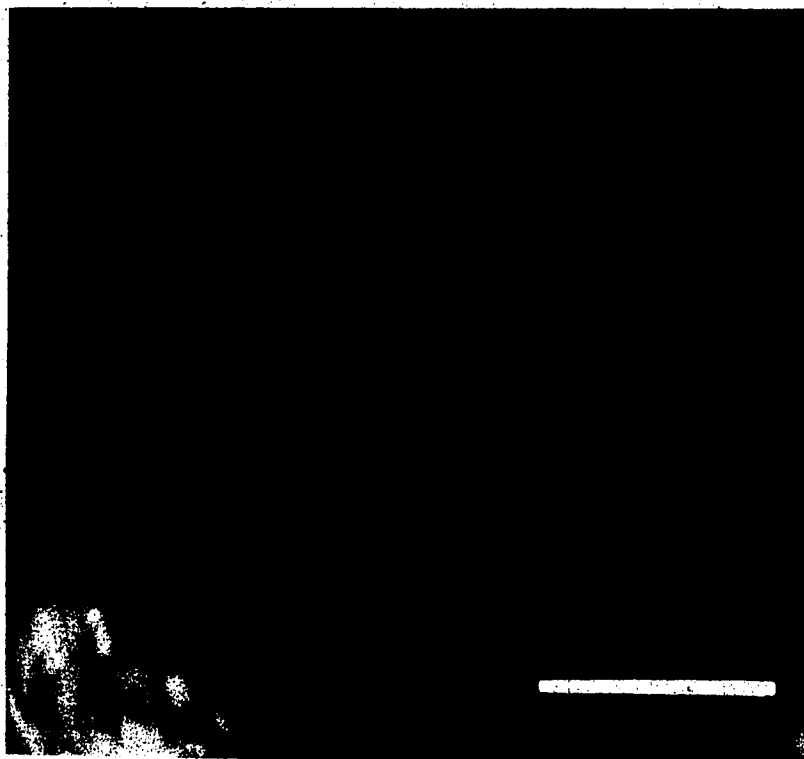
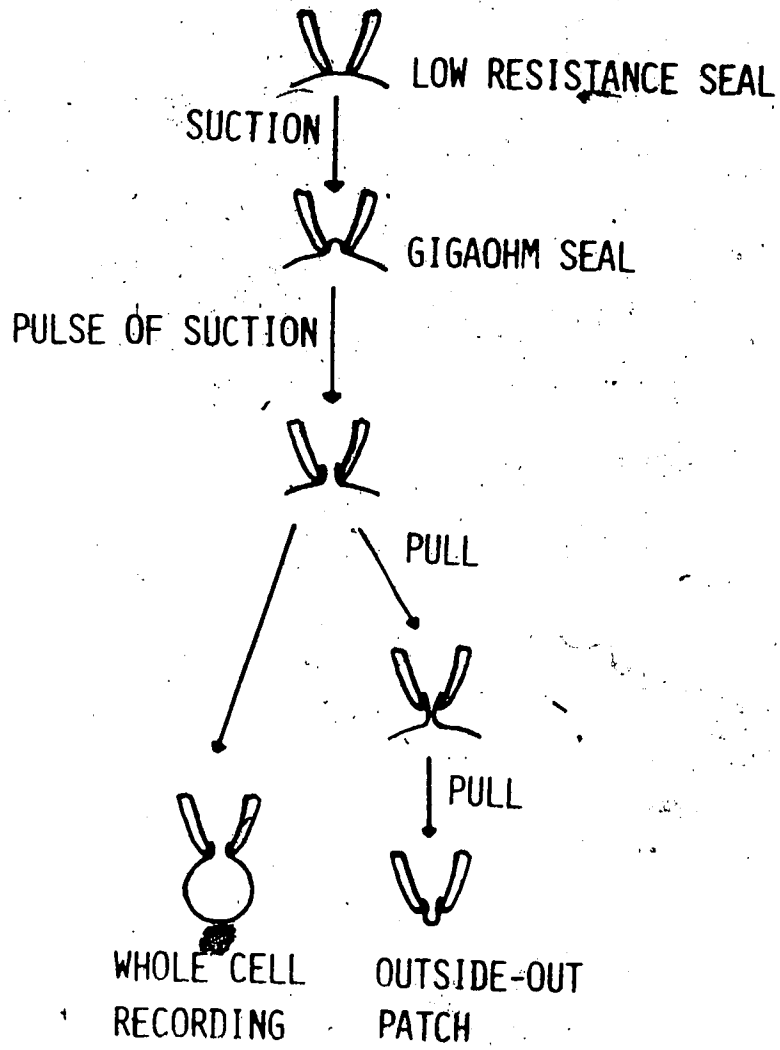


Plate 2. Light microscope photograph of a myoball grown in the presence of 10^{-8} M colchicine. Myocytes were obtained from pectoral muscles of 11 day chick embryos. Calibration bar represents 20 μm .

between pipette tip and cell membrane. The membrane patch spanning the pipette tip was disrupted by additional suction so that the suction pipette became an intracellular electrode (Figure 5). This procedure provided a low resistance pathway to the intracellular space.

Fabrication of suction pipettes: Suction pipettes were pulled according to the methods of Hamill *et al.* (1981) from microstar capillary tubing with an O.D. of 1 mm (Radnoti Glass Technology, Inc., Monrovia, CA). Pipettes were pulled in two stages on a vertical Narishige micro-electrode puller fitted with a four-turn coil of nichrome wire (1 mm diameter). In the first pre-pull, the capillary tubing was thinned over a 8-10 mm length to a minimum diameter of about 200 μm . The tubing was then recentered with respect to the heating coil and in the second pull, the thinned part broke to produce two pipettes. This two stage pull produced pipettes with short shanks and tips with steep tapers. No magnetic pull was employed. The heat setting was critical (11-11.5 A) as slight variation produced large variations in pipette resistance. In later experiments, pipettes were heat polished. This was observed at a magnification of 200x with an inverting microscope. Tips were brought to within 20-30 μm of a 25 μm Pt wire heated to a dull red glow. Pipette tips were polished when the sides were seen to collapse slightly. Pipettes were backfilled with solution using a fine gauge hypodermic needle. Pipettes with resistances of 1-5 M Ω were used. They were only used

Figure 5. Schematic of recording configurations with a suction pipette. The uppermost frame represents a suction pipette in simple mechanical contact with a cell membrane. Upon slight suction, the seal between the membrane and the pipette increases in resistance into the giga-ohm range. Further suction disrupts the patch of membrane spanning the pipette tip. Membrane currents can be recorded under voltage clamp from whole cells after disruption of the membrane patch provided that cells of sufficiently small diameter are used. The pipette can also be withdrawn from the cell to form an outside-out patch of membrane (cytoplasmic side of membrane is facing pipette solution).



once since debris on the tips prevented formation of giga-ohm seals. Pipettes were mounted in a microelectrode holder with a suction port (EH-900R, W.P. Instruments, New Haven, CT). A two foot length of polyethylene (PE) tubing (I.D. 0.032") was connected to the suction port and a three-way teflon stopcock. A 1 ml gas tight syringe (Hamilton #1001, A-M Systems, Toledo, OH) and another length of PE tubing were also connected to the stopcock. The pipette holder was carefully backfilled with solution ensuring that no bubbles remained in the shank. The holder was then connected to a preamplifier (A-M Systems, Seattle, WA); the headstage of which was mounted on a micromanipulator (Leitz, Wetzlar). The micromanipulator and the inverting microscope were mounted on an anti-vibration table (Micro-g isolator, Technical Manufacturing Co., Woburn, MA).

Voltage clamp set-up: The voltage signal from the pipette was led to the input of an electrometer with an active bridge circuit. The membrane potential signal was compared to a command voltage using a differential amplifier. The 'error' signal was applied to the suction pipette via the current passing section of the electrometer. Rectangular pulses were generated by a WPI digitimer. Current was collected from the bath by a current-voltage converter. In some experiments, a converter with a feedback resistor of 1 G Ω and a bandwidth of about 4 kHz was used. In experiments where current levels were below 1 nA, a converter with a 10 G Ω feedback resistor and a bandwidth of

about 2 kHz was used (built by Dr. T. Iwazumi, University of Texas Medical Branch). The voltage clamp circuit was designed by Dr. D.C. Eaton (UTMB) (Eaton, 1972). With the system adjusted, membrane potential could be made to settle to the command voltage within 1 ms. Membrane potential and current signals were monitored by a digital oscilloscope (Nicolet, Madison, WI) and stored on magnetic diskettes. A block diagram of the potential recording and voltage clamp circuits is shown in Figure 6.

Single channel events were recorded under voltage clamp from outside-out membrane patches (Figure 5). The pipette holder was connected to the current-voltage converter (10 G Ω feedback resistor) and the reference electrode in the bath was connected to the input of the electrometer. Bath potential could then be clamped to various potentials.

Solutions

External and pipette solutions are listed in Table 4. The composition of the pipette solution mimicked intracellular ionic composition, i.e. low Ca²⁺ and high K⁺ concentrations. All solutions were made with distilled water and the pH was adjusted to 7.4. Chemicals were purchased from local suppliers if the supplier is not listed. Tetrodotoxin (TTX) and CdCl₂ were purchased from Sigma (St. Louis, MO). SITS (4-acetamino-4'-isothiocyano-2,2'-disulfonic acid stilbene) and DIDS (4,4'-diisothiocyano-2,2'-disulfonic acid stilbene) were purchased from Pierce Chemical Co.

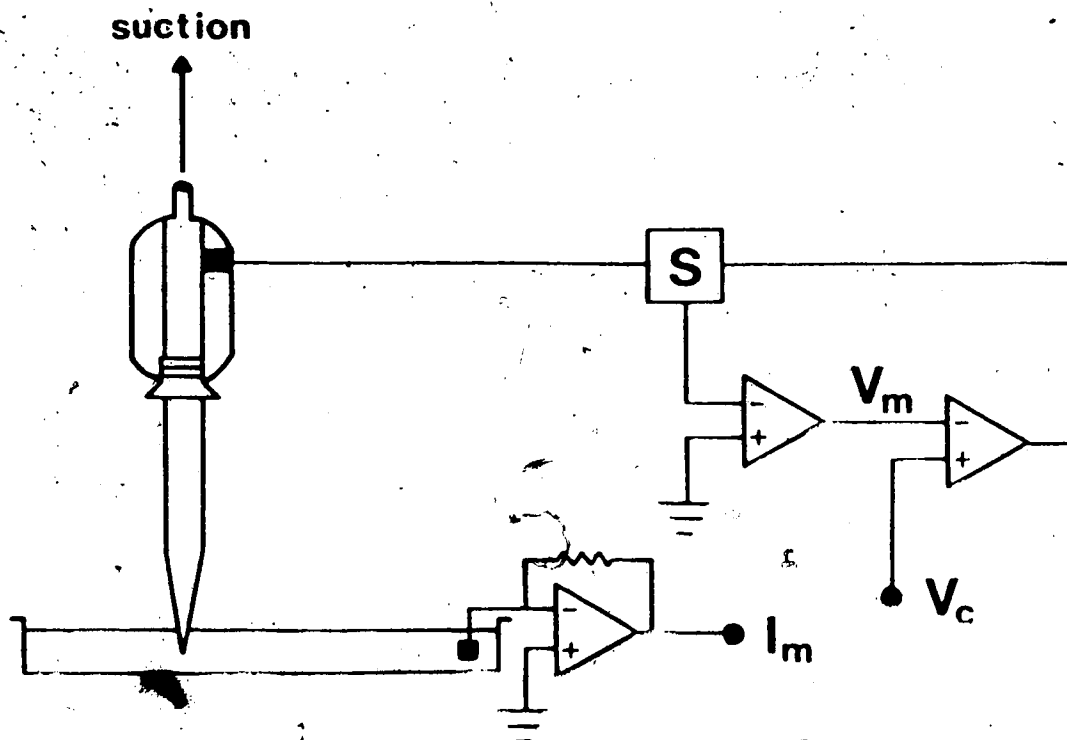


Figure 6. Experimental arrangement for voltage clamp recording. A single suction pipette is used to record voltage and pass current simultaneously. The rectangular box, denoted S, is the port on the electrometer which permits current injection. Macroscopic currents were collected from the bath by a current-voltage converter (I_m in pA). V_m is the membrane potential recorded by the electrometer (mV). V_c is the command voltage fed into the differential amplifier of the voltage clamp circuit (mV).

Table 4. External and pipette solutions for whole-cell recording. Various concentrations of external Cl^- were made by mixing the appropriate proportions of normal and Cl^- free solutions. All values are in mM.

<u>EXTERNAL</u>	<u>NaCl</u>	<u>NaCH₃SO₄</u>	<u>CaCl₂</u>	<u>MgCl₂</u>	<u>Dextrose</u>	<u>HEPES</u>
	Normal	144	---	1.8	0.8	18
Cl^- free	---	144	2.2	0.8	18	5

<u>PIPETTE</u>	<u>NaCl</u>	<u>NaCH₃SO₄</u>	<u>KCl</u>	<u>KCH₃SO₄</u>	<u>CsCl</u>	<u>TEA-Cl</u>	<u>HEPES</u>	<u>EGTA (Na salt)</u>
	Normal	10	---	50	95	---	---	5
K free	---	---	---	---	135	20	5	2
60 Cl	---	95	---	---	---	60	5	2

(Rockford, IL) and stored at -20° C. SITS and DIDS were made up as aqueous stock solutions and kept frozen in small aliquots until use. For Cl^{-} substitution experiments, NaCl or KCl were replaced by equal molar concentrations of methylsulphate ($\text{CH}_3\text{SO}_4^{-}$) (Pfaltz & Bauer, Inc., Stamford, CT) (Hutter & Noble, 1960). $\text{CH}_3\text{SO}_4^{-}$ has been reported to reduce ionized Ca^{2+} concentrations by about 20% as measured with Ca^{2+} -sensitive microelectrodes (Kenyon & Gibbons, 1977). Therefore, the Ca^{2+} concentration was increased in $\text{CH}_3\text{SO}_4^{-}$ solutions to keep the final concentration of ionized Ca^{2+} around 1.8 mM. Pipette solutions were filtered with a membrane filter (0.2 μm).

Prior to experiments, tissue culture dishes were rinsed several times with recording solution. Solution was aspirated with a Pasteur pipette to remove debris from the surface. Dishes were placed on the stage of an inverting microscope fitted with phase contrast optics (Olympus, Carsen, Don Mills, Ont.). In some experiments, the bath solution was changed by gravity-feed from an elevated reservoir. The volume of solution in the culture dish was reduced to less than 1 ml by inserting two Plexiglas wedges sealed to the dish with Vaseline. Complete exchange of solution could be accomplished in less than 1 minute.

Liquid junction potentials

Liquid junction potentials were measured for the suction pipettes. These potentials exist at the tip of

conventional microelectrodes and are brought about by the separation of ions with different mobilities at the interface of the pipette and bath solutions. Pipettes were immersed in the same solution as they were filled with and the potential was set to zero. Bath solution was changed to various recording solutions. No change in potential was observed for any combination of recording solutions. During this procedure, a salt bridge was employed in the bath to minimize changes in reference electrode potential.

Under all recording conditions, currents and potentials across the membrane were described with the usual convention. The external side of the membrane was taken as reference. Currents flowing from the internal to the external side were positive and displayed upwards.

All experiments were done at room temperature.

C. RESULTS

Whole-cell patch clamp technique

The whole-cell recording configuration of the single suction pipette voltage clamp (Hamill *et al.*, 1981) was utilized to control the membrane potential of myoballs. In order to achieve adequate voltage clamp of the surface membrane potential, several conditions had to be met: 1) the seal resistance between the pipette and the cell membrane had to be high; 2) the resistance in series with the cell membrane had to be low enough to be ignored or compensated

for and 3) the intracellular space had to be isopotential. An equivalent circuit for pipette and cell membrane is shown in Figure 7.

Establishment of giga-ohm seal: Slight positive pressure was applied to a suction pipette via a syringe and the pipette was lowered into the bath solution. The positive pressure forced solution out of the pipette and served to keep debris off the tip. For voltage clamp experiments, the clamp circuit was activated and the potential was adjusted to give zero current. This is termed zero current potential and was taken as reference potential for later measurements. A small rectangular voltage pulse was applied to the pipette and the resistance monitored continuously. Under a magnification of 200x, the tip was gently pressed against a myoball membrane and the positive pressure was relieved. Occasionally, a giga-ohm seal formed at this time as judged by a large increase in pipette input resistance to the giga-ohm range (Figure 8A). Most of the time though, negative pressure had to be applied to the pipette interior by mouth to cause a giga-ohm seal to form. The development of seals occurred abruptly within seconds of application of negative pressure. After the input resistance of the pipette increased, the voltage step was increased so that the resistance of the pipette-membrane seal could be measured. Seals in the range of 1-10 G Ω were obtained routinely with pipettes that were not heat polished. Heat polished pipettes gave seal resistances of over 10 G Ω .

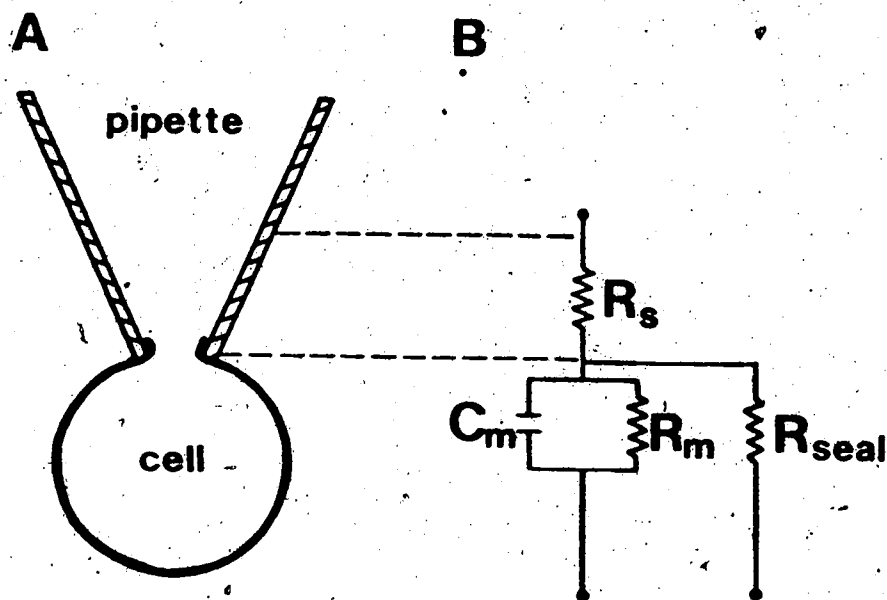
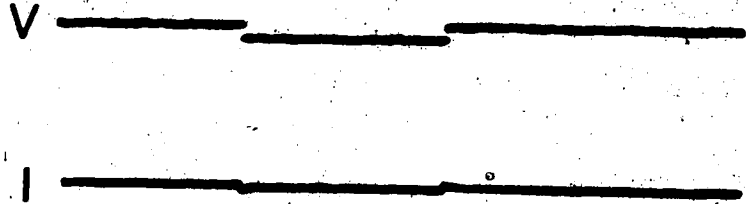


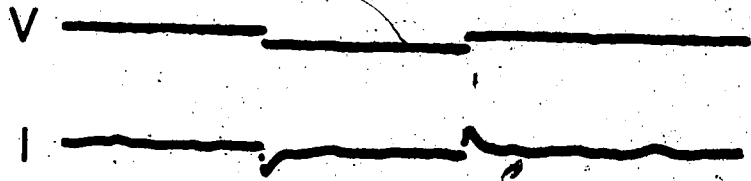
Figure 7. Equivalent circuit for pipette and cell membrane. A diagram of a cell attached to a suction pipette in the whole-cell recording configuration is shown in A and the equivalent circuit is shown in B. R_s is the resistance in series with the cell membrane ($M\Omega$). R_{seal} is the shunt resistance of the cell membrane-pipette seal ($G\Omega$). C_m and R_m are the capacitance ($\mu F/cm^2$) and the resistance ($k\Omega cm^2$) of the cell membrane, respectively.

Figure 8. Currents recorded at different stages of whole cell recording. Establishment of a giga-ohm seal was observed as a large increase in the input resistance of the pipette to the giga-ohm range (A). Response to a 12 mV hyperpolarizing voltage step indicated a seal resistance of about 3 G Ω . After applying further suction, rupture of the membrane patch spanning the pipette tip was indicated as a slight decrease in input resistance and an increase in capacitative current (B). The capacitative current increased because the capacitance of the cell now had to be charged. Input resistance of the myoball was 1.97 G Ω . The myoball had a diameter of 16 μ m which gave a surface area of 804 μ m² assuming a spherical shape. Multiplying the input resistance by the surface area gave a unit membrane resistance of 15.8 k Ω cm². The background noise was larger for the whole-cell recording configuration (B) than before rupture of the membrane patch (A) because of the additional capacitance (Cf Fenwick, Marty & Neher, 1982). Input resistance of the pipette was 5 M Ω before touching the myoball.

A



B

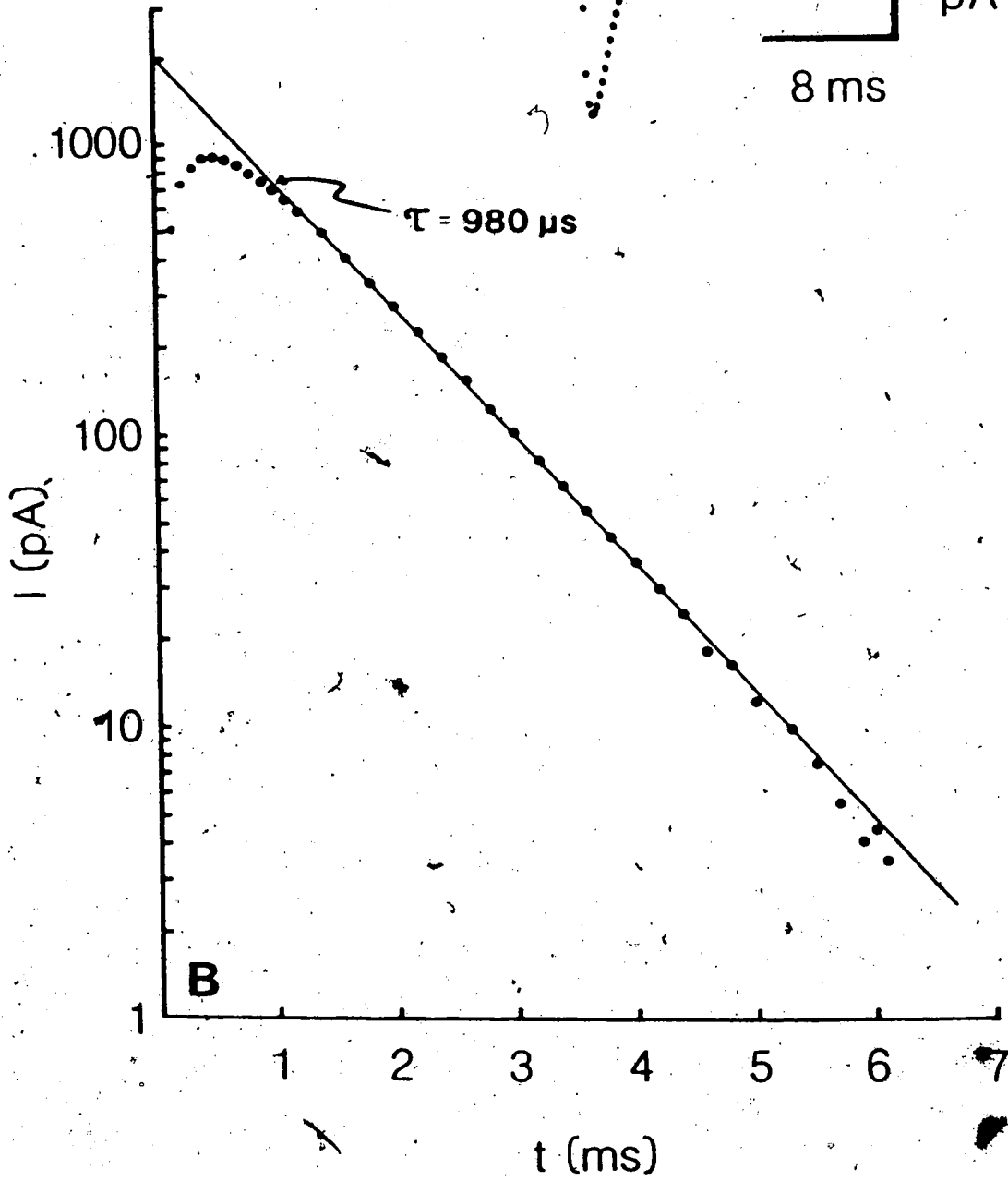
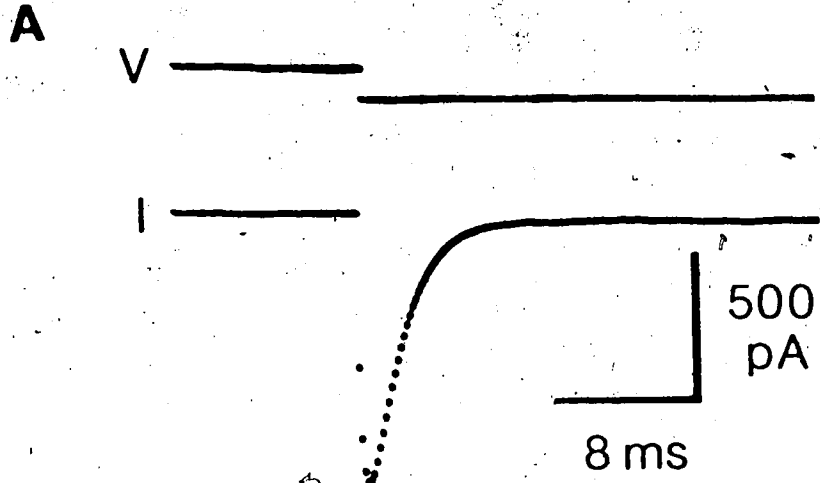


┌ 40 mV
└ 15ms

┆ 60 pA

Measurement of series resistance: To disrupt the membrane patch spanning the pipette tip, brief pulses of negative pressure were applied by mouth. Small voltage jumps showed that the disruption of the initial patch was accompanied by an increase in the input capacitance as the cell membrane now had to be charged, (Figure 8B). Cell capacitance, C , could be simply derived from the total amount of charge displaced, ΔQ , during a step command of amplitude, ΔV , according to $C = \Delta Q / \Delta V$, after subtraction of pipette capacitance. Pipette and holder capacitance were determined before disruption of the membrane patch and typically ranged from 3-10 pF. For the data shown in Figure 9, cell capacitance was calculated to be 56 pF. For 8 myoballs, the value was 58 ± 28 pF ($\bar{x} \pm$ S.D.). Assuming a spherical shape, a unit capacitance of $7 \mu\text{F}/\text{cm}^2$ was obtained for the myoball in Figure 9. For 8 myoballs, the value was $6.4 \pm 3.0 \mu\text{F}/\text{cm}^2$ ($\bar{x} \pm$ S.D.). Unit capacitance of cultured chick myotubes has been estimated at $3.9 \mu\text{F}/\text{cm}^2$ (Fischbach, Nameroff & Nelson, 1971). The unit capacitance of a cell membrane is about $1 \mu\text{F}/\text{cm}^2$ (Hodgkin, Huxley & Katz, 1952). Thus, for cultured chick muscle, there appears to be a small contribution from transverse tubular membranes or from infoldings in the surface membrane. The input resistance of the myoball (Figure 9) was measured from the steady-state current level during the voltage response and was $1.56 \text{ G}\Omega$. This gave a membrane resistance of $12.5 \text{ k}\Omega\text{cm}^2$. For 12 myoballs, membrane resistance was calculated to be

Figure 9. Capacitative current under voltage clamp. Current response to a hyperpolarizing voltage step of 44.6 mV is shown in the inset (A). Semilogarithmic plot of current as a function of time gave a single exponential fit with a time constant of 980 μ s (B). From the integral of the capacitative current recorded before the membrane patch was broken (data not shown), the capacitance of the pipette and pipette holder was determined to be 4 pF. From the integral of the capacitative current shown in A, a total capacitance of 60 pF was obtained. Subtracting pipette capacitance from this value, a cell capacitance of 56 pF was obtained. The time constant of the declining phase of the capacitative current together with the value for cell capacitance gave a value of 17 M Ω for the series resistance. The input resistance of the pipette before touching the cell was 5 M Ω . The DC current response (A) was 28 pA giving a value of 1.6 G Ω for the input resistance of the myoball. Diameter of the myoball was 16 μ m. Unit capacitance was calculated to be 7 μ F/cm². Membrane resistance was 12.5 k Ω cm².



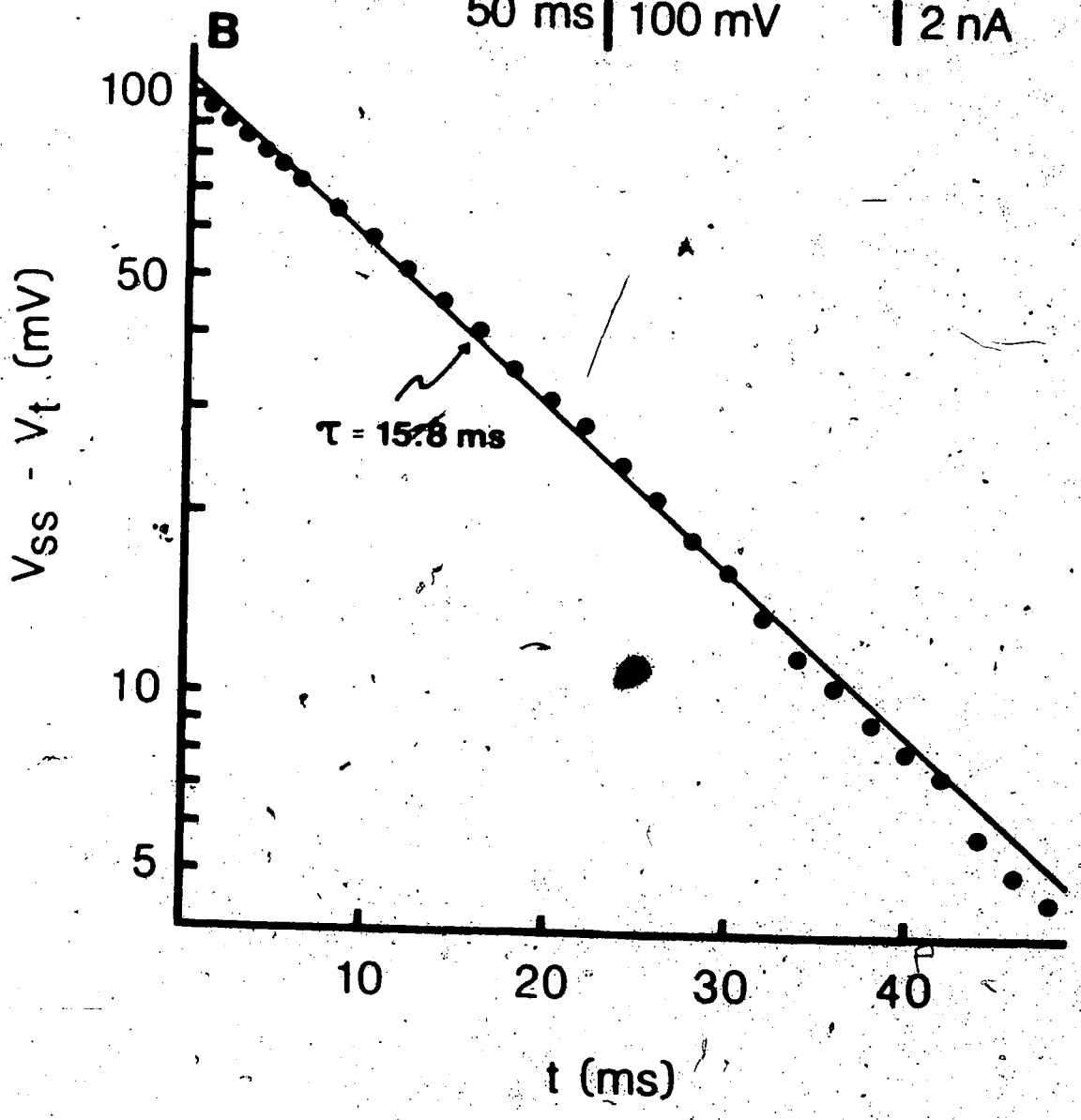
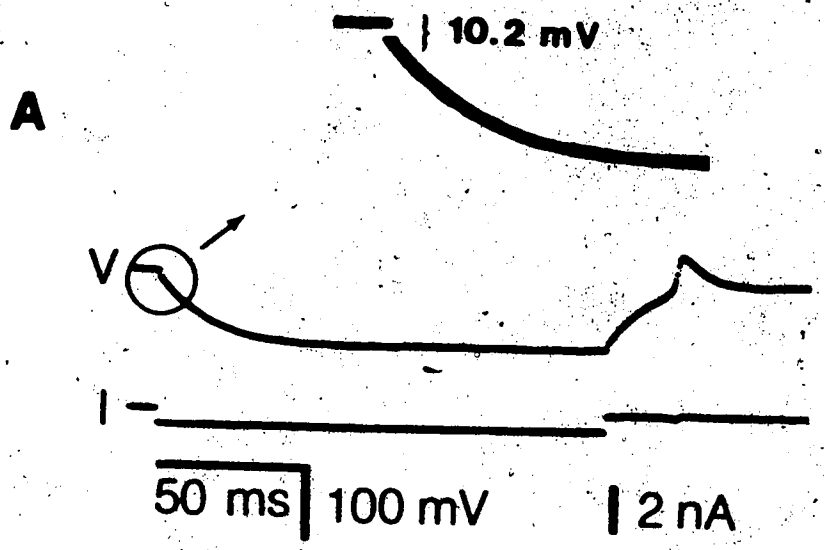
$9.9 \pm 4.3 \text{ k}\Omega\text{cm}^2$ while the input resistance was $1.2 \pm 0.6 \text{ G}\Omega$ ($\bar{x} \pm \text{S.D.}$).

The value of the series resistance (R_s) could be determined from the time constant of the decline of the capacitative current according to $R_s = \tau/C$ (Marty & Neher, 1983). In Figure 9B, the capacitative current decayed exponentially with a time constant of $980 \mu\text{s}$. R_s was calculated to be $17 \text{ M}\Omega$. The input resistance of the pipette was $5 \text{ M}\Omega$ before touching the cell. In the best cases, R_s was 3-5 times the input resistance of the pipette.

An alternative method for estimating the value of R_s was to apply a relatively large hyperpolarizing current pulse to the pipette (current-clamp) after the membrane patch had been broken. The voltage drop across R_s was manifested as an instantaneous voltage drop at the break of the pulse (Figure 10). For the myoball shown in Figure 10, the voltage drop was 10.2 mV giving a value of $16 \text{ M}\Omega$ for R_s .

The ability to use a single pipette to measure voltage and pass current simultaneously depends on the magnitudes of R_s and of the membrane currents. If the product of R_s and current is large, then the true potential across the membrane will deviate from the command voltage by that amount. For this reason, it was important to minimize the value of R_s . The following precautions were taken: 1) use of low resistance pipettes and 2) selection of small diameter myoballs. Occasionally, capacitative transients were long

Figure 10. Voltage response under current clamp. A rectangular hyperpolarizing current pulse was injected and the voltage response recorded (A). Gaps in the voltage response immediately following the turn-on and turn-off of the current step (see enlargement) were the result of voltage drops across the resistance in series (R_s) with the myoball membrane. The instantaneous voltage drop was 10.2 mV for a 0.20 pA current step giving a R_s value of 16 M Ω . The input resistance of the pipette was 5 M Ω . The input resistance of the myoball was 155 M Ω and the diameter was 27 μ m. Unit membrane resistance was calculated to be 3.7 k Ω /cm². Semi-logarithmic plot of voltage as a function of time (B) gave a single exponential. This indicated that the intracellular space was isopotential. The measured time constant (τ) was 15.8 ms. Combined with the value for membrane resistance, the unit capacitance was calculated to be 4.3 μ F/cm² or a total capacitance of 103 pF.



indicating a large R_i . Repeated applications of pulses of suction usually resulted in a sudden acceleration of the capacitative transient. This suggested that the slow time course was the result of incomplete rupture of the membrane patch or of clogging of the pipette tip with intracellular material. Most of the time, this procedure brought about a stable change in the transient. Data was only accepted for analysis if the product of R_i and maximal current was less than 3 mV. No R_i compensation (Hodgkin & Huxley, 1952a) was employed as this restriction could generally be met.

Spatial control of voltage: Another important consideration was spatial control of voltage. Because of the long, tubular morphology of muscle cells (myotubes) grown in tissue culture, the cable properties of these cells prevent adequate control of membrane potential under voltage clamp (Fukuda *et al.*, 1976b). To avoid this problem, the shape of the muscle cells was altered by including colchicine in the tissue culture media (Fukuda *et al.*, 1976a). When grown in the presence of colchicine, the muscle cells assumed a roughly spherical shape (Plate 2). The effect of colchicine on cell morphology was presumably the result of its inhibition of the microtubule cytoskeleton (Linstead & Borisy, 1970).

There were several indications that the intracellular space was not isopotential. Under current clamp, a rectangular pulse of current gave a voltage response which could be

(Fukuda *et al.*, 1975)

(Figure 10B). As well, the capacitative current recorded under voltage clamp had an exponential decline (Figure 9B). Spatial control of voltage was also reflected in current voltage plots of time-dependent currents (cf. Back *et al.*, 1975). Adequate spatial control was reflected in current voltage plots if the curve was nearly symmetrical around the peak inward current. Whereas peak current levels were attained within a few millivolts of threshold if voltage control was poor (see Figure 39). This is because the voltage clamp cannot oppose the depolarization caused by the opening of channels. In general, current-voltage plots of inward currents were symmetrical. Poor voltage control was also apparent from the membrane voltage traces as deviations from the rectangular shape. This was generally not seen except when membrane currents were very large (several nA).

Exchange of pipette and intracellular solutions: The whole-cell recording technique offered the opportunity to alter intracellular ion composition and to apply drugs to the cytoplasmic side of the membrane. There was every evidence that, provided the capacitative transient was fast, exchange occurred between pipette and myoball solutions within about one minute. The myoballs had outward currents (Figure 11) which quickly disappeared if the pipette was filled with K-free solution (Ca replacement) containing tetraethylammonium (TEA). Both TEA and Cs are known to

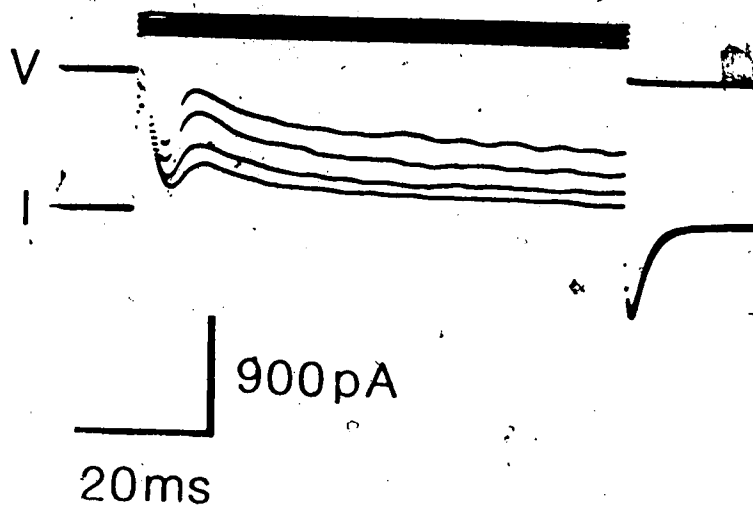


Figure 11. Outward membrane currents. Depolarizing voltage steps were applied from a holding potential of -60 mV. Four traces are superimposed. The currents appeared to exhibit voltage dependent inactivation. Repetitive voltage steps (every 200 ms) reduced the outward current level. After a several second rest, the current level returned to the initial level (data not shown). External solution was normal containing 10^{-7} M $10X$ and 1.0 mM Ca^{2+} . Pipette solution was normal (145 mM K^+).

(Hille, 1970) and the outward currents were most likely carried by K^+ . Also, as will be shown later, membrane Cl^- currents could be made to reverse at different potentials by altering the intracellular concentration of Cl^- .

It was my experience that the use of suction pipettes to penetrate a cell inflicted much less damage than conventional microelectrode impalement. Whole-cell recording could be performed for periods up to one hour without visual or electrical signs of deterioration.

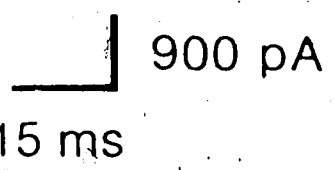
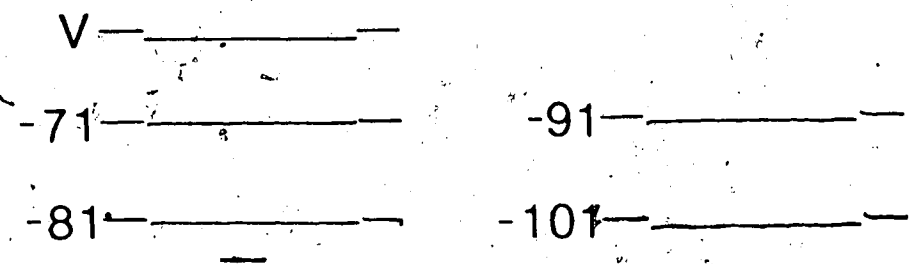
In summary, the use of single suction pipettes for whole-cell voltage clamp had the following characteristics: 1) adequate control of membrane potential; 2) opportunity to alter intracellular ion concentrations and to apply drugs to the internal surface of the membrane and 3) minimal damage to the cells. In addition, the membrane-pipette seal was mechanically stable. This allowed the formation of outside-out patches for the recording of single channel currents (see Discussion).

Membrane currents under voltage clamp

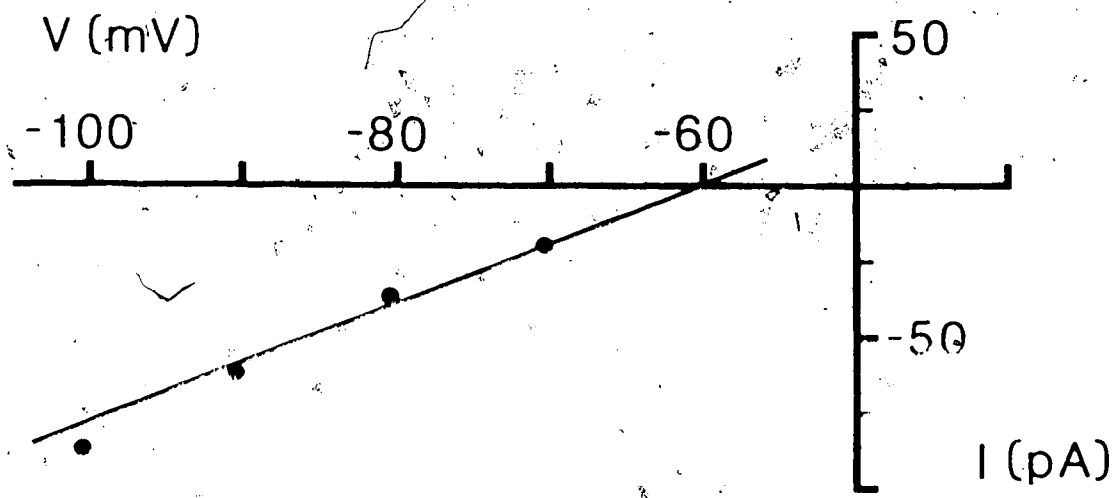
Leakage currents: Time-independent currents are termed leakage currents and must be subtracted from time-dependent currents. Leakage conductance was assumed to be linearly related to potential over the range of potentials at which time-dependent currents were studied. Leakage conductance was determined by applying small, hyperpolarizing voltage steps to the cell under voltage clamp.

Figure 12. Determination of leakage conductance. Records of voltage and current during hyperpolarizing voltage steps from a holding potential of -60 mV (A). Potential to which the membrane potential was stepped is indicated beside each current trace. Current magnitude was plotted as a function of test potential (B). The slope of the line gave an input resistance of $0.55 \text{ G}\Omega$. Myoball diameter was $25 \text{ }\mu\text{m}$. Value calculated for membrane resistance was $10.8 \text{ k}\Omega\text{cm}^2$. The seal resistance was $2 \text{ G}\Omega$.

A



B



was constructed and conductance was determined from the slope of the line. This value was used to calculate leakage currents for depolarizing voltage steps.

Voltage- and time-dependent currents: Under voltage clamp conditions and with the pipette and bath solutions approximating normal ionic composition, responses to depolarizing voltage steps were recorded (Figure 13). There was a fast inward current which was blocked by 10^{-7} M TTX and was presumably carried by Na^+ (Narahashi et al., 1964). At more depolarized potentials, outward currents developed. They were probably carried by K^+ since the outward currents were absent when the pipette solution contained 20 mM TEA (Stanfield, 1970b; Armstrong, 1975). The ~~slow~~ inward current and the slow inward current flowing during repolarization to the holding potential were identified as Cl^- currents. They are described in more detail in the following sections. Ca^{2+} currents have also been reported in these cells (Fukuda et al., 1976b), but they were probably masked by the other currents. Under current clamp, a long duration action potential (Figure 14A) and a short, fast spike (not shown) were observed.

Voltage- and time-dependent chloride currents: To isolate the current flowing through the voltage-dependent Cl^- conductance, currents flowing through the other permeability pathways were minimized by including channel blockers in the solutions and by substituting impermeant ions for

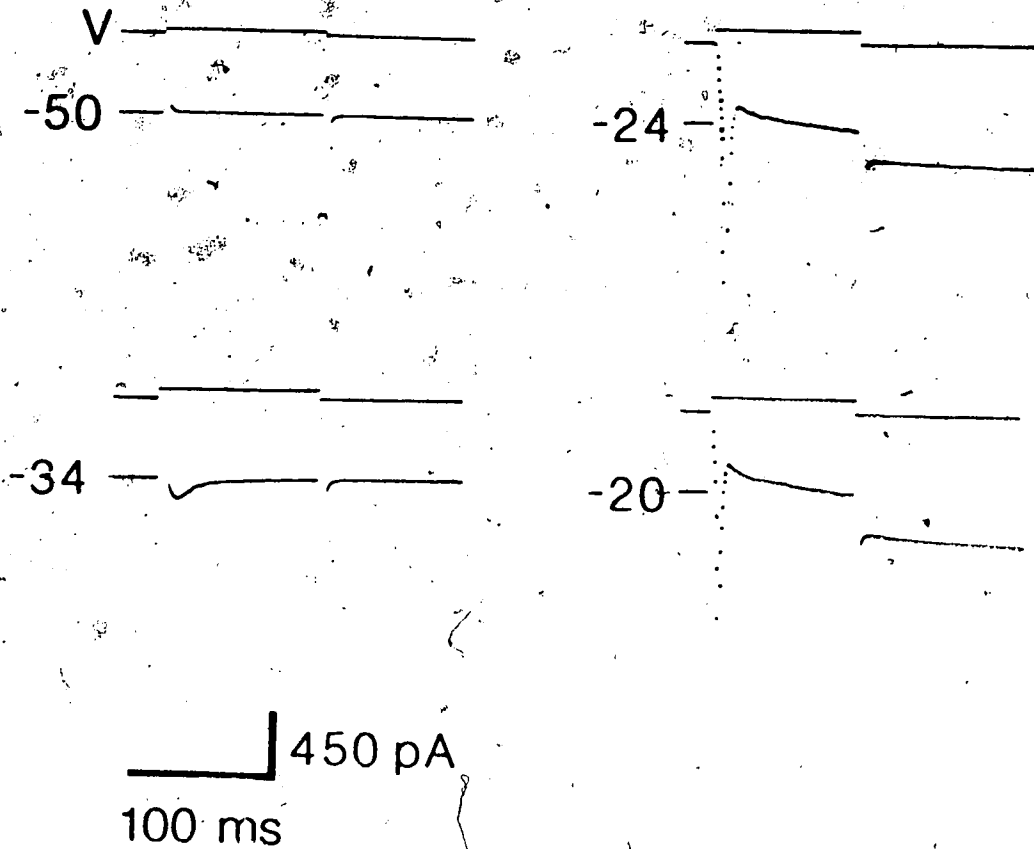
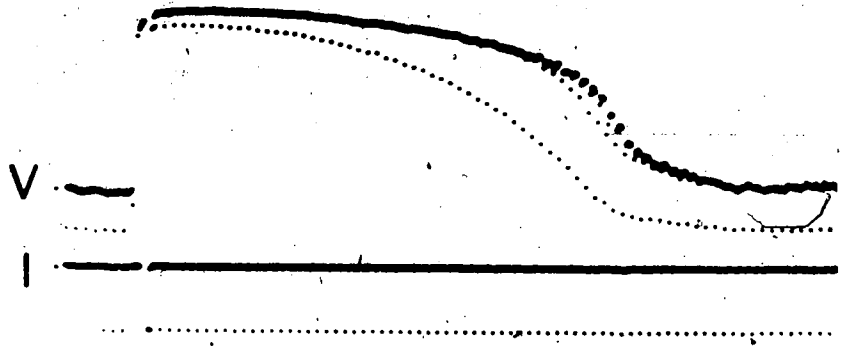


Figure 13. Membrane currents under voltage clamp. Depolarizing voltage steps were applied from a holding potential of -60 mV. The potential to which the membrane potential was stepped is indicated beside each current trace. External and pipette solutions were normal. Last two current traces were retouched.

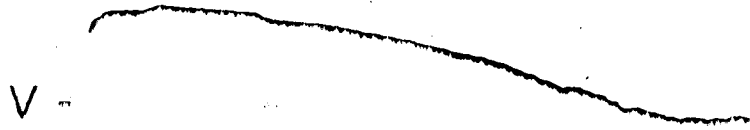
Figure 14. Chloride action potentials. Under current clamp, a long duration action potential was elicited (A). Small hyperpolarizing current pulses were given continuously to show the change in membrane resistance during the action potential. Resting input resistance was $0.6 \text{ G}\Omega$. At the top of the plateau of the action potential, input resistance dropped to $0.2 \text{ G}\Omega$. During the repolarization phase of the action potential, input resistance increased to $1.3 \text{ G}\Omega$. Resting potential was -70 mV . Duration of action potential was 38 s and height was 60 mV . External and pipette solutions were normal. Part B shows an action potential recorded in the presence of 20 mM TEA intracellularly. The duration was 85 s and the height was 39 mV . Resting potential was -63 mV and the potential at the top of the action potential was -28 mV . Reversal potential for Cl^- given by the Nernst equation was 23 mV . External solution was normal containing 10^{-7} M TTX and 1.0 mM Cd^{2+} . Pipette solution was 60 Cl^- .

A



40 mV 225 pA
10 s

B



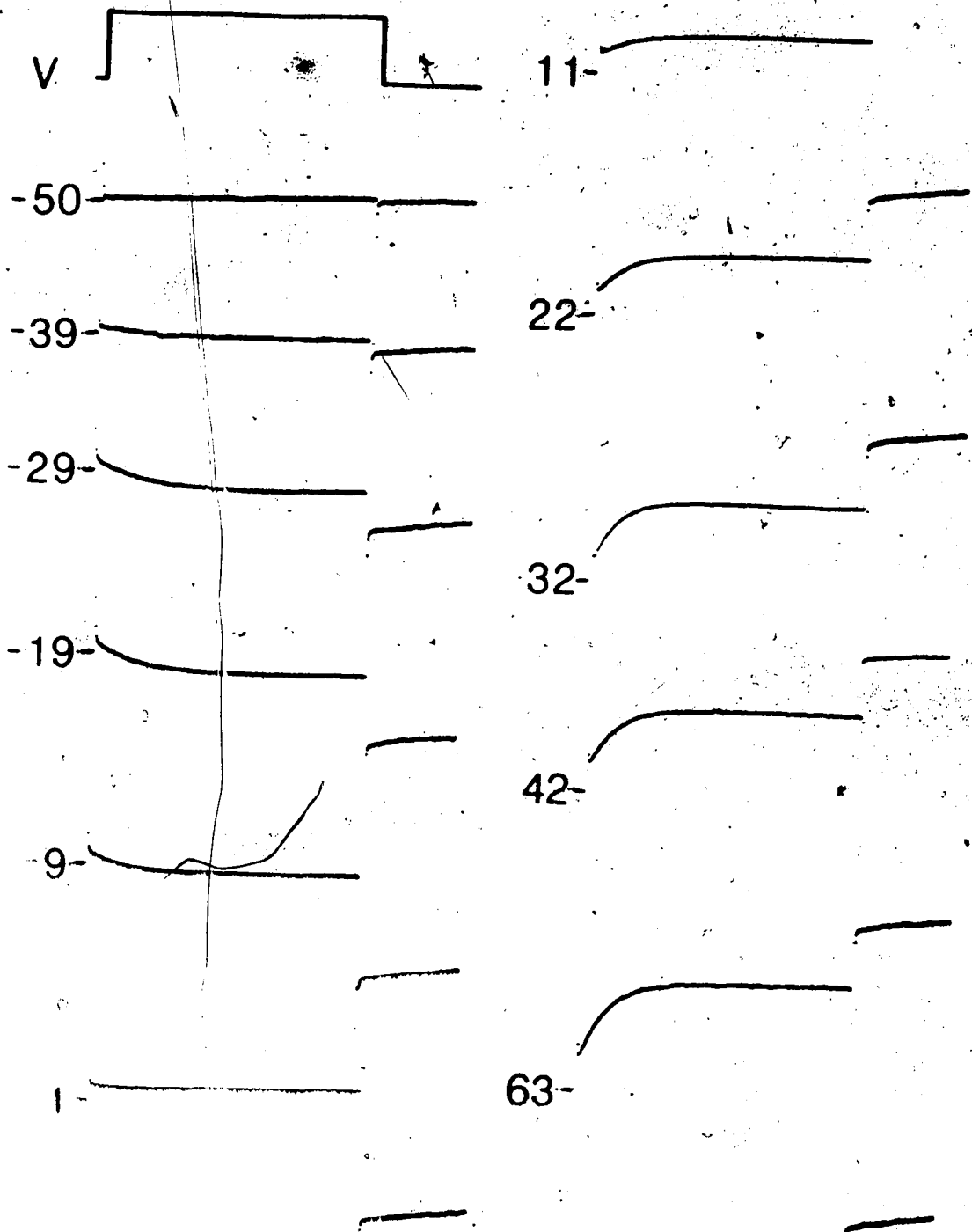
40 mV
20 s

permeant ones. Na^+ currents were blocked by including 10^{-7} M TTX in the bath solution (Narahashi *et al.*, 1964) and Ca^{2+} currents were blocked by 1.0 mM Cd^{2+} in the bath (Hagiwara & Byerly, 1981). K^+ currents were eliminated by using K^+ -free pipette solution with Cs^+ as the major cation and by including 20 mM TEA (Stanfield, 1970b; Armstrong, 1975).

Figure 15 shows records of currents elicited with 10 ms depolarizing voltage steps from a holding potential of -60 mV. As the potential was stepped further away from the holding potential, an inward current developed slowly and did not decline during maintained depolarization. As the potential was stepped to more positive values, the inward current rose more quickly and became larger. Near 0 mV, the current trace was flat, i.e. that was the reversal potential for the currents as no net current was flowing. This also showed that the other currents were successfully blocked. Above 0 mV currents were outward and rose more quickly than at less positive potentials. Following the depolarizing steps, inward currents were recorded which did not decline for several seconds (only partially shown in Figure 15). Under current clamp, an extremely long duration action potential was recorded (Figure 14B). Cl^- action potentials recorded under 'normal' ionic conditions (Figure 14A) had much shorter durations. Consequently, outward K^+ currents must play a role in repolarizing the membrane potential.

The currents were corrected for leakage currents and steady state current levels were plotted against

Figure 15. Membrane chloride currents. Membrane currents were recorded under voltage clamp during step depolarizations (V) from a holding potential of -60 mV. Voltage steps were to the potential listed beside each current trace. Currents through Na^+ , and K^+ and Ca^{2+} channels were minimized by including 10^{-7} M TTX and 1.0 mM Cd^{2+} in the external solution and by having 20 mM TEA in a K^+ -free solution inside the pipette. Seal resistance was 2 G Ω , Pipette input resistance was 2 M Ω , R_s was 6 M Ω . Diameter of the myoball was 16 μm . Membrane resistance was calculated to be 8 k Ωcm^2 . External solution was normal plus the additions mentioned above (149 mM Cl). Pipette solution was K^+ -free (155 mM Cl). Current traces are not corrected for leakage conductance.



350 ms

400 pA

depolarizing test potential (Figure 16). Currents were detectable above -45 mV and were initially inward. Peak inward current occurred at about -25 mV and then became less inward and reversed polarity above 0 mV. Measured reversal potential was 3 mV. Peak current density was $12 \mu\text{A}/\text{cm}^2$. Peak current densities ranged from 3 to 30 with a mean of $17 \mu\text{A}/\text{cm}^2$ for 12 myoballs.

In two experiments, external Cl^- concentration was changed during the recording. When the external Cl^- concentration was reduced, inward currents became larger indicating participation of Cl^- in the currents (Figure 17A).

To demonstrate quantitatively that the slow membrane currents were carried by Cl^- , reversal potentials for steady-state currents were measured in a variety of internal and external Cl^- concentrations. Care was taken to select pipettes with wide tips and myoballs with small diameters so as to achieve the best possible control of intracellular ion concentrations. Cl^- was replaced with the impermeant ion, methylisophate (Kutter & Noble, 1960). Figure 17B shows the results for two different myoballs. For currents recorded in 16 mM external and 155 mM internal Cl^- the measured reversal potential was 15 mV. The equilibrium potential calculated from the Nernst equation is 18 mV. For another myoball in 140 mM external and 150 mM internal Cl^- the measured reversal potential was 11 mV. The equilibrium potential calculated from the Nernst equation is 14 mV.




Figure 16. Current-voltage plot of chloride currents. Magnitudes of steady-state currents were corrected for leakage currents and plotted as a function of depolarizing test potential. Measured reversal potential was 3 mV. Peak current density was $12 \mu\text{A}/\text{cm}^2$ (measured at -25 mV). Data from currents shown in Figure 15.

0

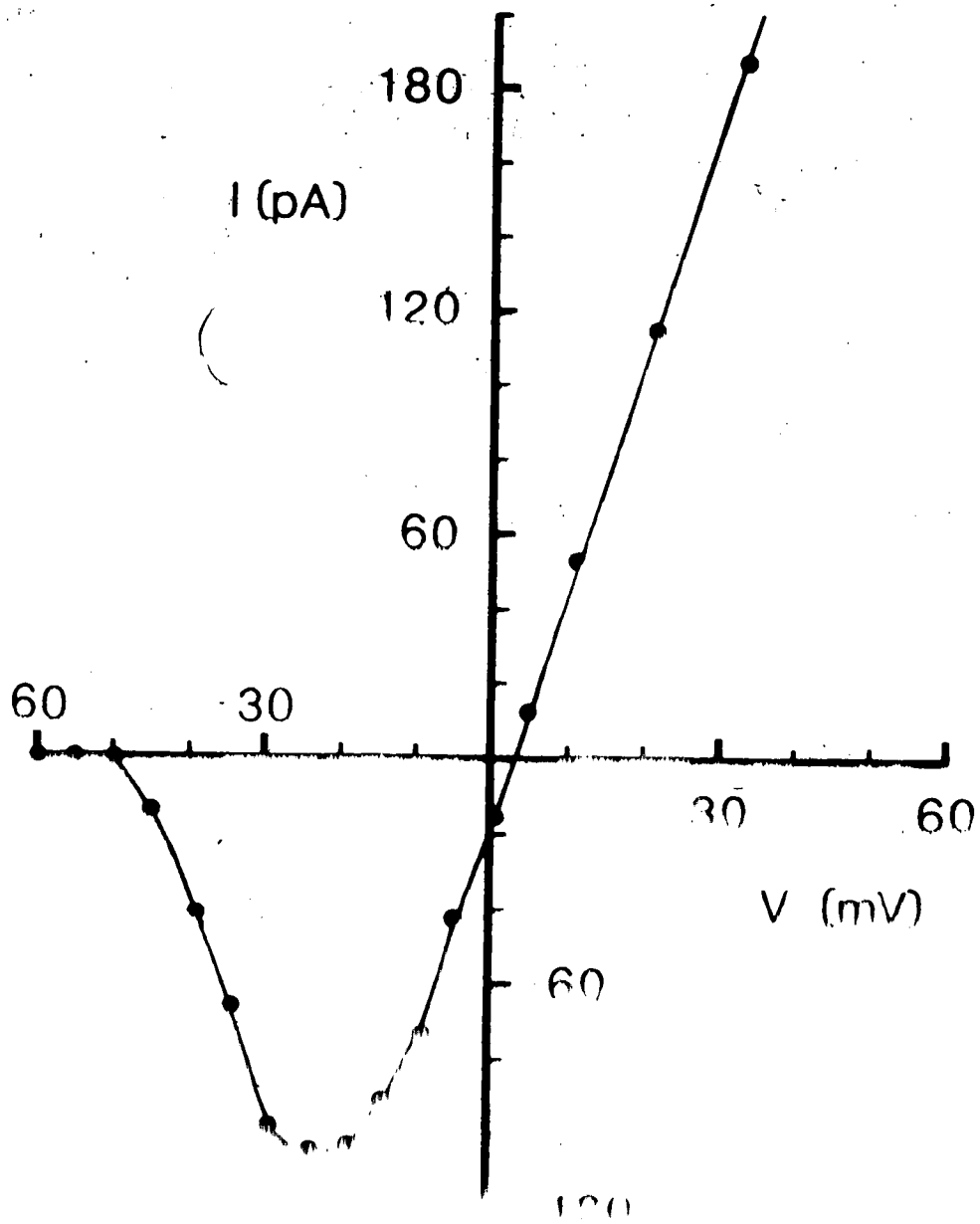
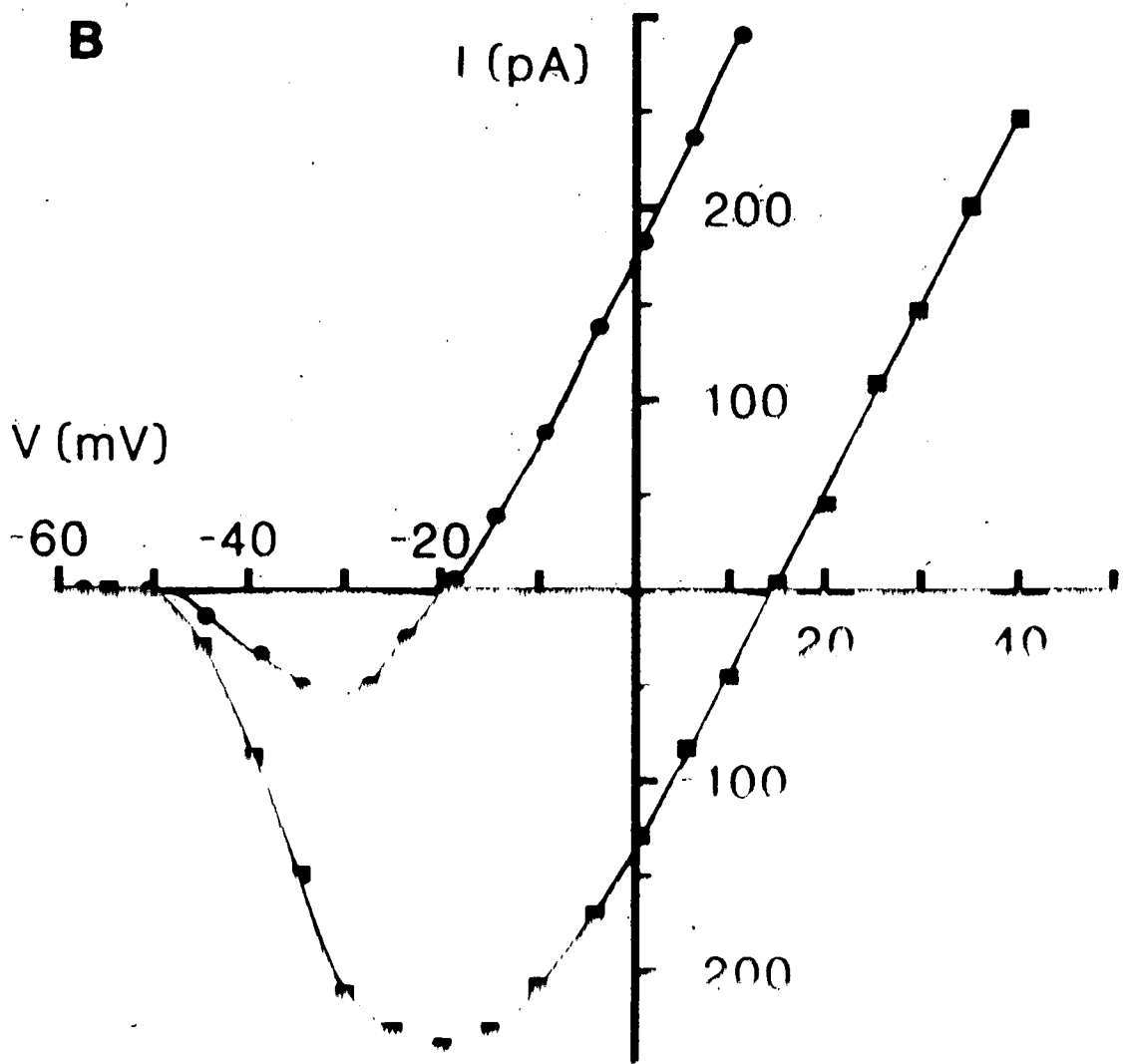
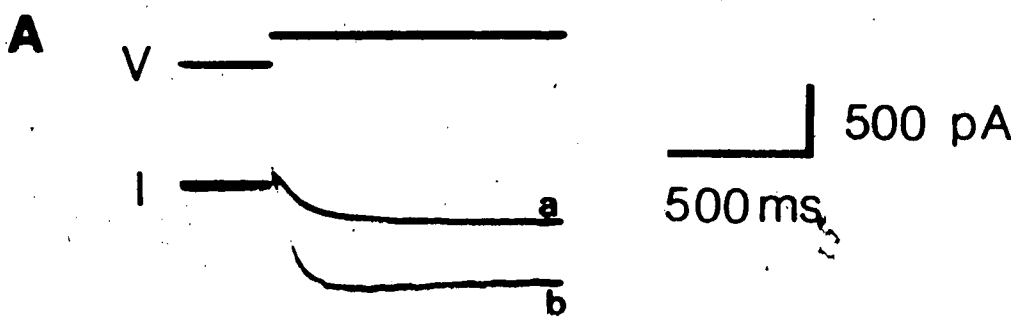


Figure 17. Effects of changing external chloride concentrations on membrane currents. Currents recorded during depolarizing voltage steps to -19 mV from a holding potential of -60 mV (A). External Cl^- concentration was reduced from 149 mM (current trace a) to 3 mM (current trace b) while continuously recording from the same myoball. Cl^- was replaced with methylsulphate. Current-voltage plots for currents recorded from two different myoballs in different Cl^- concentrations are shown in B. The curve drawn through the circles is data from recordings done in 60 mM intracellular Cl^- and 149 mM external Cl^- . Measured reversal potential was -19 mV. The curve drawn through the squares is data from recordings done in 155 mM intracellular Cl^- and 76 mM external Cl^- . Measured reversal potential was 15 mV. Holding potential was -60 mV for both. External solution contained 10^{-7} M TTX and 1.0 μM Cd²⁺. Pipette solution contained 60 mM TEA.



The graph in Figure 18 shows the cumulative results from 21 myoballs. The reversal potential for the steady-state current was plotted as a function of Cl^- concentrations. The regression line through the data points has a slope of 53 mV per decade which is close to the 58 mV per decade predicted by the Nernst equation. The slope of the line probably would have been closer to the predicted value if better control of intracellular ion concentrations was possible. This data gave very strong evidence that the slow currents were carried by Cl^- .

Block by SITS, DIDS, and SCN^- : Stilbene derivatives have been shown to block Cl^- permeability in a wide variety of cell types: red blood cells (Knauf & Rothstein, 1971; Cabantchik & Rothstein, 1974); epithelial cells (Ehrenspeck & Brodsky, 1976) and invertebrate (Russell & Brodwick, 1979) and vertebrate (Vaughan & Fong, 1978) skeletal muscle. It has been suggested that SITS and DIDS act at the Cl^- binding site (Shami, Rothstein & Knauf, 1978). It was found that SITS (1 mM) blocked the currents in a reversible manner (Figure 19). DIDS (10 μM) also blocked the currents, but the block could not be reversed by repeated washing. The irreversibility of the block by DIDS has also been observed in other preparations (Cabantchik & Rothstein, 1974). SCN^- (10 mM) was found to block the currents in a reversible manner as has been reported for the Cl^- channel in electroplax membranes (White & Miller, 1981).

Figure 18. Reversal potentials as a function of chloride concentrations. Reversal potentials for steady-state currents were measured in various Cl^- concentrations as demonstrated in Figure 17. Data from 21 myoballs. Values are means \pm S.D. The straight line was drawn according to the Nernst equation:

$$E_{\text{Cl}} = \frac{RT}{zF} \ln \frac{(\text{Cl})_o}{(\text{Cl})_i}$$

E_{Cl} is the equilibrium potential for Cl^- (mV); $(\text{Cl})_o$ and $(\text{Cl})_i$ are external and internal Cl^- concentrations (mM), respectively. R, T, z and F have their usual meanings.

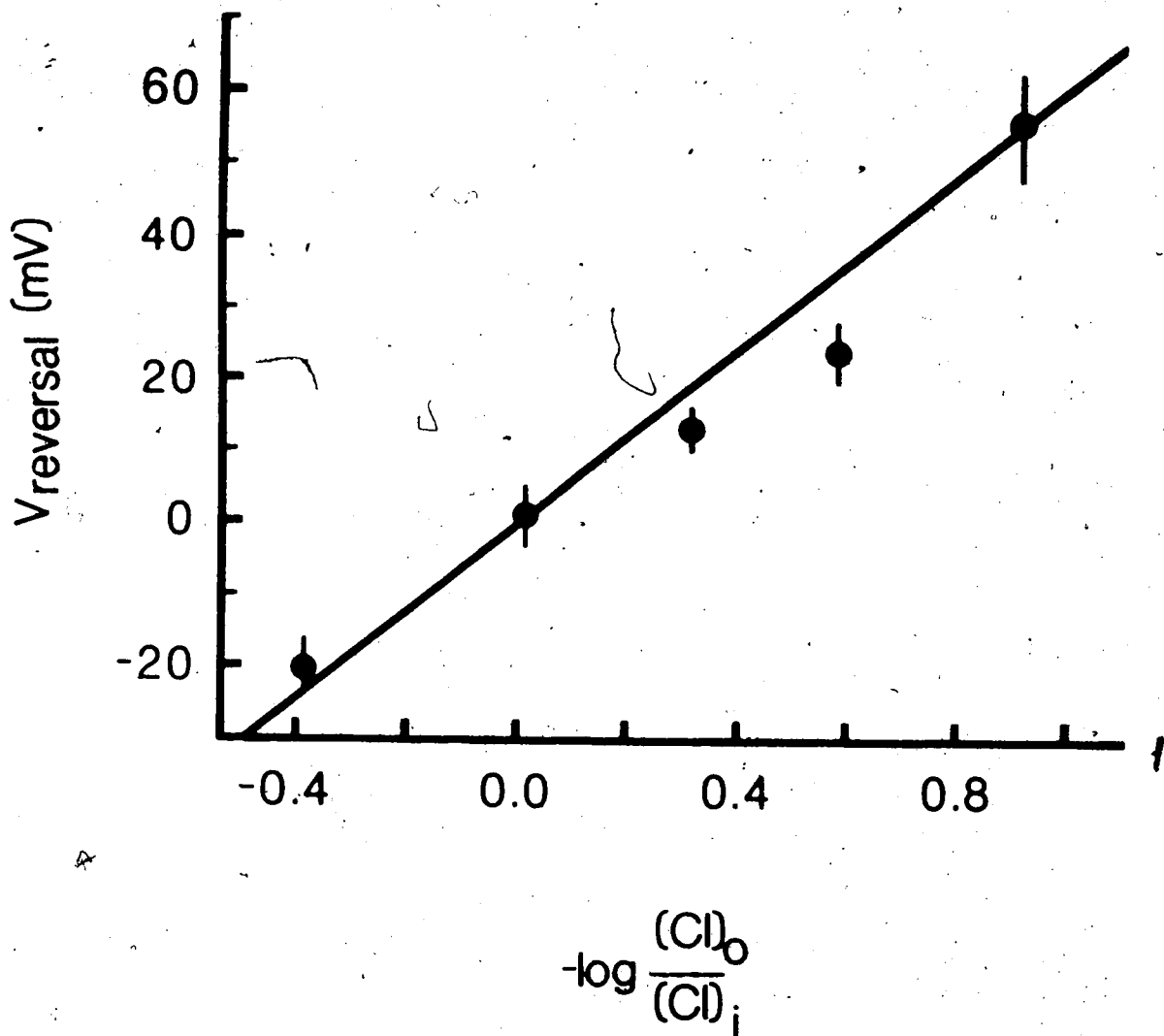
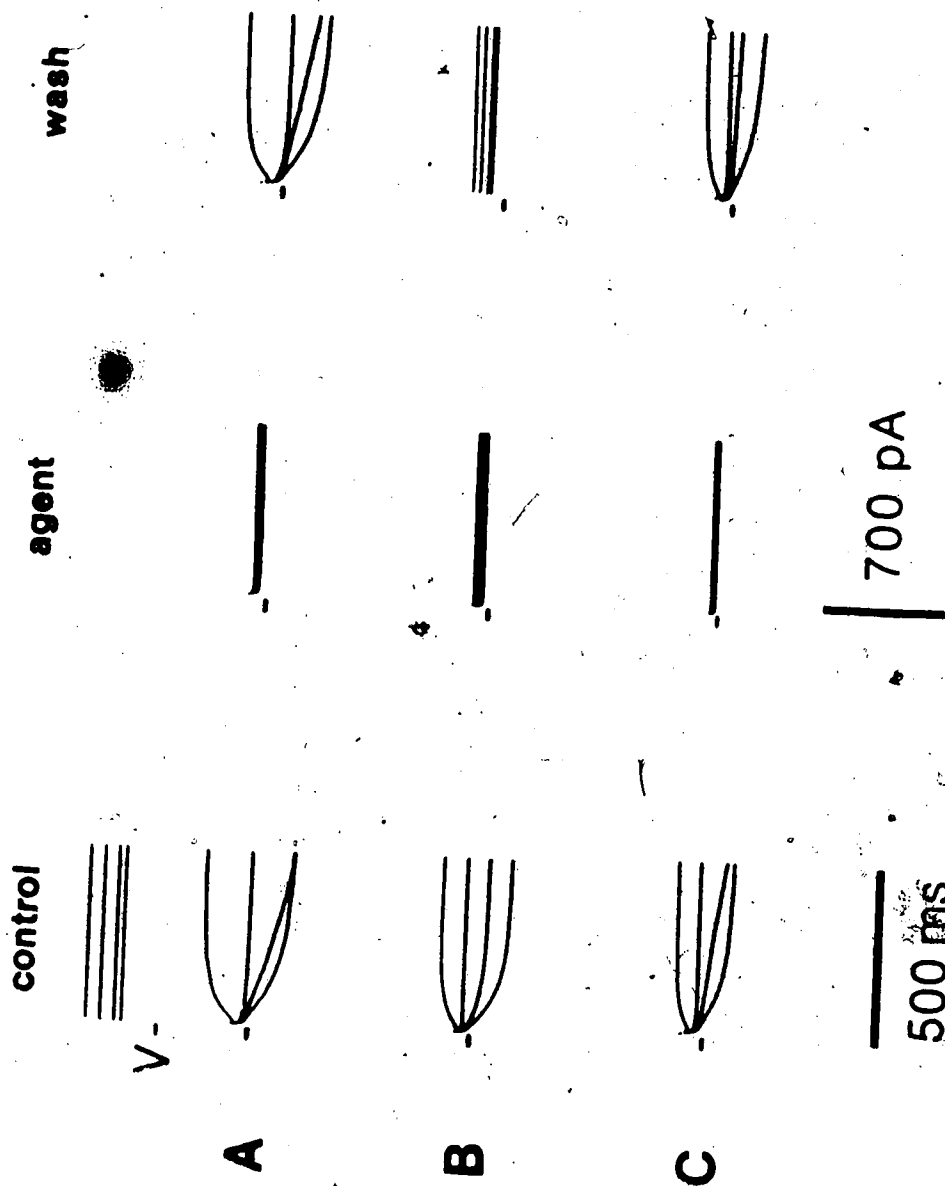


Figure 19. Effects of SITS, DIDS and SCN^- on membrane currents. Currents were recorded under voltage clamp. A control series was taken in normal external solution containing 10^{-7} M TTX and 1.0 mM Cd^{2+} . Pipette solution was K^+ -free. Bath solution was then changed to one containing the different agents while continuously recording from the same myoball. Four current traces are superimposed in each frame. The voltage step protocol is denoted V. Currents were reversibly blocked by 1 mM SITS (row A). Block by 10 μM DIDS was apparently irreversible as extensive washing with normal external solution did not reverse the effect (row B). Block by 10 mM SCN^- was reversible (row C). Holding potentials were -60 mV in B and -80 mV in A and C.



Cl currents lack an inactivation mechanism: Since the currents did not decline during maintained depolarization (see Figure 15), this indicated that the conductance lacked an inactivation mechanism. To test whether there was any steady-state voltage dependent inactivation operating at negative potentials, the holding potential was varied and depolarizing voltage steps to the same potential were applied (Figure 20). It can be seen that the magnitude of the inward currents elicited by the test pulses did not change. Therefore, over the range of potentials tested, there was no evidence of voltage-dependent inactivation.

Tail currents: Following depolarizing voltage steps that activated Cl^- currents, currents became inward and decayed slowly and completely (Figure 21). Currents that flow during repolarization are termed tail currents. They were examined with a two pulse protocol. First, a large depolarizing voltage step was applied in order to open as many channels as possible. Then the potential was stepped back to various levels (Figure 22A). Magnitudes of the tail currents were measured following the break the depolarizing step. They were plotted as a function of repolarization potential in order to construct an 'instantaneous' current-voltage plot (Figure 22B). Data points could be fitted a straight line with an extrapolated reversal potential of -1 mV. This value was very close to the calculated Cl^- equilibrium potential of 1 mV and indicated that the tail currents were carried by Cl^- . The straight line fit to

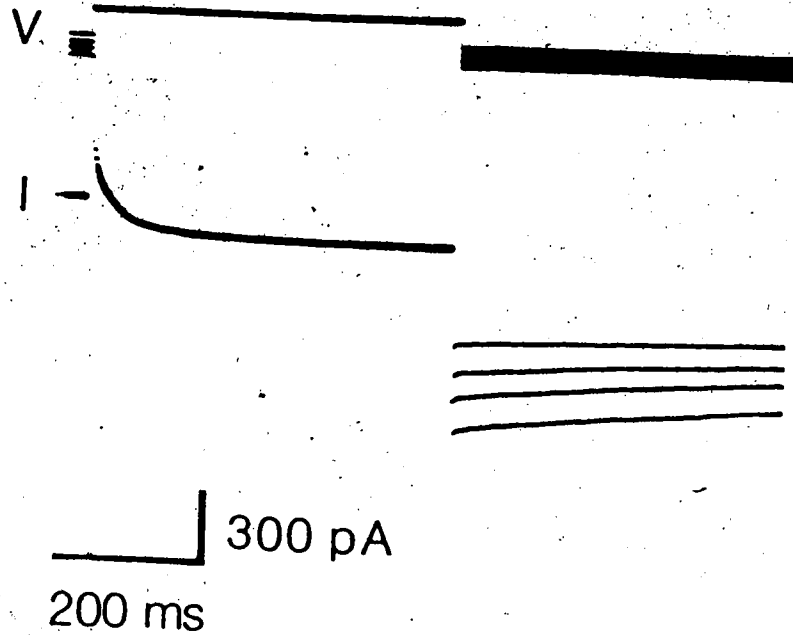


Figure 20. Lack of voltage-dependent inactivation. Cl^- currents were recorded under voltage clamp. The holding potential was varied, -60, -70, -80 and -89 mV, and a depolarizing voltage step to -23 mV was applied. Four traces are superimposed. Note that the steady-state current level was identical in all four runs. External solution was normal containing 10^{-7} M TTX and 1.0 mM Cd^{2+} . Pipette solution was K^+ -free.

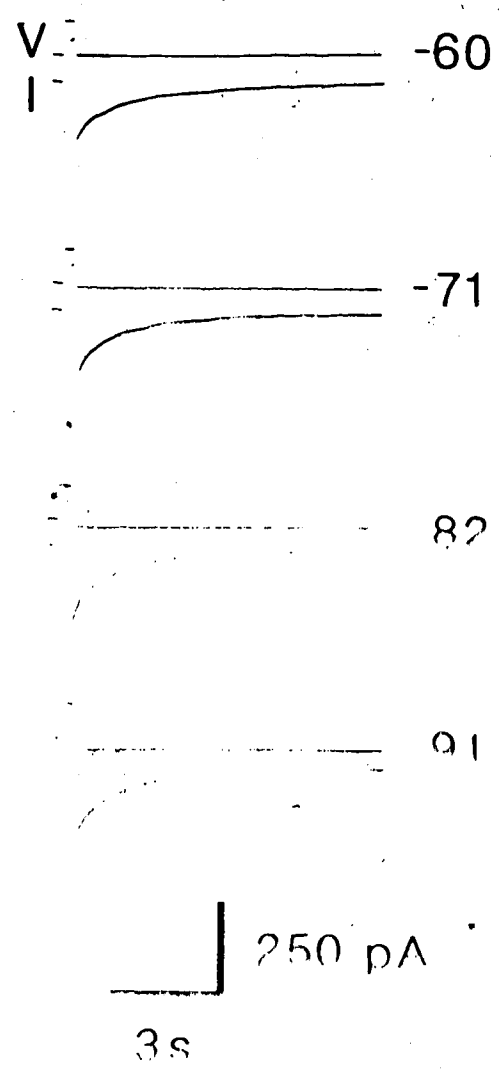
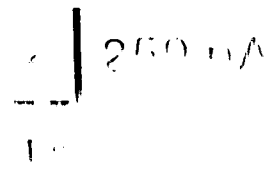
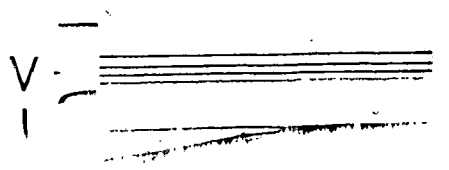


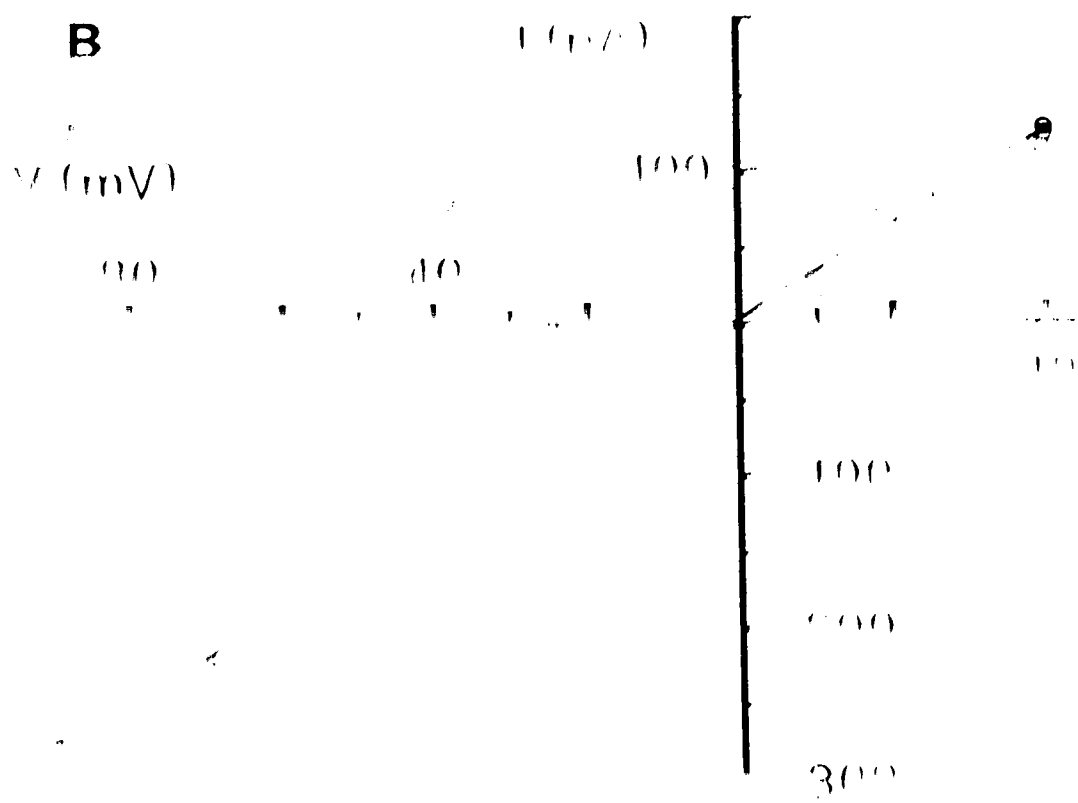
Figure 21. Tail currents. Currents flowing during repolarization to various potentials following a depolarizing step to 38 mV for 300 ms are shown. Potential during repolarization is listed beside each trace. Holding potential was -60 mV. External solution was normal containing 10^{-7} M TTX and 1.0 mM Ca^{2+} . Pipette solution was K^{+} -free. Seal resistance was 4 GΩ. Input resistance of the pipette was 2 MΩ.

Figure 22. Instantaneous current-voltage plot. Four superimposed traces show the protocol for collecting data for instantaneous current-voltage plots (A). Following a depolarizing voltage step to 40 mV, the potential was stepped to various potentials. Tail current magnitudes were measured following the break of the depolarizing pulse and corrected for leakage conductance. Values were plotted against repolarization potential (B). Data from tail currents are represented by filled circles and from steady-state currents by circles. Data points fell on a straight line with a slope of 3.2 nS. Diameter of myoball was 13.6 μm which gave a conductance of 0.55 mS/cm^2 . Measured reversal potential was -1 mV. Holding potential was -60 mV. External solution was normal containing 10^{-7} M TTX and 1.0 mM Ca^{2+} . Pipette solution was K^+ -free. Seal resistance was 1.00 G Ω . R_{in} of pipette was 8 M Ω . R_{in} of pipette was

A



B



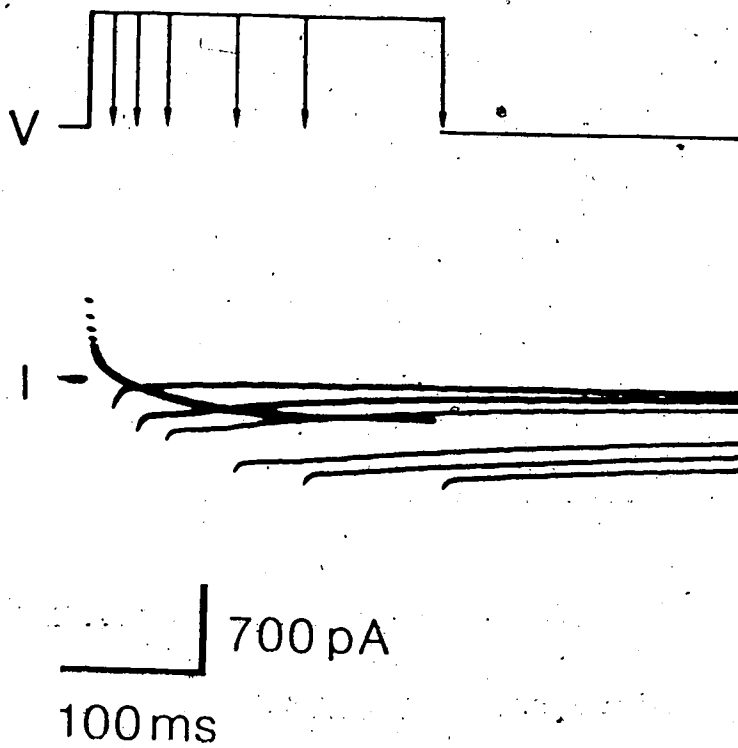
the data also indicated that the open channels behaved ohmically. The slope of the line gave a conductance value of 3.1 nS. The mean value for 10 myoballs was 8.3 ± 3.9 nS ($\bar{x} + S.D.$). Calculated per unit area the mean conductance was 0.63 ± 0.3 mS/cm².

Tail currents were also examined by varying the duration of the depolarizing test pulse (Figure 23). Membrane conductance was calculated from the steady-state and the tail currents at the end of the depolarizing test pulse. The values were plotted as a function of time and it can be seen that the time course of the conductance changes calculated from both steady state and tail currents was similar. This result supported the idea that the tail currents were flowing through the conductance mechanism activated during the depolarizing pulse.

(1) conductance as a function of voltage: Since the open channels were found to behave ohmically, the following relationship could be applied: $I = G(V - V_{rev})$. I is current (pA); G is conductance (nS); V is voltage at which current was measured (mV) and V_{rev} is the reversal potential (mV). Using this relation, conductance was calculated and normalized with respect to the maximum value for each myoball (Figure 24). The resulting curve reflects the fraction of channels open at a given membrane potential. The relationship between conductance and voltage was sigmoid. It rose sharply between -40 and -20 mV and leveled off at positive potentials. The mean value for maximal Cl

Figure 23. Envelope of tails. Currents recorded in response to depolarizing steps to -29 mV from a holding potential of -60 mV are superimposed (A). The duration of the depolarizing pulse was lengthened as indicated in the diagram (V). Pulse durations shown are: 12, 30, 50, 100, 150 and 250 ms. Conductance was calculated at the termination of the depolarizing pulse from both the steady-state currents (circles) and from the tail currents (triangles) (B). The values are plotted as a function of time. Note that the time course of the conductance changes calculated from either the steady-state or the tail currents followed a similar time course. Reversal potential was 0 mV. External solution was normal containing 10^{-7} M TTX and 1.0 mM Cd^{2+} . Pipette solution was K^+ -free. Seal resistance was 5 G Ω . R_s was 6 M Ω . R_p of pipette was 1 M Ω .

A



B

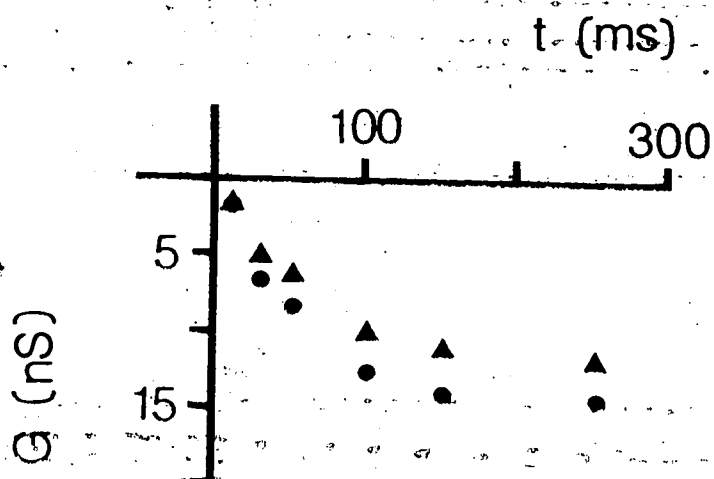
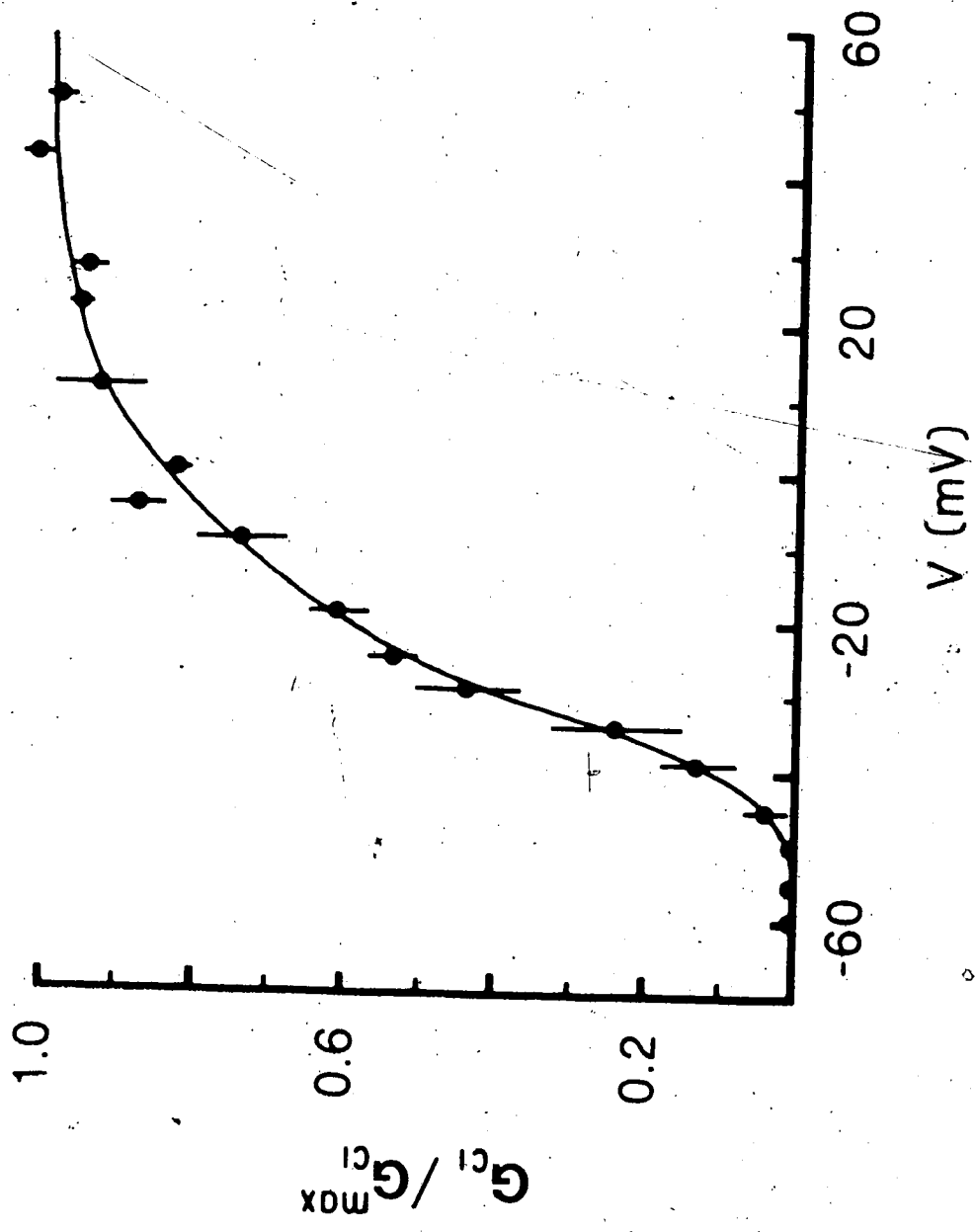


Figure 24. Conductance as a function of voltage. Conductance was calculated according to: $I = G(V - V_{rev})$. I is current (pA); G is conductance (nS); V is membrane potential (mV); V_{rev} is measured reversal potential (mV). Conductance values (G_{Cl}) were normalized with respect to the maximal conductance (G_{Cl}^{max}) for each myoball. Data from 5 myoballs. Values are means \pm S.E. Smooth curve drawn by eye.



conductance was 1.03 ± 0.7 mS/cm² ($\bar{x} \pm$ S.D.; $n = 13$).

The relationship between Cl⁻ conductance and membrane potential could also be seen in the current-voltage plots, if the magnitudes of the tail currents were measured for each of the depolarizing steps (Figure 25). The resulting tail current amplitude versus voltage curve should be proportional to the fraction of open channels at each potential. The curve resembled the curve in Figure 24 in that it rose steeply from -40 to 0 mV and then started leveling off above 0 mV.

Plotting Cl⁻ conductance as a function of voltage on a semilogarithmic plot showed that the values approached a limiting value of 8 mV for an e-fold change in conductance (Figure 26). Thus, the Cl⁻ conductance exhibited high voltage sensitivity. The Na⁺ conductance of frog skeletal muscle has been reported to rise e-fold for a 3.7 mV depolarization (Ildefonse & Rougier, 1972; Hille & Campbell, 1976).

Cl current activation kinetics: Semilogarithmic plots of Cl currents as a function of time gave straight line fits suggesting a monoexponential time course for current activation (Figure 27). However, it was found that the currents could not be completely described by a single exponential as the first 6-10 ms of current development did not fit. There appeared to be delays of several milliseconds in the development of the Cl⁻ currents. Unfortunately, the capacitative transients obscured most of the delays. In

Figure 25. Current-voltage plot of tail current magnitude.

Steady-state currents (circles) were plotted against depolarizing test potential. Tail current magnitudes (squares) were measured immediately after the turn-off of the depolarizing test pulse and plotted against test potential. The resulting tail current amplitude curve should be proportional to the fraction of channels that were activated at the depolarizing test potential. Compare to the conductance versus voltage curve in Figure 24. Data taken from the currents shown in Figure 15.

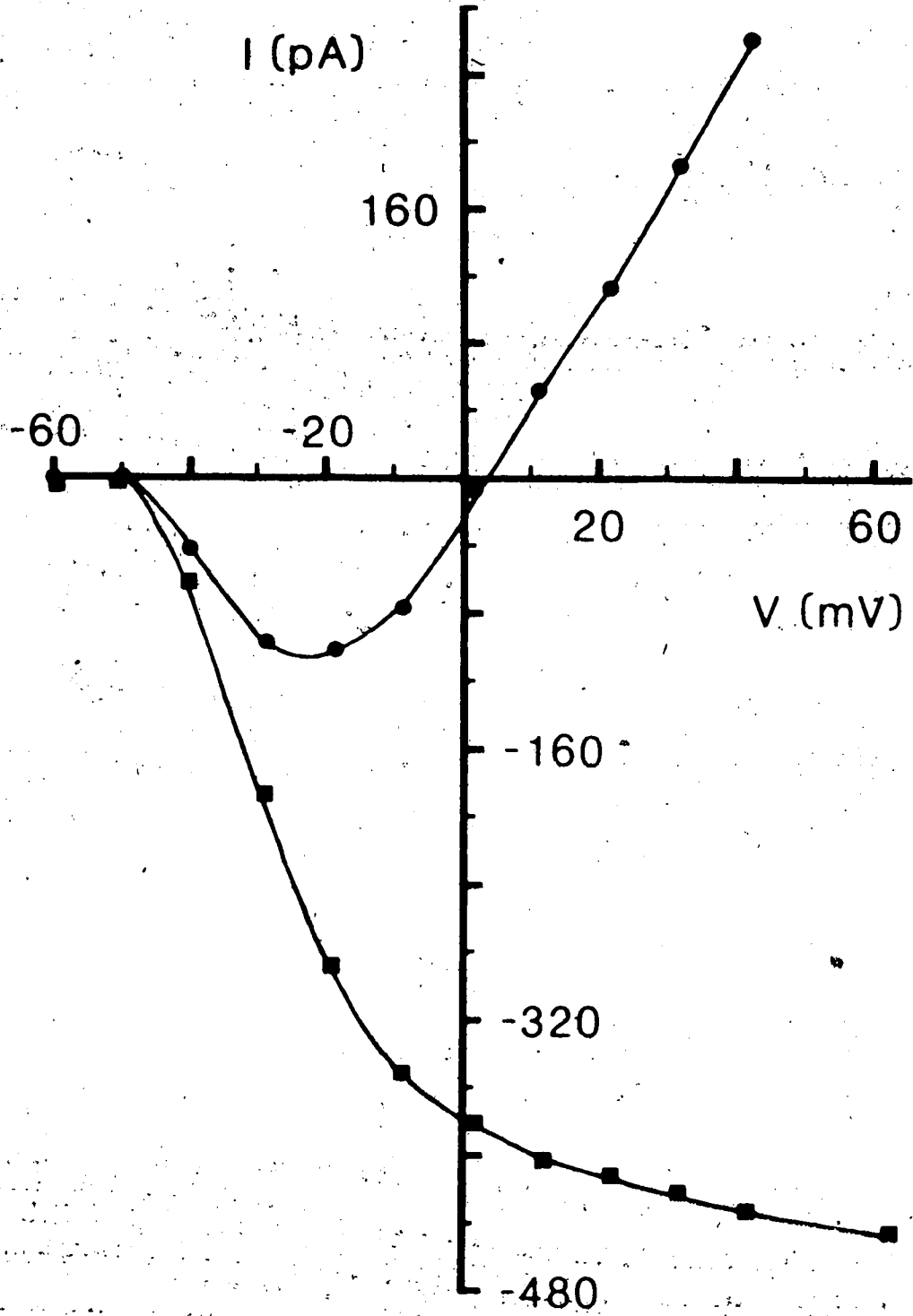
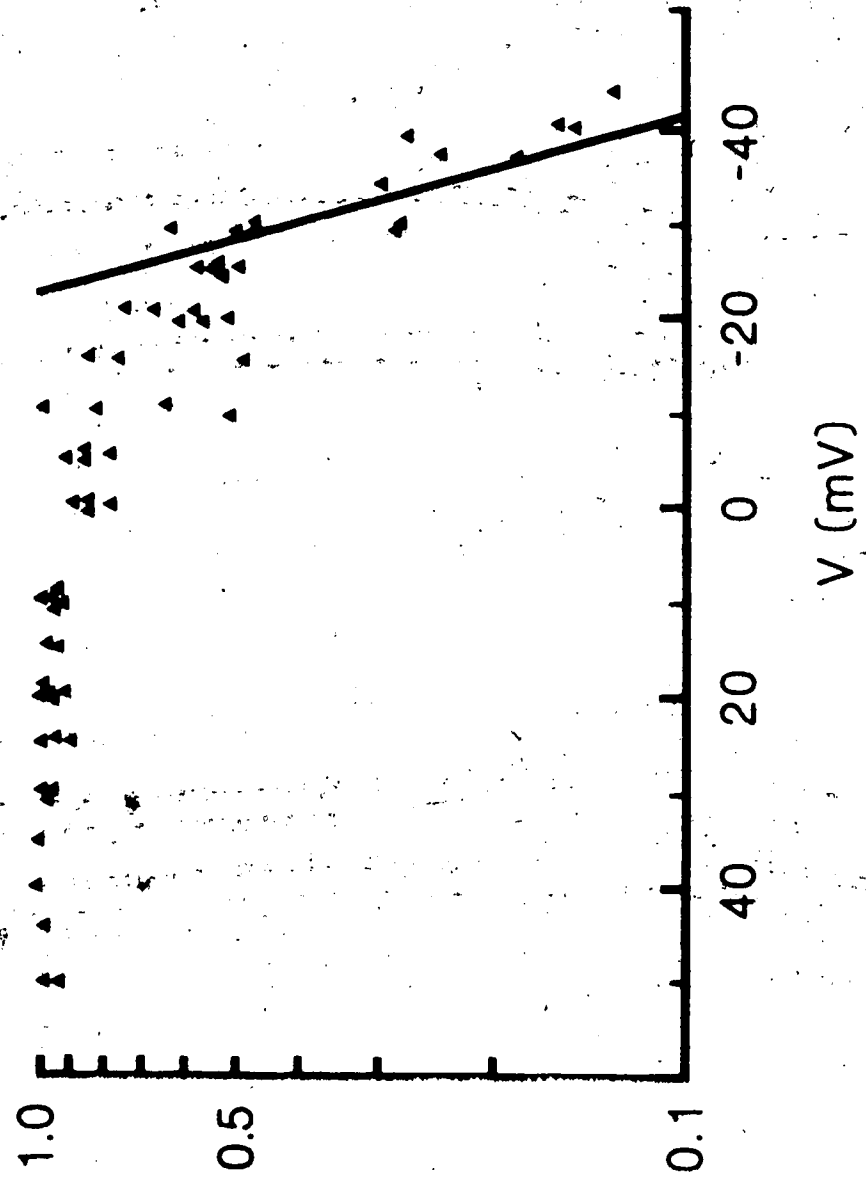
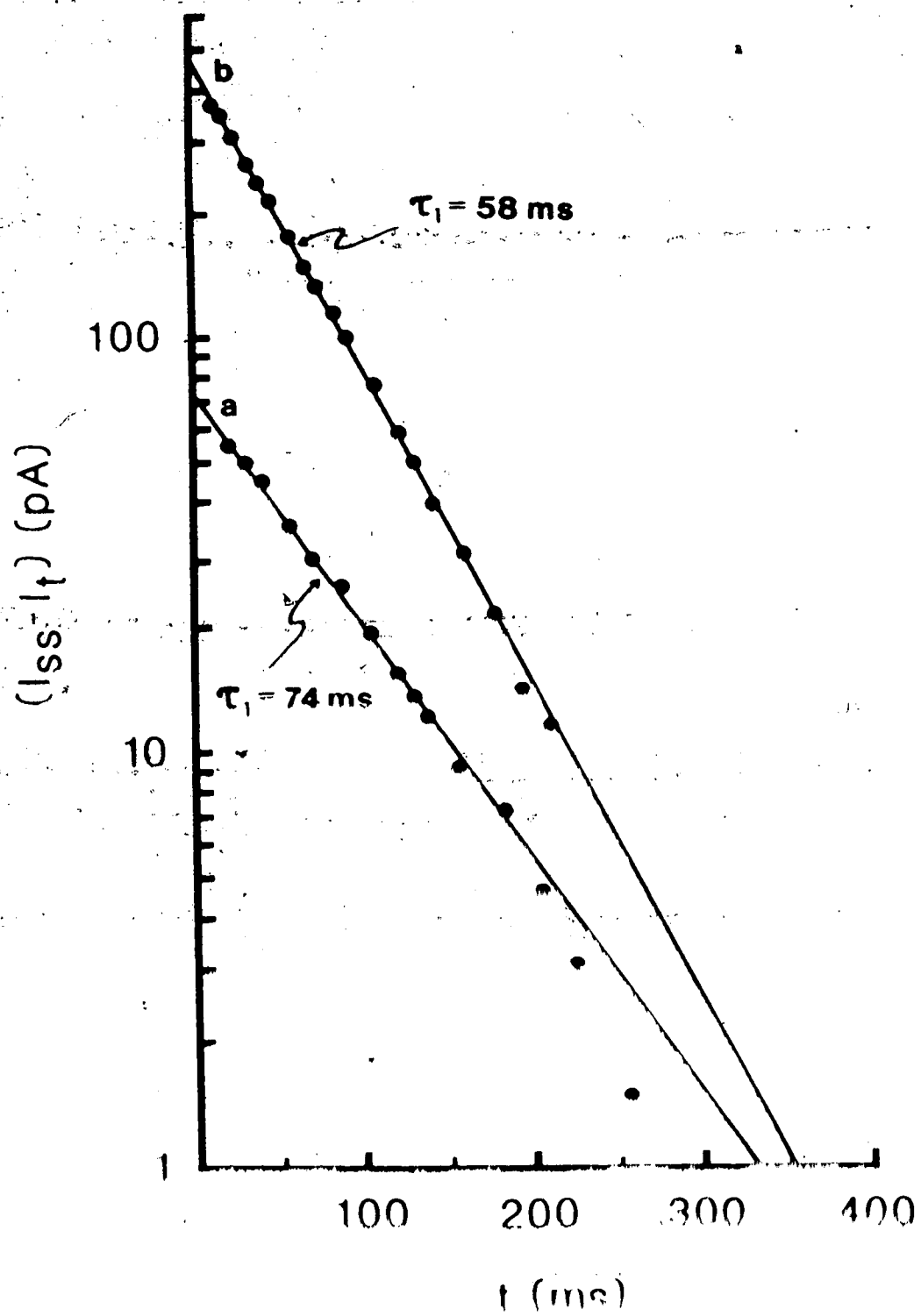


Figure 26. Semilogarithmic plot of conductance as a function of voltage. Normalized values of Cl⁻ conductance (G_{Cl}/G_{Cl}^{max}) were plotted against voltage on semilog paper. Data same as in Figure 24. Line through the data is a regression line fit to the conductance values for potentials more negative than -25 mV. Slope of the line gives an e-fold change in conductance for an 8 mV depolarization.



G_{max}^{Cl} / G^{Cl}

Figure 27. Semilogarithmic plot of current activation. Inward current magnitudes for voltage steps to -9 mV (line a) and to 63 mV (line b) were plotted as a function of time. The time constant (τ_1) for the voltage step to -9 mV was 74 ms with an amplitude (A_1) of 73 pA. The time constant (τ_1) for the step to 63 mV was 58 ms and the amplitude (A_1) was 473 pA. Turn-on of the depolarizing voltage step was set as time equal to zero. Same current traces as in Figure 15.



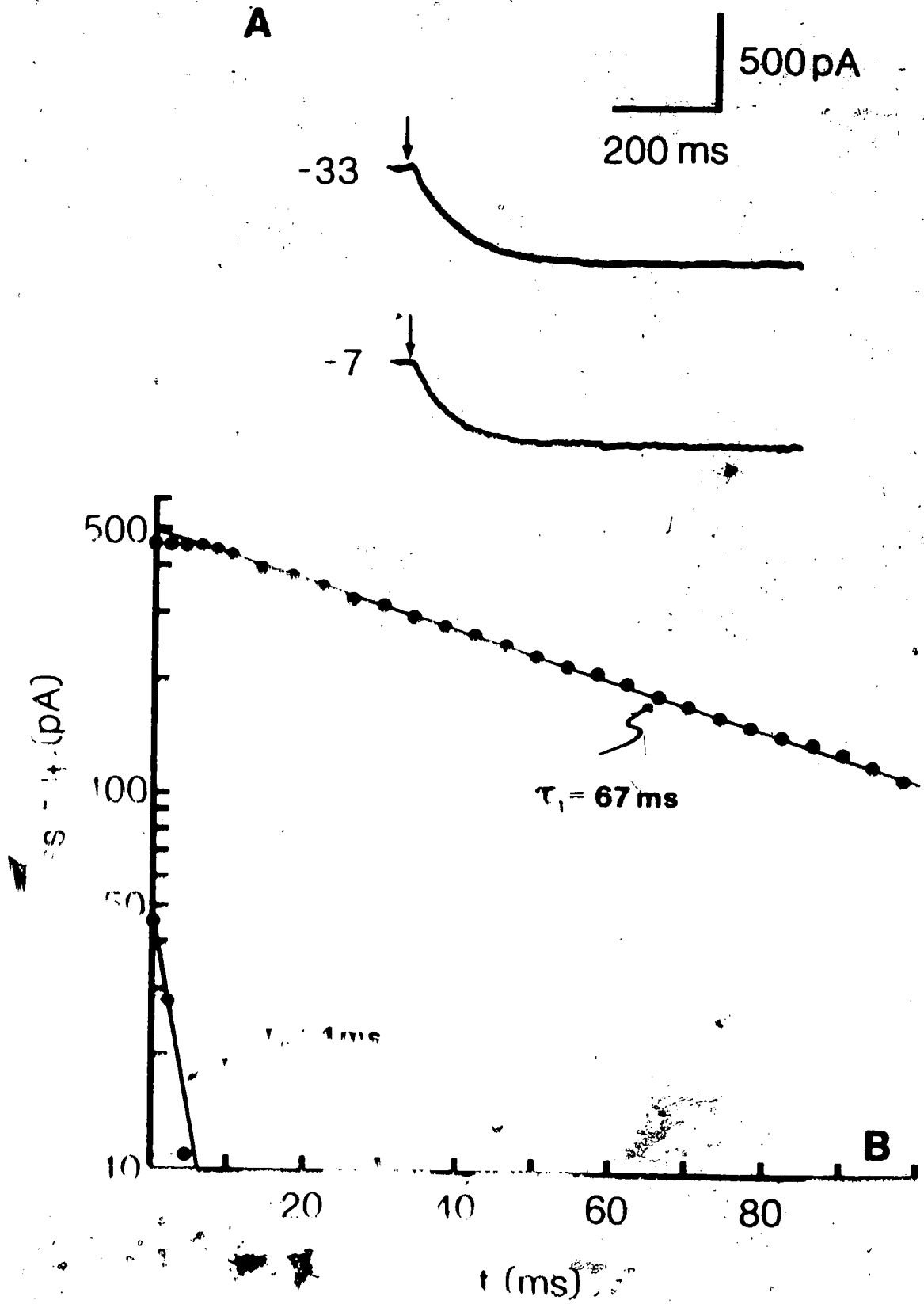
order to visualize the delays, the capacitative currents were eliminated from the current records by adding current responses to hyperpolarizing voltage steps of equal magnitude. For the traces shown in Figure 28, there was about a 6 ms delay in inward current development for a depolarizing step to -33 mV and about a 4 ms delay for a step to -7 mV. Delays were found to be slightly shorter for currents recorded at more positive potentials. Plotting current records of this type versus time on semilogarithmic plots showed that the initial slope was close to zero (Figure 28B).

To account for these observations, the time course of activation of the Cl currents was fit with the sum of two exponentials: a major component with amplitude A_1 (pA) and time constant τ_1 (ms) and a minor component with amplitude A_0 (pA) and time constant τ_0 (ms). The amplitude of the minor exponential component had the opposite polarity to the amplitude of the major exponential component in order to account for the delay in current activation. The sum of the two exponentials gave an initial slope close to zero. The values of A_0 , A_1 and τ_1 were obtained by fitting a straight line to a semilogarithmic plot of current (see Figure 28). τ_0 was roughly estimated by fitting the model curve to the actual current record. The equation used to fit the currents had the following form:

$$I(t) = I_{\infty} [A_0 \exp(-t/\tau_0) + A_1 \exp(-t/\tau_1)]$$

where $I(t)$ is the current at time t and I_{∞} is the steady state current.

Figure 28. Delay of activation. Cl^- currents recorded in response to depolarizing voltage steps to -33 and -7 mV from a holding potential of -70 mV are shown in Part A. Linear leakage and capacitive currents were subtracted from the inward current records by adding the current responses to voltage steps opposite in polarity. Arrows indicate the turn-on of the voltage steps. There was a slight delay in the development of the inward currents which was about 6 ms for the step to -33 mV and about 1 ms for the step to -7 mV. Semilogarithmic plot of current as a function of time for a voltage step to -18 mV was fitted with a straight line (B). The time constant for the major exponential (τ_1) was 67 ms and had an amplitude (λ_1) of 518 pA. The initial slope was close to zero. Another exponential with a time constant (τ_2) of roughly 4 ms and an amplitude (λ_2) of 46 pA gave an initial slope of zero if subtracted from the major exponential. The original solution was a mixture of 10% and 90% of the high and low concentrations of the solution. The concentration of the solution was 10% and the concentration of the solution was 90%.



(pA), respectively. Figure 29 shows that the fit of the equation to the currents was excellent.

The time constants of the major exponential component (τ_1) were found to vary with membrane potential (Figure 30). They decreased from 150-200 ms at potentials more negative than -20 mV to about 50 ms at potentials more positive than 0 mV. The time constants (τ_0) of the minor exponential seemed to vary little with voltage, but the values were very uncertain. The presence of this component (delay) suggests that there are at least two kinetically distinct closed states.

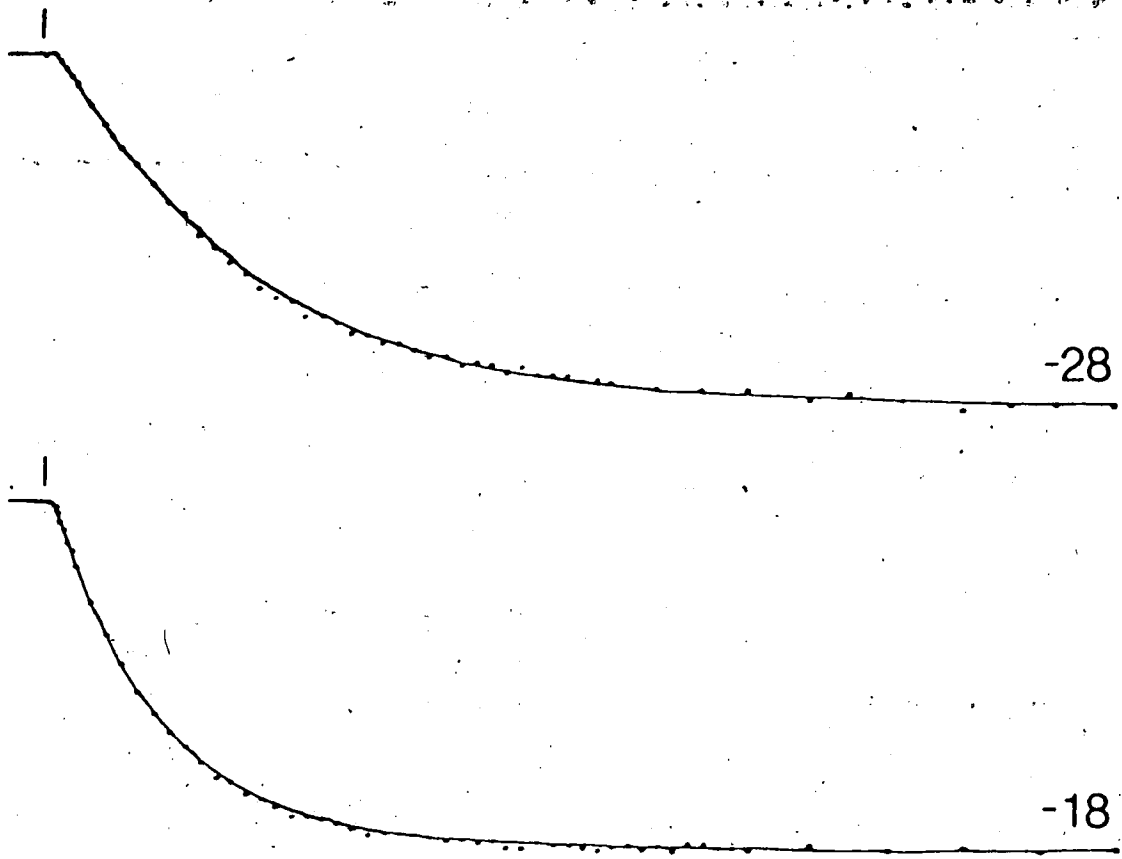
Cl current deactivation kinetics: Tail currents had an unusually slow time course (Figure 21). Therefore, consideration had to be given to the possibility that there was a component of the tail currents that did not reflect the closing behavior of the Cl channels. There was no indication that voltage control was lost since the voltage trace was perfectly flat and the tail currents declined with exponential time courses (discussed later). Another source of artifact could have been polarization of the Ag/AgCl electrode during the prolonged current flow. However, this seemed unlikely as polarization would be expected to distort the recording of slow and steady state events (cf Katz, 1966). A more likely explanation would have been the effects of ion accumulation and/or depletion in a restricted space. The following experiment was designed to evaluate this possibility.

Figure 29. Fit of model equation to currents. Curves modelling activation of Cl^- currents were drawn according to:

$$I_t = I_{ss} - [A_0 \exp(-t/\tau_0) + A_1 \exp(-t/\tau_1)].$$

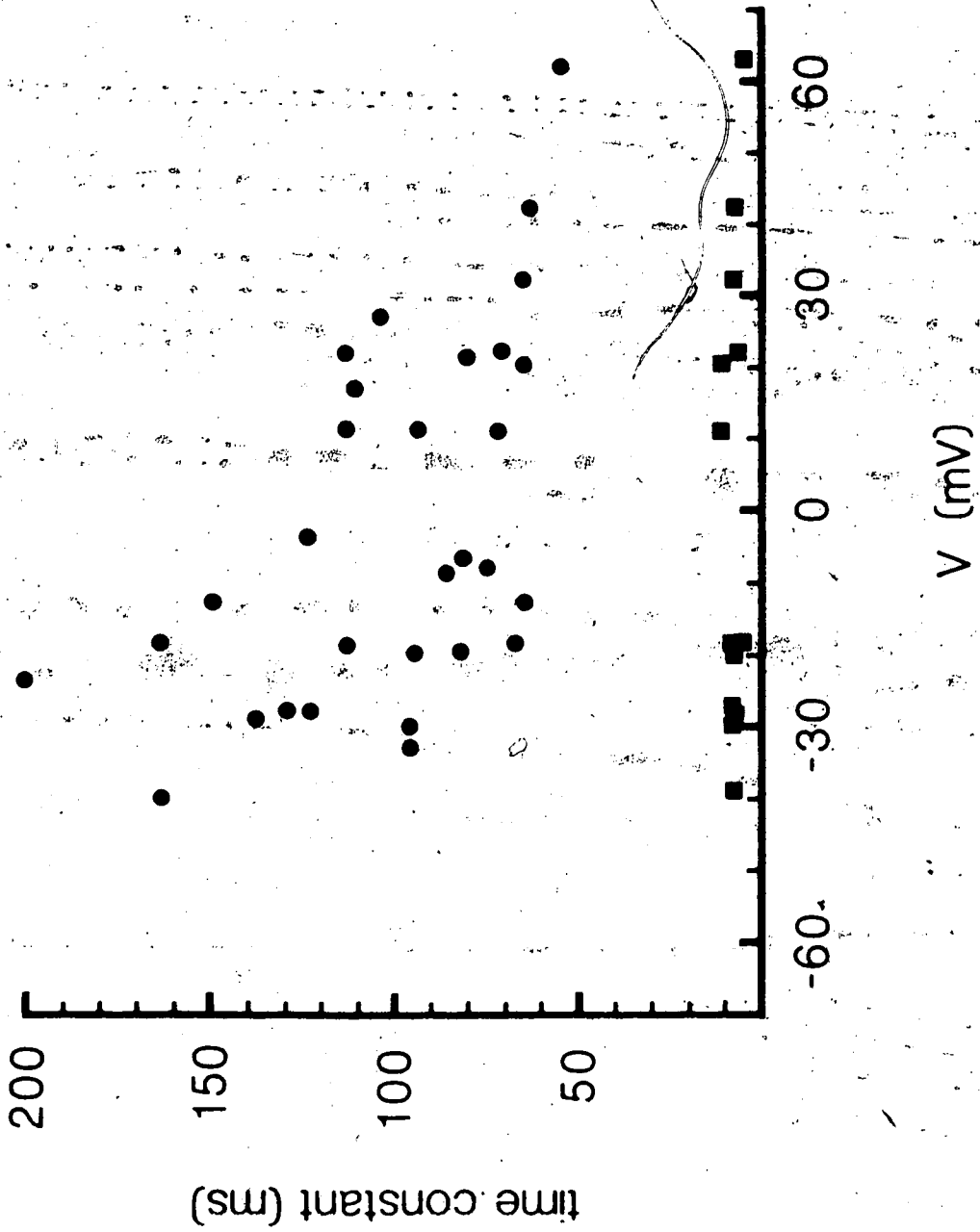
I_t is current at time t (pA); I_{ss} is steady-state current (pA); A_0 is amplitude of minor exponential (pA); τ_0 is time constant of minor exponential (ms); A_1 is amplitude of major exponential (pA); τ_1 is time constant of major time exponential (ms).

For a depolarizing voltage step to -28 mV, $I_{ss} = -464$ pA; $A_0 = 54$ pA; $\tau_0 = 9$ ms; $A_1 = -518$ pA; $\tau_1 = 128$ ms. For a depolarizing step to -18 mV, $I_{ss} = -452$ pA; $A_0 = 46$ pA; $\tau_0 = 4$ ms; $A_1 = -498$ pA; $\tau_1 = 67$ ms. Turn-on of voltage step indicated by vertical bars. Data points from steps to -28 and -18 mV from a holding potential of -70 mV were superimposed on the model curves. Linear leakage and capacitative currents were eliminated by adding current responses to voltage steps of opposite polarity. Currents were from same myoball as in Figure 28.



200 pA
100 ms

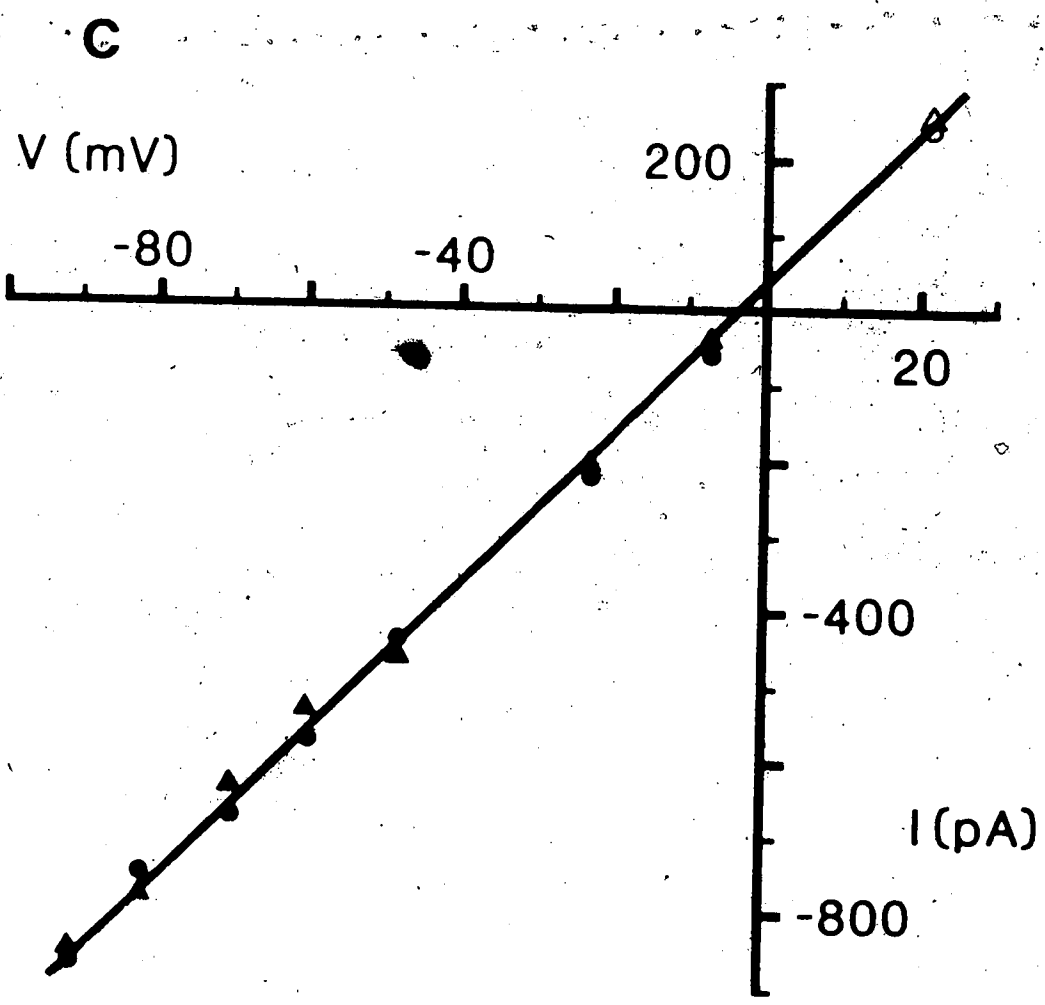
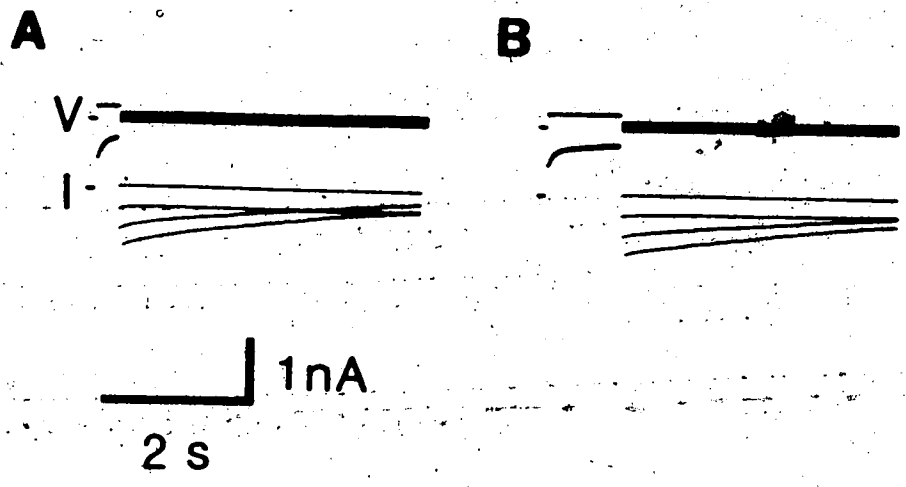
Figure 30. Time constants of activation as a function of voltage. Time constants for the activation of Cl^- currents were obtained as shown in Figures 27, 28 and 29. Circles represent time constants for the major exponential component (τ_1). Data from 5 myoballs. Squares represent time constants for the minor exponential component (τ_0). Data from 3 myoballs.



The reversal potential for tail currents was determined following depolarizing voltage steps of varying durations. The expectation was that if ion concentration gradients were changing significantly during current flow, then a shift in the reversal potential would be observed when short and long duration pulses were compared (Figure-31). For the experiment shown, the reversal potential did not shift when the conditioning pulse was lengthened from 300 to 1000 ms. Similar experiments, with depolarizing conditioning potentials varying from 200 ms to 3 s, also did not show a shift in the reversal potential ($n = 7$). Therefore, it did not appear that the effects of changes in ion concentration gradients were causing the slow tail currents. It should be pointed out that tail currents had slow time courses even for depolarizing pulses to the reversal potential (see step to -1 mV in Figure 15). At the reversal potential, there should be no net ion movement and consequently, no accumulation or depletion. In conclusion, the slow tail currents did not appear to be artifacts and must have reflected the closing behavior of the Cl^- channels.

Tail currents were fitted with the sum of two exponentials: a major component with amplitude A_2 (pA) and time constant τ_2 (ms) and a minor component with amplitude A_1 and time constant τ_1 (ms). At all potentials, the time constant was first determined for the slow, major component by fitting an exponential to the later data points and then peeling this fit away from the total current to reveal the

Figure 31. Reversal potential of tail currents for different duration test pulses. Instantaneous current-voltage plots were constructed according to the protocol in Figure 22. Depolarizing voltage step was to 21 mV from a holding potential of -70 mV. Duration of depolarizing voltage step was 300 ms in Part A and 1 s in Part B. Current-voltage plot of the data showed that the points fell along the same line with a reversal potential of -4 mV (C). Tail current magnitudes for 300 ms test pulse (filled triangles) and for 1 s pulse (filled circles). Steady-state current magnitude for the 300 ms pulse (triangle) and for the 1 s (circle). Slope of the line gave a conductance of 9.3 nS. Diameter of myoball was 30 μ m which gave a unit conductance of 3.3 mS/cm². External solution was normal containing 10⁻⁷ M TTX and 1.0 mM Cd²⁺. Pipette solution was K⁺-free. Seal resistance was 10 G Ω . R_s was 6 M Ω . R_{in} of pipette was 1 M Ω .



faster exponential (Figure 32). τ_2 was 8-15 times slower than τ_1 and both time constants were slightly longer at more positive potentials. For example, in one myoball, τ_1 increased from 200 ms at -90 mV to 260 ms at -60 mV. τ_2 increased from 1.74 s at -90 mV to 2.64 s at -60 mV. More time constant values are given in a later figure.

The presence of the extremely slow tail current component suggested that the channels entered a long-lived open state from which they returned very slowly to the closed states. The time constant for this transition at a more positive membrane potential was obtained from the following experiment. It was noted that the relative amplitude of the fast component of the tail currents depended on the duration of the conditioning pulse (Figure 33). As the depolarizing voltage step was lengthened, the amplitude of the fast tail component became smaller while the amplitude of the slow tail component became larger (Table 5). With short duration pulses (80 ms), the fast component amplitude constituted 35% of the total current while for long duration pulses (1 s), its contribution fell to about 15%. These values were plotted as a function of depolarizing test pulse duration on semilogarithmic paper (Figure 34). Data points were well fit with a single exponential with a time constant of 700 ms. This then, would be the time constant (τ_2) for the transition from the short to the long-lived open state.

Figure 35 shows the two time constants (τ_1 and τ_2) determined from activation and deactivation of the currents.


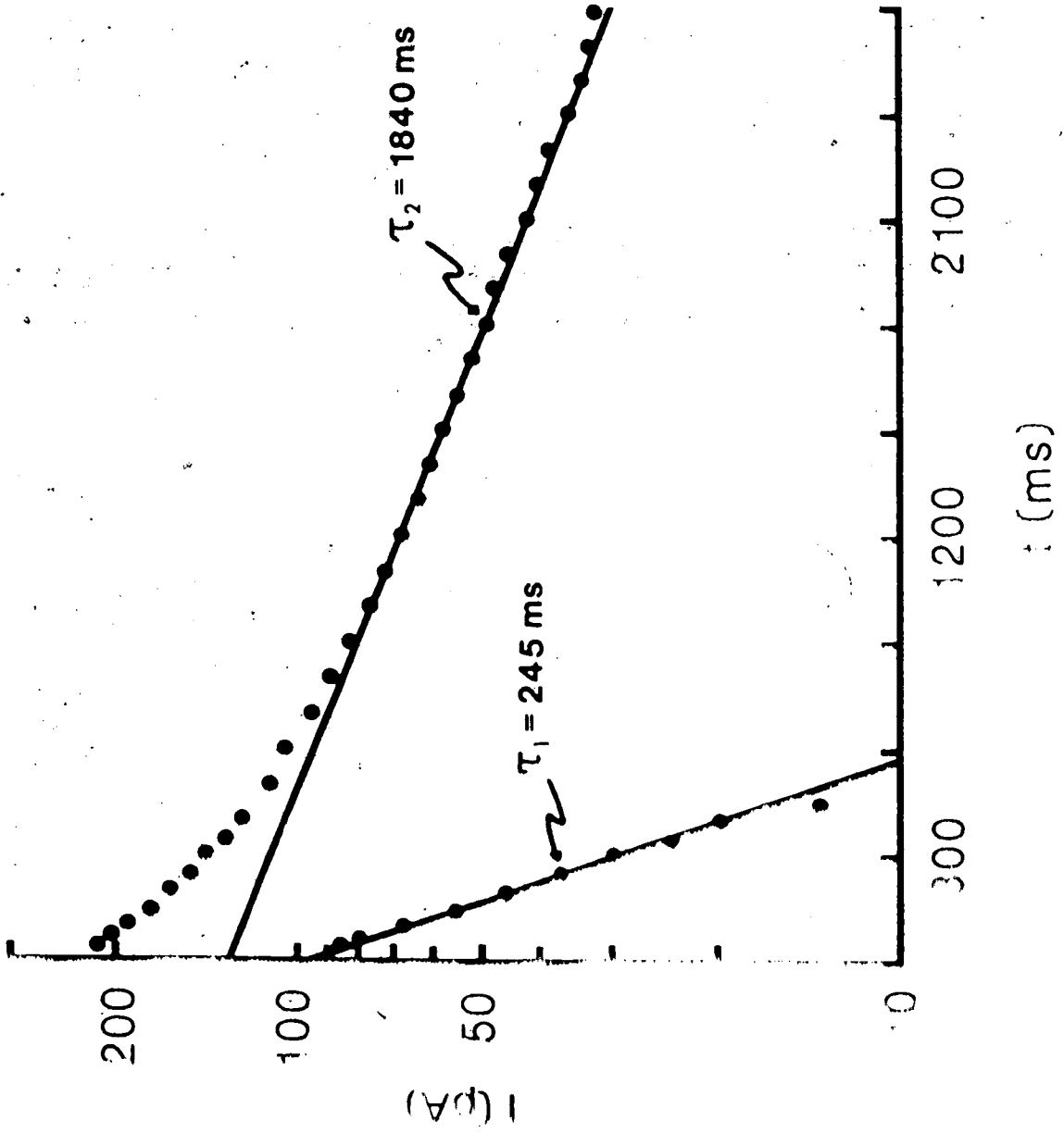


Figure 32. Semilogarithmic plot of tail current. Tail current following a depolarization to 38 mV was plotted as a function of time on semilog paper. Repolarization potential was -70 mV (same trace as in Figure 21). The major exponential had a time constant (τ_2) of 1840 ms and an amplitude (A_2) of 131 pA. The faster exponential is the difference between the total current and the straight line fit to the late portion of the current. The minor exponential had a time constant (τ_1) of 245 ms and an amplitude (A_1) of 100 pA).



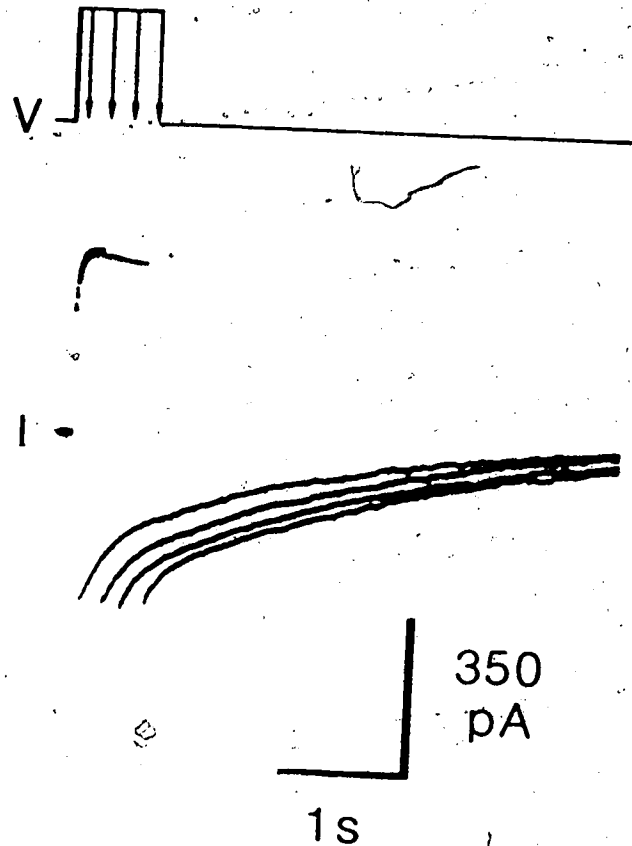


Figure 33. Effect of test pulse duration on tail currents. Depolarizing test pulse duration was varied as indicated (V). Test pulse was to 22 mV from a holding potential of 70 mV. Four current responses are superimposed (80, 240, 400, 600 ms). External solution was normal containing 10^{-7} M TTX and $1.0 \text{ } \mu\text{M}$ Ca^{2+} . Pipette solution was 60 Cl. Seal resistance was $1.00 \text{ } \Omega$, was $2 \text{ M}\Omega$. Input resistance of the amplifier was $2 \text{ } \times 10^9$.

Table 5. Effect of depolarizing test pulse duration on tail currents. Test pulse was to 22 mV from a holding potential of -70 mV. Duration was increased from 80 to 1,000 msec. Tail currents were plotted on semilog paper and the two exponentials separated (see Figure 32). Data from same myoball as in Figure 33.

Duration (msec)	A_1 (pA)	A_2 (pA)	$(A_1 + A_2)$ (pA)	$A_1 / (A_1 + A_2)$
80	141	272	413	0.35
120	139	295	434	0.32
160	129	317	446	0.29
200	121	311	432	0.28
240	111	300	411	0.27
400	88	319	407	0.22
600	66	314	380	0.17
1,000	55	311	366	0.15

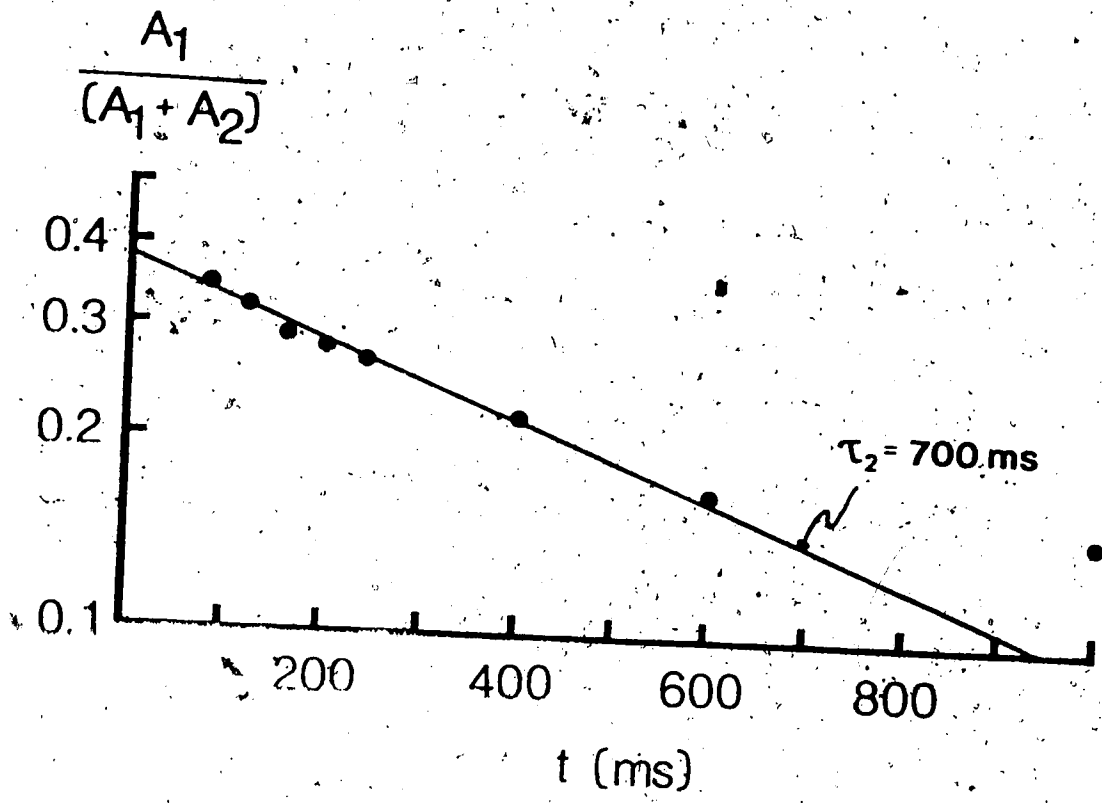
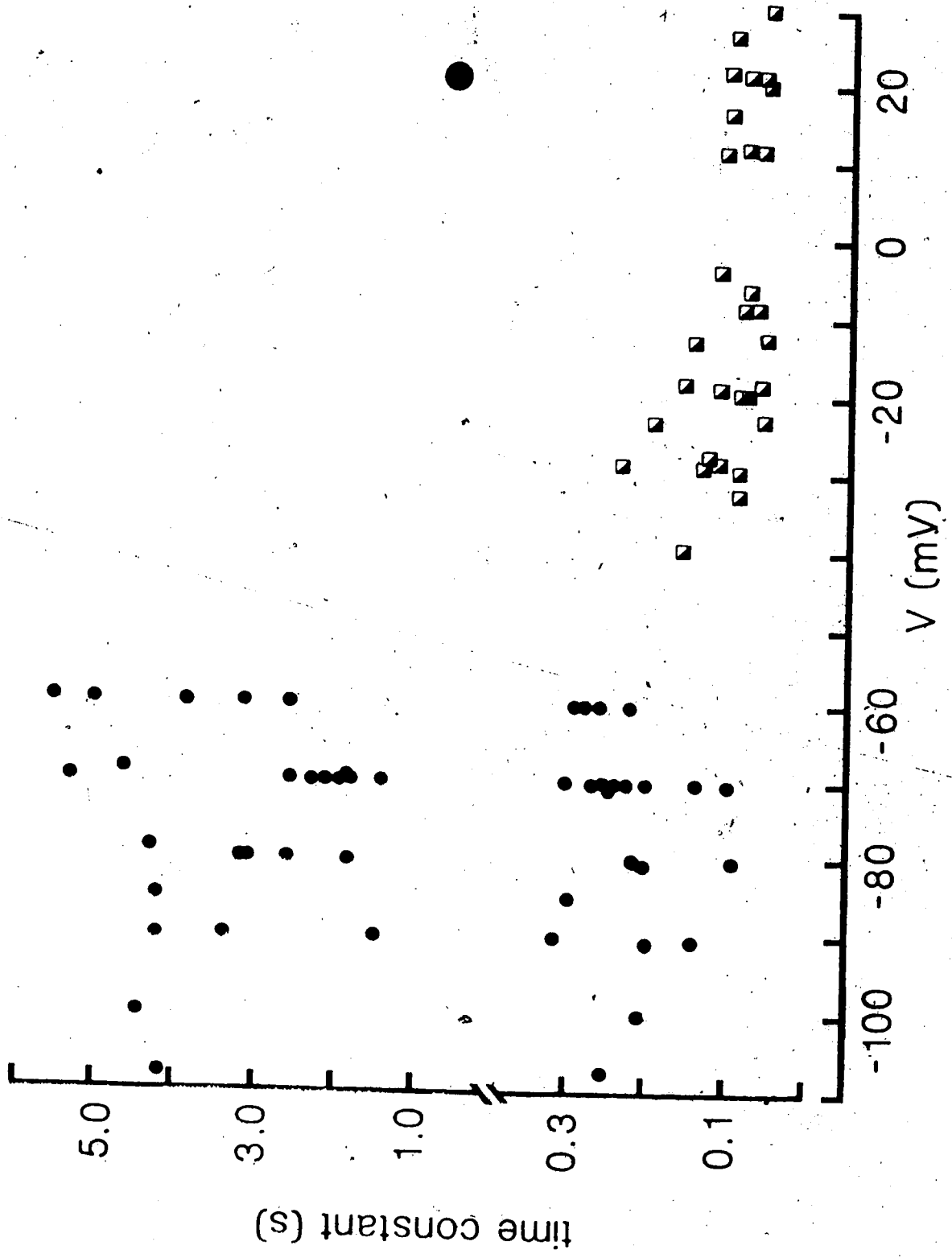


Figure 34. Semilogarithmic plot of tail current amplitude as a function of test pulse duration. $A_1/(A_1 + A_2)$ was plotted semilogarithmically versus duration of the depolarizing test pulse. Data from Table 5.

Figure 35. Time constants as a function of voltage. Time constants obtained from activation and deactivation of Cl^- currents are plotted versus membrane potential. Tail currents were fit with the sum of two exponentials as shown in Figure 32. Time constants from tail currents are represented by small circles. Time constant represented by the large circle is from Figure 34. Time constants obtained from activation of currents are represented by half-filled squares (data same as Figure 31). Note that the ordinate is broken.

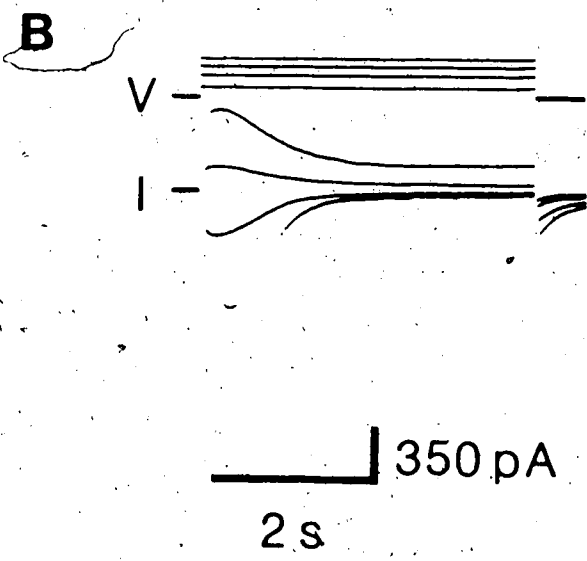
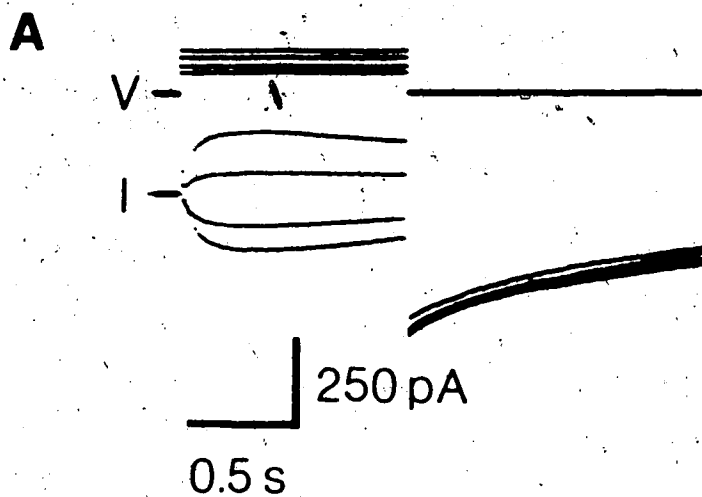


The other time constant (τ_0) obtained from activation is not shown (see Figure 30). In all, there were three measurable time constants.

Membrane currents in isolated myoballs

Chloride currents: Cl^- currents were recorded from myoballs that had formed spontaneously from enzymatically dissociated muscle fibers. Cl^- currents were found in myoballs obtained from 15 to 21 day embryos. The currents reversed at the potential predicted for Cl^- and showed the same kinetic properties as the currents recorded from myoballs grown in tissue culture (Figure 36A). In some myoballs, the currents declined under maintained depolarization (Figure 36B). This decline in current was also observed by Fukuda *et al* (1976b). The declining phase of the current could be fitted with a single exponential. Time constants for the decline were longer at positive than at negative membrane potentials. For example, in one myoball, current declined with a time constant of 410 ms for a step to -45 mV. For steps to more positive potentials, the time constants became longer and for a step to 52 mV, the time constant was 1400 ms. This behavior is opposite to that exhibited by currents which have voltage-dependent inactivation, i.e. the rate of decline is faster at more depolarized potentials (Hodgkin & Huxley, 1952b). Also, a plot of current magnitude versus rate of decline was nearly linear, i.e. the larger the current, the faster it declined. These

Figure 36. Chloride currents from isolated myoballs. Cl^- currents were recorded under voltage clamp from a myoball obtained from 19 day embryonic intercostal muscles. Part A shows the currents recorded during step depolarizations from a holding potential of -60 mV. Four traces are superimposed. Diameter of myoball was $32 \mu\text{m}$. Peak current density was $7 \mu\text{A}/\text{cm}^2$. Records in B were obtained from a myoball isolated from 20 day intercostal muscles. Diameter was $27 \mu\text{m}$. Peak inward current density was $31 \mu\text{A}/\text{cm}^2$. External solution was normal containing 10^{-7} M TTX and 1.0 mM Cd^{2+} . Pipette solution was K^+ -free.



observations suggested that the decline of the currents resulted from ion accumulation and/or depletion. Perhaps some of the Cl^- channels may be located in a place where they see a restricted space, e.g. the transverse tubular system.

Other currents: Myoballs obtained from muscles of a particular age showed great variability with regard to the type and density of membrane currents. Hence, only very general conclusions could be made about the development of excitability. At the earliest ages studied, 13-14 days, most of the myoballs had no voltage- and time-dependent currents. Outward currents were found in a small percentage of myoballs. Figure 37 shows outward currents recorded from a myoball obtained from a 16 day muscle. These types of currents were absent when the pipette solution contained TEA and were presumably K^+ currents.

Small, TTX-sensitive currents were found in myoballs obtained from 17 to 21 day muscles and were probably carried by Na^+ . An interesting observation was made for this current. If the myoballs were kept overnight in tissue culture, the current density increased about 25 fold. For example, for fresh 17 day myoballs the inward current density averaged $13 \mu\text{A}/\text{cm}^2$. After overnight incubation, current density had increased to around $300 \mu\text{A}/\text{cm}^2$. This value was much greater than for freshly isolated 18 day myoballs (Figure 38 & 39). It was as if the expression of Na^+ channels was being suppressed by something in the embryo.

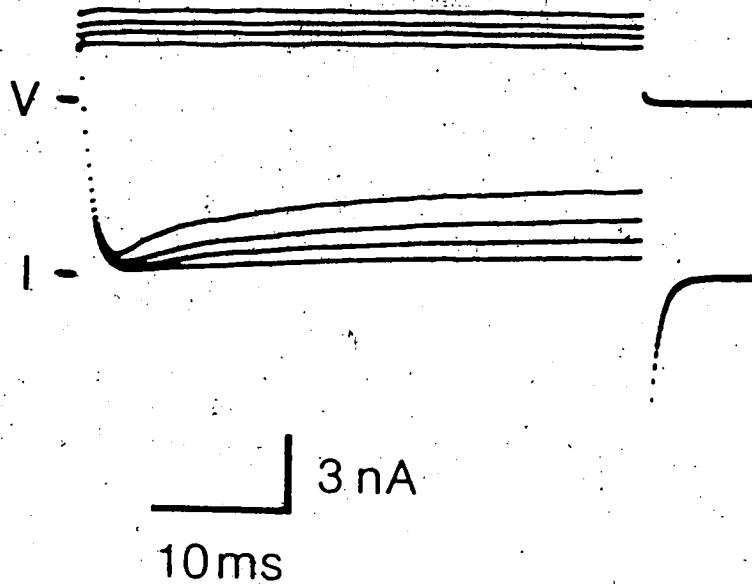


Figure 37. Outward currents from isolated myoball. Currents were recorded under voltage clamp. Depolarizing voltage steps were applied from a holding potential of -70 mV. Four traces are superimposed. Myoball was obtained from 16 day embryonic intercostal muscles. External and pipette solutions were normal.

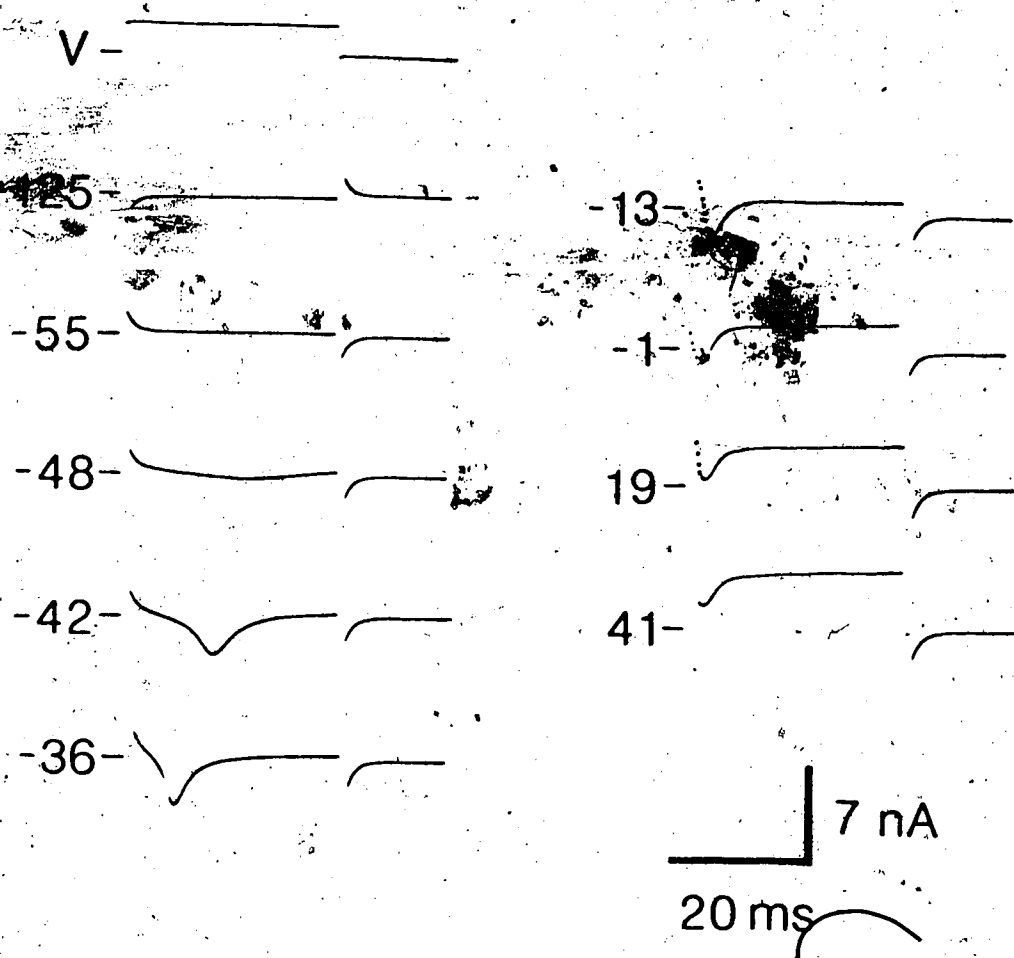
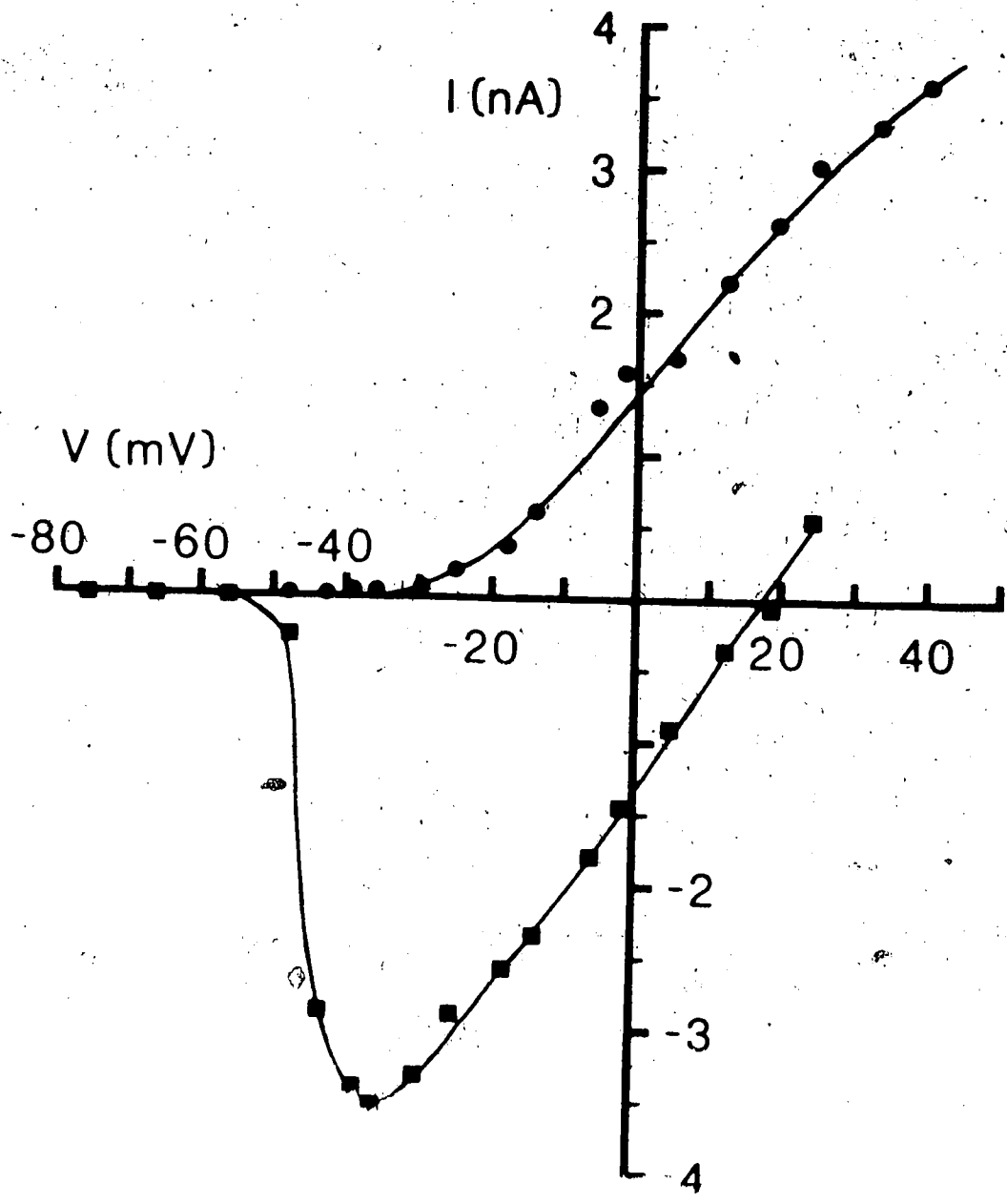


Figure 38. Inward and outward currents from isolated myoballs. Currents were recorded under voltage clamp from a myoball that had been obtained from 18 day intercostal muscles and kept overnight in tissue culture. Depolarizing test potential is noted beside each trace. Holding potential was -90 mV. External and pipette solutions were normal. Seal resistance was 5 G Ω . R_s was 17 M Ω . Input resistance of pipette was 5 M Ω . Traces 7, 8 and 9 were retouched.

Figure 39. Current-voltage plot of inward and outward currents. Plot of peak inward currents (squares) and steady-state current (circles) as a function of depolarizing test potential. Diameter of myoball was $27.5 \mu\text{m}$. Peak inward current density was 14.9 mA/cm^2 and outward current density was 15.4 mA/cm^2 (measured at -40 mV). Data from currents shown in Figure 38 and from additional steps.



Sherman *et al.* (1982) have also observed an increase, although not as large, in Na^+ channel density following denervation of developing rat muscle. In addition, it has been reported that slow-tonic muscle of the frog, which normally does not have Na^+ channels, expresses them following denervation (Cull-Candy, Miledi & Uchitel, 1980).

In summary, it appeared that the outward currents were the first to appear during development. The inward Cl^- currents appeared next and then the Na^+ currents.

D. DISCUSSION

Chloride currents in embryonic chick muscle

The whole-cell patch clamp technique (Hamill *et al.*, 1981) was found to provide adequate voltage control of the surface membranes of myoballs obtained from chick skeletal muscles. Slow membrane currents were recorded from myoballs grown in tissue culture (Figure 15) and from myoballs obtained from muscle that had developed *in vivo* (Figure 36). The currents were shown to be carried by Cl^- . The reversal potential for the currents varied with Cl^- concentrations according to the values predicted by the Nernst equation (Figure 18). Also, the currents were blocked by the stilbene derivatives, STS and DIDS (Figure 19) which have been shown to block Cl^- permeability in a variety of cell types (Knauf & Pothslein, 1971; Vaughan & Fong, 1977). Presumably, the

openings of 'Cl⁻ channels', as yet hypothetical macromolecules embedded in the membrane which permit transmembrane Cl⁻ movements.

The Cl⁻ currents were shown to produce a long duration action potential (Figure 14). Depolarization of the membrane potential was brought about by inward Cl⁻ currents, i.e. Cl⁻ ions were moving out of the myoballs. In order for a Cl⁻ action potential to be generated, the equilibrium potential for Cl⁻ must be more positive than the resting membrane potential. Therefore, the intracellular Cl⁻ concentration must be higher than that which would occur as a result of passive equilibration. This suggests that the embryonic chick fibers have an inward Cl⁻ pump. Inward Cl⁻ pumps have been shown to exist in squid axon (Keynes, 1963; Russell, 1979) and suggested to exist in some mammalian skeletal muscles (Dulhunty, 1978). Outward Cl⁻ pumps have been demonstrated in *Aplysia* neurones (Russell & Brown, 1972; Russell, 1978), in barnacle skeletal muscle (Russell & Brodwick, 1979) and in cat motor neurones (Lux, 1971; Llunas, Baker & Precht, 1974). The reversal potential of the Cl⁻ action potentials was around 20 to 25 mV in chick muscle fibers (Figure 2) (Kane, 1975). From the Nernst equation, this gives an intracellular Cl⁻ concentration of about 60 mM. The concentration was probably not as high in cultured chick muscle as the reversal potential of the action potential was more negative (-50 mV). This may be the reason that the membrane potential of the action potential must be

injected intracellularly in order to elicit Cl^- action potentials in cultured muscle (Fukuda, 1974; Spector & Prives, 1977).

In cultured chick myotubes, it has been observed that the depolarization phase of the Cl^- action potential coincided with the development of contractures, while the repolarization phase coincided with relaxation (Spector & Prives, 1977). In developing p.l.d. muscles of the chick, extremely long duration contractions have been recorded in response to 1 ms extracellular stimulation (Reiser & Stokes, 1982). The time course of these unusual contractions and the ages at which they occurred strongly suggest that the Cl^- action potential was involved. Thus, the Cl^- action potential appears to be involved in excitation-contraction coupling in the embryonic fibers.

Comparison with other chloride channels

Very few voltage independent Cl^- channels have been studied in detail. Of the other Cl^- channels, only the channel from *Loxopoda* electroplex membranes is similar to the Cl^- channel studied here. *Loxopoda* Cl^- channels were incorporated into planar phospholipid bilayers and studied under voltage clamp. Single channel conductance has been reported to be about 15 pS (White & Miller, 1972; 1981). Single channel behavior is extremely complex and the channels displayed multiple conductance levels and non-linear I-V characteristics. The channels were reported to be

channels showed sigmoidal dependence of conductance on voltage (Figure 24). Conductance was low (channels closed) at negative potentials and high (channels open) at positive potentials (White & Miller, 1979). An exact correlation of conductance with absolute membrane potential is not possible since the position of the conductance curve along the voltage axis was affected by the phospholipid composition of the bilayers. The voltage sensitivity of chick and *Torpedo* Cl⁻ channels was very similar. Conductance changed e-fold for an 11 mV depolarization as compared to an 8 mV change determined for chick Cl⁻ channels (Figure 26). Both conductances were blocked by SITS and DIDS (Figure 19) (White & Miller, 1979) and by SCN⁻ (Figure 19) (White & Miller, 1979). The kinetics of the macroscopic currents were not studied in detail for the *Torpedo* Cl⁻ channels. However, the currents did not show any inactivation which was the case for the Cl⁻ currents in this study (Figure 15, 20). The turn-on and the turn-off of the macroscopic currents followed single exponential time courses. The rise times appeared to be much longer, on the order of tens of seconds, than those seen for chick Cl⁻ currents (Figure 15). Also, chick Cl⁻ currents clearly showed two exponentials during deactivation (Figure 32) while *Torpedo* Cl⁻ currents did not.

Interestingly, the kinetics of the channel-forming protein, voltage dependent anion conductance (VDAC), from outer mitochondrial membranes (Colombini, 1979) are reminiscent of the kinetics of the Cl⁻ currents studied here. The

kinetics of the macroscopic VDAC currents have not been studied in detail, but the following similarities were apparent (Colombini, 1979). Turn-on of the macroscopic current appeared to follow a single exponential time course with the rise time being very close to the 50-100 ms range found for chick Cl^- currents. Closing of the VDAC channels was very slow, on the order of seconds. There also appeared to be two exponential phases. This is very similar to the properties found for the chick Cl^- currents (Figure 32). However, the similarity between the two channels stops there. Single channel conductance for VDAC channels has been reported to be about 500 pS (Colombini, 1979). It is unlikely that the conductance of chick Cl^- channels is that high as the macroscopic currents would have been very noisy. Also, the dependence of conductance on voltage for the two channels is radically different. VDAC channels have been shown to open only over a very narrow range of potentials around 0 mV (Doring & Colombini, 1984)

Chloride current kinetics

The kinetics of the Cl^- currents were more complex than could be described by a simple Hodgkin Huxley kinetic model (1952b). According to their model, tail currents measured at very negative potentials should display a single exponential component. For chick Cl^- currents, however, there were clearly two exponential components even at very negative potentials (Figure 32). An alternative to the Hodgkin Huxley

model is to suppose that the channels must pass through a sequence of kinetically distinct states. Since three distinct time constants were measured (Figure 30, 35), there must be at least four kinetic states (Colquhoun & Hawkes, 1983). The following kinetic model was developed:



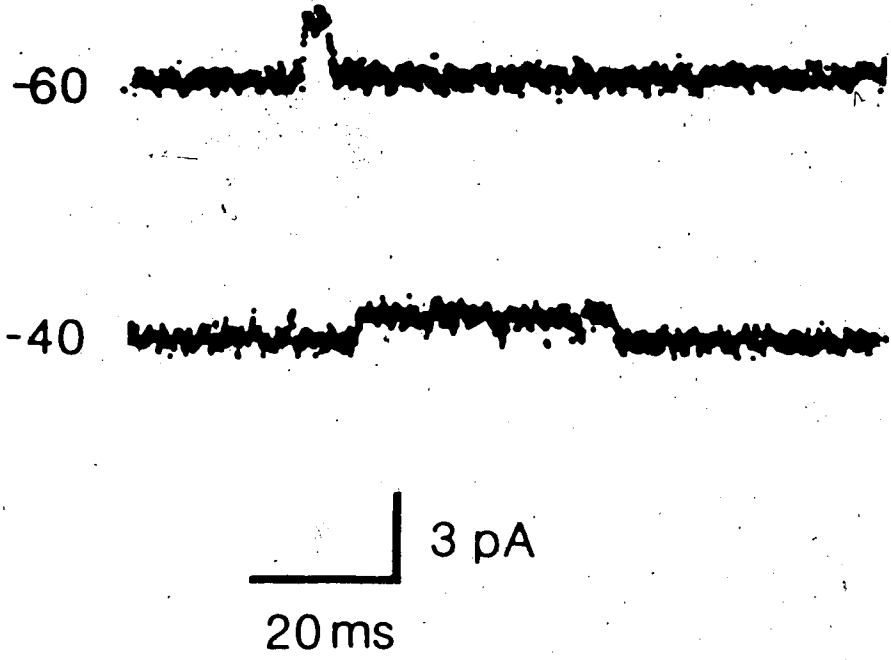
In this scheme, C_2 and C_1 represent closed states of the channel and O_1 and O_2 represent open states. The presence of the second closed state (C_2) was needed to account for the delay in activation (Figure 28). Although two closed states are indicated, the exact number may be greater than 2. The second open state (O_2) was needed to account for the slow exponential tail current component (Figure 21). Thus, during a depolarizing pulse, channels would enter the open states sequentially. When the membrane potential is repolarized, Cl^- current would decline rapidly as channels proceeded from O_1 to C_1 . But a slowly declining phase of current would also be present as channels in O_2 returned slowly to the closed states by way of O_1 .

Evidence to support the hypothesis that the channels have two kinetically distinct open states can be obtained by observing the kinetics of single channel currents. The amount of time spent in a given kinetic state (dwell time) has been shown to be exponentially distributed (cf Horn & Lange, 1983). Thus, it is predicted that the open time histograms of the Cl^- channels could be fitted with the sum of two exponentials. Attempts were made to record single

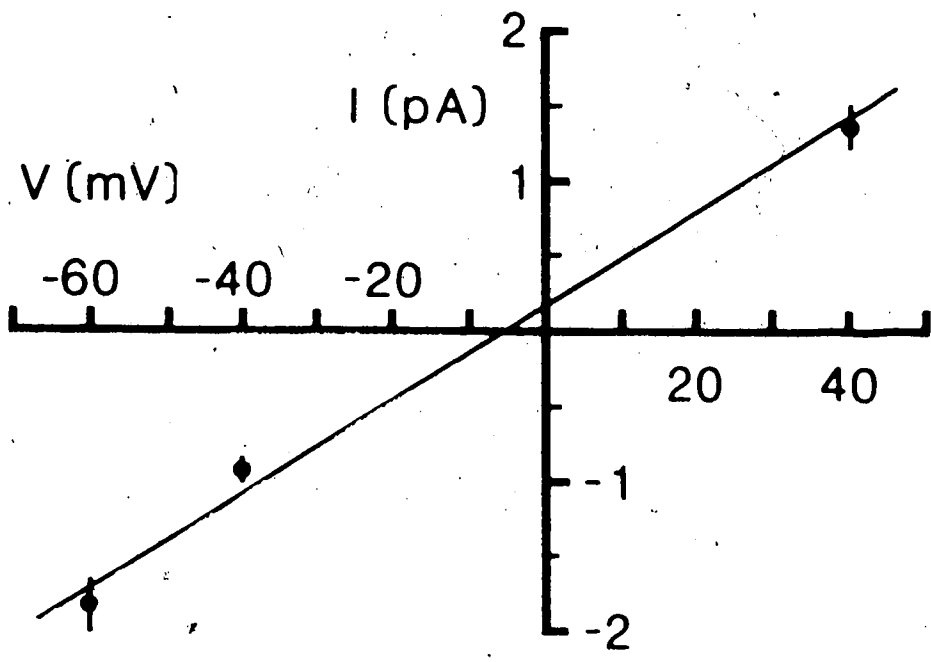
channel Cl^- currents in outside-out membrane patches. Single channel events could be recorded (Figure 40); however, no Cl^- channels with the appropriate voltage-dependent behavior were consistently observed. It was quite possible that the conductance was too small to be detected with the noise level of my set-up (any channel under 10 pS would have been difficult to detect). Or, perhaps the channel did not survive in outside-out membrane patches. Some channels, for example Ca^{2+} channels (Hagiwara & Byerly, 1981), require intracellular components for activity and do not survive long in excised membrane patches.

Figure 40. Single channel events. Single channel currents were recorded in outside-out membrane patches (see Figure 5) from cultured chick myoballs. Channel openings are displayed upwards (A). Holding potentials are indicated beside each current trace. External solution was normal containing 10^{-7} M TTX and 1.0 mM Cd^{2+} . Pipette solution was K^+ -free. Current-voltage plot gave a single channel conductance of 31 pS (B). Measured reversal potential was -5 mV. Values are means \pm S.D. for 15 channel openings.

A



B



REFERENCES

- Adrian, R.H. (1969). Rectification in muscle membrane. *Prog. Biophys. Molec. Biol.* 19: 339-369.
- Adrian, R.H. & Bryant, S.H. (1974). On repetitive discharge in myotonic muscle fibres. *J. Physiol.* 240: 505-515.
- Adrian, R.H., Chandler, W.K. & Hodgkin, A.L. (1970a). Voltage clamp experiments in striated muscle fibres. *J. Physiol.* 208: 607-644.
- Adrian, R.H., Chandler, W.K. & Hodgkin, A.L. (1970b). Slow changes in potassium permeability in skeletal muscle. *J. Physiol.* 208: 645-688.
- Adrian, R. & Freygang, W.H. (1962). The potassium and chloride conductance of frog muscle membrane. *J. Physiol.* 163: 61-103.
- Adrian, R.H. & Marshall, M.W. (1977). Sodium currents in mammalian muscle. *J. Physiol.* 268: 223-250.
- Adrian, R.H. & Peachey, L.D. (1965). The membrane capacity of frog twitch and slow fibres. *J. Physiol.* 181: 324-336.
- Albuquerque, E.X. & McIsaac, R.J. (1970). Fast and slow mammalian muscles after denervation. *Exper. Neurol.* 26: 183-202.
- Albuquerque, E.X. & Thesleff, S. (1968). A comparative study of membrane properties of innervated and chronically denervated fast and slow muscles of the rat. *Acta Physiol. Scand.* 73: 471-480.
- Almers, W. (1972). Potassium conductance changes in skeletal muscle and the potassium concentration in the transverse tubules. *J. Physiol.* 225: 33-56.
- Almers, W. (1976). Differential effects of tetracaine on delayed potassium channels and displacement currents in frog muscle. *J. Physiol.* 312: 159-176.
- Almers, W., Fink, R. & Palade, P.T. (1981). Calcium depletion in muscle tubules: the decline of calcium current under maintained depolarization. *J. Physiol.* 312: 177-207.

- Almers, W. & Levinson, S.R. (1975). Tetrodotoxin binding to normal and depolarized frog muscle and the conductance of a single sodium channel. *J. Physiol.* 247: 483-509.
- Almers, W. & Palade, P.T. (1981). Slow calcium and potassium currents across frog muscle membrane: measurements with a vaseline-gap technique. *J. Physiol.* 312: 159-176.
- Armstrong, C.M. (1975). Potassium pores of nerve and muscle membranes. In: *Membranes: A Series of Advances*, Vol. 3, ed. Eisenman, G. pp. 325-358. New York: Dekker.
- Armstrong, C.M. (1981). Sodium channels and gating currents. *Physiol. Rev.* 61(3): 644-683.
- Askanas, V. & Hee, D. (1973). Histochemistry of cultured embryonic and regenerating rat muscle. *J. Histochem. Cytochem.* 21: 785-793.
- Askanas, V., Hee, D. & Milhorat, A.T. (1972). Histochemistry of aneural chicken and rat muscle in tissue culture. *J. Histochem. Cytochem.* 20: 849-850.
- Askanas, V., Shafiq, S.A. & Milhorat, A.T. (1972). Histochemistry of cultured aneural chick muscle. Morphological maturation of fiber type. *Exp. Neurol.* 37: 218-230.
- Atsumi, S. (1977). Development of neuromuscular junctions of fast and slow muscles in the chick embryo: a light and electron microscopic study. *J. Neurocyt.* 6: 691-709.
- Atwood, H.L. & Kwan, I. (1978). Dystrophic and normal mice show age-dependent divergence of muscle Na concentrations. *Exper. Neurol.* 60: 386-392.
- Bacou, F. & Nougues, J. (1980). Alterations of enzymatic activities during red and white muscle differentiation *in vitro*. *Exp. Cell Res.* 129: 455-460.
- Barchi, R.L. & Weigele, J.B. (1979). Characteristics of saxitoxin binding to the sodium channel of sarcolemma isolated from rat skeletal muscle. *J. Physiol.* 295: 383-396.
- Barlow, J.S. & Manery, J.F. (1954). The changes in electrolytes, particularly chloride, which accompany growth in chick muscle. *J. Cell Physiol.* 43: 165-191.

- Barrett, J.N., Magleby, K.L. & Pallotta, B.S. (1982). Properties of single calcium-activated potassium channels in cultured rat muscle. *J. Physiol.* 331: 211-230.
- Bastian, J. & Nakajima, S. (1974). Action potential in the transverse tubules and its role in the activation of skeletal muscle. *J. Gen. Physiol.* 63: 257-278.
- Beam, K.G. & Donaldson, P.L. (1983a). A quantitative study of potassium channel kinetics in rat skeletal muscle from 1 to 37°C. *J. Gen. Physiol.* 81: 485-512.
- Beam, K.G. & Donaldson, P.L. (1983b). Slow components of potassium tail currents in rat skeletal muscle. *J. Gen. Physiol.* 81: 513-530.
- Bekoff, A. & Betz, W.J. (1977a). Physiological properties of dissociated muscle fibres obtained from innervated and denervated adult rat muscle. *J. Physiol.* 271: 25-40.
- Bekoff, A. & Betz, W.J. (1977b). Properties of isolated adult rat muscle fibres maintained in tissue culture. *J. Physiol.* 271: 537-547.
- Bennett, M.V.L. (1961). Modes of operation of electric organs. *Ann. N.Y. Acad. Sci.* 94: 458-509.
- Bennett, R. & Pettigrew, A.G. (1974). The formation of synapses in striated muscle during development. *J. Physiol.* 241: 515-545.
- Betz, W.J. & Sakmann, B. (1973). Effects of proteolytic enzymes on function and structure of frog neuromuscular junctions. *J. Physiol.* 230: 673-688.
- Bezanilla, F., Caputo, C., González-Serratos, H. & Venosa, H. (1972). Sodium dependence on the inward spread of activation in isolated twitch muscle fibres of the frog. *J. Physiol.* 223: 507-523.
- Blatz, A.L. & Magleby, K.L. (1983). Single voltage-dependent chloride-selective channels of large conductance in cultured rat muscle. *Biophys. J.* 43: 237-241.
- Bondi, A.Y. & Chiarandini, D.J. (1979). Ionic basis for electrical properties of tonic fibres in rat extraocular muscles. *J. Physiol.* 295: 273-281.
- Bryant, S.H. & Morales-Aguilera, A. (1971). Chloride conductance in normal and myotonic fibres and the action of monocarboxylic aromatic acids. *J. Physiol.* 219: 367-383.

- Burke, W. & Ginsborg, B.L. (1956). The electrical properties of the slow muscle fibre membrane. *J. Physiol.* 132: 586-598.
- Cabantchik, Z.I., Knauf, P.A. & Rothstein, A. (1978). The anion transport system of the red blood cell. The role of membrane protein evaluated by the use of 'probes'. *Biochim. Biophys. Acta* 515: 240-302.
- Cabantchik, Z.I. & Rothstein, A. (1974). Membrane proteins related to anion permeability of human red blood cells. I. Localization of disulfonic stilbene binding sites in proteins involved in permeation. *J. Membrane Biol.* 15: 207-226.
- Camerino, D. & Bryant, S.H. (1976). Effects of denervation and colchicine treatment of rat skeletal muscle. *J. Neurobiol.* 7: 221-228.
- Campbell, D.T. (1976). Ionic selectivity of the sodium channel of frog skeletal muscle. *J. Gen. Physiol.* 67: 295-307.
- Campbell, D.T. & Hille, B. (1976). Kinetic and pharmacological properties of the sodium channel of frog skeletal muscle. *J. Gen. Physiol.* 67: 309-323.
- Caputo, C. & Dipolo, R. (1973). Ionic diffusion delays in the transverse tubules of frog twitch muscle fibres. *J. Physiol.* 229: 547-557.
- Chenoy-Marchais, D. (1982). A Cl^- conductance activated by hyperpolarization in *Aplysia* neurones. *Nature* 299: 359-361.
- Chiarandini, D.J. & Stefani, E. (1979). Electrophysiological identification of two types of fibres in rat extra ocular muscles. *J. Physiol.* 290: 453-465.
- Chutkow, J.G. (1973). Magnesium, potassium and sodium in 'red' and 'white' muscle in the rat (37337). *Proc Soc. Exp. Biol. Med.* 143: 430-432.
- Colombini, M. (1979). A candidate for the permeability pathway of the outer mitochondrial membrane. *Nature* 279: 643-645.
- Colquhoun, D. & Hawkes, A.G. (1983). The principles of the stochastic interpretation of ion-channel mechanisms. In: *Single channel Recording*. eds. Sakmann, B. & Neher, E. New York: Plenum Press.

- Colquhoun, D., Rang, H.P. & Ritchie, J.M. (1974). The binding of tetrodotoxin and α -bungarotoxin to normal and denervated mammalian muscle. *J. Physiol.* 240: 199-226.
- Coronado, R. & Latorre, R. (1982). Detection of K and Cl channels from calf cardiac sarcolemma in planar bilayer membranes. *Nature* 298: 849-852.
- Costantin, L.L. (1970). The role of sodium current in the radial spread of contraction in frog muscle fibers. *J. Gen. Physiol.* 55: 703-715.
- Cota, G., Nicola Siri, L. & Stefani, E. (1983). Calcium-channel gating in frog skeletal muscle membrane: effect of temperature. *J. Physiol.* 338: 395-412.
- Cull-Candy, S.G., Miledi, R. & Uchitel, O.D. (1980). Induction of action potentials in cultured slow muscle fibres of frog. *J. Physiol.* 299: 197-202.
- Cullen, M.J., Harris, J.B., Marshall, M.W. & Ward, M.R. (1975). An electrophysiological and morphological study of normal and denervated chicken latissimus dorsi muscles. *J. Physiol.* 245: 371-385.
- DeCoursey, T.E., Dempster, J. & Hutter, O.F. (1984). Inward rectifier current noise in frog skeletal muscle. *J. Physiol.* 349: 299-327.
- Diamond, J. & Miledi, R. (1962). A study of foetal and new-born rat muscle fibres. *J. Physiol.* 162: 393-408.
- Doring, C. & Colombini, M. (1984). On the nature of the molecular mechanism underlying the voltage dependence of the channel-forming protein, voltage-dependent anion selective channel (VDAC). *Biophys. J.* 45: 44-46.
- Dulhunty, A.F. (1978). The dependence of membrane potential on extracellular chloride concentration in mammalian skeletal muscle fibres. *J. Physiol.* 276: 67-82.
- Dulhunty, A.F. (1979). Distribution of potassium and chloride permeability over the surface and T-tubule membrane of mammalian skeletal muscle. *J. Membrane Biol.* 45: 293-310.
- Duval, A. & Léoty, C. (1978). Ionic currents in mammalian fast skeletal muscle. *J. Physiol.* 278: 403-423.

- Duval, A. & Léoty, C. (1980a). Ionic currents in slow twitch skeletal muscle in the rat. *J. Physiol.* 307: 23-41.
- Duval, A. & Léoty, C. (1980b). Comparison between the delayed outward current in slow and fast twitch skeletal muscles in the rat. *J. Physiol.* 307: 43-57.
- Eaton, D.C. (1972). Potassium ion accumulation near a pace-making cell of *Aplysia*. *J. Physiol.* 224: 421-440.
- Ehrenspeck, G. & Brodsky, W.A. (1976). Effects of 4-acetamido-4'-isothiocyano-2,2'-disulfonic stilbene on ion transport in turtle bladders. *Biochim. Biophys. Acta* 419: 555-558.
- Eisenberg, R.S. & Gage, P.W. (1969). Ionic conductances of the surface and transverse tubular membranes of frog sartorius fibers. *J. Gen. Physiol.* 53: 279-297.
- Engel, E., Barcilon, V. & Eisenberg, R.S. (1972). The interpretation of current-voltage relations recorded from a spherical cell with a single microelectrode. *Biophys. J.* 12: 384-403.
- Farnbach, G.C., Brown, M.J. & Barchi, R.L. (1978). A maturational defect in passive membrane properties of dystrophic mouse muscle. *Exp. Neurol.* 62: 539-554.
- Fedde, M.R. (1969). Electrical properties and acetylcholine sensitivity of singly and multiply innervated avian muscle fibers. *J. Gen. Physiol.* 53: 624-637.
- Fenwick, E.M., Marty, A. & Neher, E. (1982). A patch clamp study of bovine chromaffin cells and of their sensitivity to acetylcholine. *J. Physiol.* 331: 577-597.
- Fleiss, R. & Lüttgau, H.C. (1974). An evaluation of the membrane constants and the potassium conductance in metabolically exhausted muscle fibers. *J. Physiol.* 263: 215-238.
- Fleiss, R., G.D., Nameroff, M. & Nelson, P.G. (1971). Electrical properties of chick skeletal muscle fibers developing in cell culture. *J. Cell Physiol.* 78: 289-300.
- Fleiss, R., Lombet, A., Vigne, P., Romey, G. & Lazdunski, M. (1981). The appearance of voltage-sensitive Na⁺ channels during the *in vitro* differentiation of embryonic chick skeletal muscle. *J. Physiol.* 313: 239-254.

- Fukuda, J. (1974). Chloride spike: a third type of action potential in tissue-cultured skeletal muscle cells from the chick. *Science* 185: 76-78.
- Fukuda, J. (1975). Voltage clamp study on inward chloride currents of spherical muscle cells in tissue culture. *Nature* 257: 408-410.
- Fukuda, J., Henkart, M.P., Fischbach, G.D. & Smith, T.G. Jr. (1976a). Physiological and structural properties of colchicine-treated chick skeletal muscle cells grown in tissue culture. *Devl. Biol.* 49: 395-411.
- Fukuda, J., Fischbach, G.D. & Smith, T.G. Jr. (1976b). A voltage clamp study of the sodium, calcium and chloride spikes of chick muscle cells grown in tissue culture. *Devl. Biol.* 49: 412-424.
- Gaffney, C.T. & Mullins, L.J. (1958). Ion fluxes during the action potential in *Chara*. *J. Physiol.* 144: 505-524.
- Gardner, W. & Eisenberg, R.S. (1969). Action potentials, afterpotentials and excitation-contraction coupling in frog sartorius fibers without transverse tubules. *J. Gen. Physiol.* 53: 298-310.
- Gilly, W.F. & Hui, C.S. (1980). Membrane electrical properties of frog slow muscle fibres. *J. Physiol.* 301: 157-173.
- Ginsborg, B.L. (1960a). Spontaneous activity in muscle fibres of the chick. *J. Physiol.* 150: 707-717.
- Ginsborg, B.L. (1960b). Some properties of avian skeletal muscle fibres with multiple neuromuscular junctions. *J. Physiol.* 154: 581-598.
- González-Serratos, H. (1971). Inward spread of activation in muscle fibres. *J. Physiol.* 212: 777-799.
- Groves, T., Perry, R., Tuffery, A.R. & Vrbová, G. (1974). Possible mechanisms determining synapse formation in developing skeletal muscles of the chick. *Cell Tiss. Res.* 155: 13-25.
- Groves, T., Purves, R.D. & Vrbová, G. (1977). Differentiation of electrical and contractile properties of slow and fast muscle fibres. *J. Physiol.* 269: 535-547.
- Groves, T., Vrbová, G. & Wilcock, G. (1981). The influence of innervation on differentiating tonic and twitch muscle fibres of the chick. *J. Physiol.* 319: 161-169.

- Hagiwara, S. & Byerly, L. (1981). Calcium channel. *Ann. Rev. Neurosci.* 4: 69-125.
- Hamill, O.P., Marty, A., Neher, E., Sakmann, B. & Sigworth, F.J. (1981). Improved patch-clamp techniques for high-resolution current recording from cells and cell-free membrane patches. *Pflugers Arch.* 391: 85-100.
- Hanke, W. & Miller, C. (1983). Single chloride channels from *Torpedo* electroplax. Activation by protons. *J. Gen. Physiol.* 82: 25-45.
- Hansen Bay, C.M. & Strichartz, G.R. (1980). Saxitoxin binding to sodium channels of rat skeletal muscles. *J. Physiol.* 300: 89-103.
- Harris, A.J. (1974). Inductive functions of the nervous system. *Ann. Rev. Physiol.* 36: 251-305.
- Harris, J.B. & Marshall, M.W. (1973). Tetrodotoxin-resistant action potentials in newborn rat muscles. *Nature, New Biol.* 243: 191-192.
- Harris, J.B. & Thesleff, S. (1971). Studies of tetrodotoxin resistant action potentials in denervated skeletal muscle. *Acta Physiol. Scand.* 83: 382-388.
- Harvey, A.L. (1980). Action of drugs on developing skeletal muscle. *Pharmac. Ther.* 11: 1-41.
- Hess, A. (1970). Vertebrate slow muscle fibers. *Physiol. Rev.* 50: 40-62.
- Hess, A. & Pilar, G. (1963). Slow fibres in the extraocular muscles of the cat. *J. Physiol.* 169: 780-798.
- Hess, S. (1981). The interaction of potassium with the activation of anomalous rectification in frog muscle membrane. *J. Physiol.* 317: 497-508.
- Hille, B. (1970). Ionic channels in nerve membranes. In *Progress in Biophysics*, Vol. 21, ed. Butler, J.A.V. & Noble, D. pp. 3-32. Oxford: Pergamon.
- Hille, B. (1975). Ionic selectivity of Na and K channels of nerve membranes. In *Membranes - A Series of Advances*, Vol. 3, Dynamic Properties of Lipid Bilayers and Biological Membranes, ed. Eisenman, G., Chap. 4. New York: Marcel Dekker, Inc.
- Hille, B. (1976). Gating in sodium channels of nerve. *Ann. Rev. Physiol.* 38: 139-152.

- Hille, B., Bennett, M.V.L. & Grundfest, H. (1965). Voltage clamp measurements of the Cl^- conductance changes in skate electroplaques. *Biol. Bull.* 129: 407-408.
- Hille, B. & Campbell, D.T. (1976). An improved vaseline gap voltage clamp for skeletal muscle fibers. *J. Gen. Physiol.* 67: 265-293.
- Hodgkin, A.L. & Horowicz, P. (1959). The influence of potassium and chloride ions on the membrane potential of single muscle fibres. *J. Physiol.* 148: 127-160.
- Hodgkin, A.L. & Horowicz, P. (1960). The effect of sudden changes in ionic concentrations of the membrane potential of single muscle fibres. *J. Physiol.* 153: 370-385.
- Hodgkin, A.L. & Huxley, A.F. (1952a). Currents carried by sodium and potassium ions through the membrane of the giant axon of *Loligo*. *J. Physiol.* 116: 449-472.
- Hodgkin, A.L. & Huxley, A.F. (1952b). A quantitative description of membrane current and its application to conduction and excitation in nerve. *J. Physiol.* 117: 500-544.
- Hodgkin, A.L., Huxley, A.F. & Katz, B. (1952). Measurement of current-voltage relations in the membrane of the giant axon of *Loligo*. *J. Physiol.* 116: 424-448.
- Hodgkin, A.L. & Nakajima, S. (1972). The effect of diameter on the electrical constants of frog skeletal muscle fibres. *J. Physiol.* 221: 105-120.
- Horn, R. & Lange, K. (1983). Estimating kinetic constants from single channel data. *Biophys. J.* 43: 207-223.
- Hubbard, S.J. (1963). The electrical constants and the component conductances of frog skeletal muscle after denervation. *J. Physiol.* 165: 443-456.
- Huerta, M. & Stefani, E. (1981). Potassium and caffeine contractures in fast and slow muscles of the chicken. *J. Physiol.* 318: 181-190.
- Hutter, O.F. & Noble, D. (1960). The chloride conductance of frog skeletal muscle. *J. Physiol.* 151: 89-102.
- Hutter, O.F. & Warner, A.E. (1967). The effect of pH on ^{36}Cl efflux from frog skeletal muscle. *J. Physiol.* 189: 127-143.

- Hutter, O.F. & Warner, A.E. (1972). The voltage dependence of the chloride conductance of frog muscle. *J. Physiol.* 227: 275-290.
- Ildefonse, M. & Rougier, O. (1972). Voltage-clamp analysis of the early current in frog skeletal muscle fibre using the double sucrose gap method. *J. Physiol.* 222: 373-395.
- Ildefonse, M. & Roy, G. (1972). Kinetic properties of the sodium current in striated muscle fibres on the basis of the Hodgkin-Huxley theory. *J. Physiol.* 227: 419-431.
- Ito, S. (1972). Effects of media of different ionic composition on the activation potential of anuran egg cells. *Dev. Growth & Differen.* 14: 217-227.
- Jack, J.J.B., Noble, D. & Tsien, R.W. (1975). *Electric Current Flow in Excitable Cells*. Oxford: Clarendon Press.
- Jaimovich, E., Venosa, R.A., Shrager, P. & Horowicz, P. (1976). Density and distribution of tetrodotoxin receptors in normal and detubulated frog sartorius muscle. *J. Gen. Physiol.* 67: 399-416.
- Jolesz, F. & Sreter, F.A. (1981). Development, innervation and activity-pattern induced changes in skeletal muscle. *Ann. Rev. Physiol.* 43: 531-552.
- Kano, M. (1975). Development of excitability in embryonic chick skeletal muscle cell. *J. Cell Physiol.* 86: 503-510.
- Kano, M. & Shimada, Y. (1973). Tetrodotoxin-resistant electric activity in chick skeletal muscle cells differentiated *in vitro*. *J. Cell Physiol.* 81: 85-90.
- Kano, M., Shimada, Y. & Ishikawa, K. (1972). Electrogenesis of embryonic chick skeletal muscle cells differentiated *in vitro*. *J. Cell Physiol.* 79: 363-366.
- Kano, M. & Yamamoto, M. (1977). Development of spike potentials in skeletal muscle cells differentiated *in vitro* from chick embryo. *J. Cell Physiol.* 90: 439-444.
- Katz, B. (1966). *Nerve, Muscle and Synapse*. pp. 16-19. New York: McGraw-Hill Book Co.
- Kenyon, J.L. & Gibbons, W.R. (1977). Effects of low-chloride solutions on action potentials of sheep cardiac Purkinje fibers. *J. Gen. Physiol.* 70: 635-660.

- Keynes, R.D. (1963). Chloride in the squid giant axon. *J. Physiol.* 169: 690-705.
- Kidokoro, Y. (1973). Development of action potentials in a clonal rat skeletal muscle cell line. *Nature, New Biol.* 241: 158-159.
- Kidokoro, Y. (1975a). Developmental changes of membrane electrical properties in a rat skeletal muscle cell line. *J. Physiol.* 244: 129-143.
- Kidokoro, Y. (1975b). Sodium and calcium components of the action potential in a developing skeletal muscle cell line. *J. Physiol.* 244: 145-159.
- Kirsch, G.E., Nichols, R.A. & Nakajima, S. (1977). Delayed rectification in the transverse tubules. Origin of the late after-potential in frog skeletal muscle. *J. Gen. Physiol.* 70: 1-21.
- Knauf, P.A. & Rothstein, A. (1971). Chemical modification of membranes. I. Effects of ~~sulphydryl and amino-reactive reagents on anion and cation permeability of the human red blood cell.~~ *J. Gen. Physiol.* 58: 190-210.
- Kolb, H.A. & Schwarze, W. (1984). Properties of a cation channel of large unit conductance in lymphocytes, macrophages and cultured muscle cells. *Biophys. J.* 45: 136-138.
- Kostyuk, P.G. (1984). Intracellular perfusion of nerve cells and its effect on membrane currents. *Physiol. Rev.* 64(2): 435-454.
- Kuffler, S.W. & Vaughan Williams, E.M. (1953a). Small nerve junctional potentials. The distribution of small motor nerves to frog skeletal muscle and the membrane characteristics of the fibres they innervate. *J. Physiol.* 121: 289-317.
- Kuffler, S.W. & Vaughan Williams, E.M. (1953b). Properties of the "slow" skeletal muscle fibres of the frog. *J. Physiol.* 121: 318-340.
- Land, B.R., Sastre, A. & Podleski, T.R. (1973). Tetrodotoxin-sensitive and -insensitive action potentials in myotubes. *J. Cell Physiol.* 82: 497-510.
- Latorre, R., Vergara, C. & Hidalgo, C. (1982). Reconstitution in planar lipid bilayers of a Ca-dependent K channel from transverse tubule membranes isolated from rabbit skeletal muscle. *Proc. Natl. Acad. Sci. USA* 79: 805-809.

- Lawrence, J.C. & Catterall, W.A. (1981). Tetrodotoxin-insensitive sodium channels. Ion flux studies of neurotoxin action in a clonal rat muscle cell line. *J. Biol. Chem.* 256: 6213-6222.
- Lebeda, F.J. & Albuquerque, E.X. (1975). Membrane cable properties of normal and dystrophic chicken muscle fibers. *Exp. Neurol.* 47: 544-557.
- Lebeda, F.J., Warnick, J.E. & Albuquerque, E.X. (1974). Electrical and chemosensitive properties of normal and dystrophic chicken muscles. *Exp. Neurol.* 43: 21-37.
- Leech, C.A. & Stanfield, P.R. (1981). Inward rectification in frog skeletal muscle fibres and its dependence on membrane potential and external potassium. *J. Physiol.* 319: 295-309.
- Llinas, R., Baker, R. & Precht, W. (1974). Blockage of inhibition by ammonium acetate action on chloride pump in cat trochlear motoneurons. *J. Neurophysiol.* 37(3): 522-532.
- Loo, D.D.F., McLarnon, J.G. & Vaughan, P.C. (1981). Some observations on the behaviour of chloride current-voltage relations in *Xenopus* muscle membrane in acid solutions. *Can. J. Physiol. Pharmacol.* 59: 7-13.
- Lorković, H. & Tomanek, R.J. (1977). Potassium and chloride in normal and denervated rat muscles. *Am. J. Physiol.* 232(3): C109-C114.
- Lux, H.D. (1971). Ammonium and chloride extrusion: hyperpolarizing synaptic inhibition in spinal motoneurons. *Science* 173: 555-556.
- Marty, A. & Neher, E. (1983). Tight-seal whole-cell recording. In: *Single-channel Recording*; eds. Sakmann, B. & Neher, E. New York: Plenum Press.
- McArdle, J.J., Michelson, L. & D'Alonzo, A.J. (1980). Action potentials in fast- and slow-twitch mammalian muscles during reinnervation and development. *J. Gen. Physiol.* 75: 655-672.
- Merickel, M., Gray, R., Chauvin, P. & Appel, S. (1981). Electrophysiology of human muscle in culture. *Exp. Neurol.* 72: 281-293.
- Miledi, R., Stefani, E. & Steinbach, A.B. (1971). Induction of the action potential mechanism in slow muscle fibres of the frog. *J. Physiol.* 217: 737-754.

- Moczydlowski, E. & Latorre, R. (1983). Gating kinetics of Ca-activated K channels from rat muscle incorporated into planar bilayers: evidence for two voltage-dependent Ca-binding reactions. *J. Gen. Physiol.* 82: 511-542.
- Morgan, D.L. & Proske, U. (1984). Vertebrate slow muscle: its structure, pattern of innervation and mechanical properties. *Physiol. Rev.* 64(1): 103-169.
- Mullins, L.J. (1962). Efflux of chloride ions during the action potential of *Nitella*. *Nature* 196: 986-987.
- Narahashi, T., Moore, J.W. & Scott, W.R. (1964). Tetrodotoxin blockage of sodium conductance increase in lobster giant axons. *J. Gen. Physiol.* 47: 965-974.
- Neher, E. & Stevens, C.F. (1977). Conductance fluctuations and ionic pores in membranes. *Ann. Rev. Biophys. Bioeng.* 6: 345-381.
- Nicola Siri, L., Sánchez, J.A. & Stefani, E. (1980). Effect of glycerol treatment on the calcium current of frog skeletal muscle. *J. Physiol.* 305: 87-96.
- Nougués, J. & Bacou, F. (1977). Enzymatic activities of muscle fibres differentiated *in vitro* from pectoralis major (white) and adductor magnus (red) muscles of chick embryo. *Experientia* 33: 714-716.
- Ohmori, H., Yoshida, S. & Hagiwara, S. (1981). Single K channel currents of anomalous rectification in cultured rat myotubes. *Proc. Natl. Acad. Sci. USA* 78(8): 4960-4964.
- Olmsted, J.B. & Borisy, G. (1973). Microtubules. *Ann. Rev. Biochem.* 42: 507-540.
- Page, S.G. (1969). Structure and some contractile properties of fast and slow muscles of the chicken. *J. Physiol.* 205: 131-145.
- Palade, P.T. & Barchi, R.L. (1977). Characteristics of the chloride conductance in muscle fibers of the rat diaphragm. *J. Gen. Physiol.* 69: 325-342.
- Pappone, P.A. (1980). Voltage-clamp experiments in normal and denervated mammalian skeletal muscle fibres. *J. Physiol.* 306: 377-410.
- Potreau, D. & Raymond, G. (1980). Calcium-dependent electrical activity and contraction of voltage-clamped frog single muscle fibres. *J. Physiol.* 307: 9-22.

- Purves, D. & Sakmann, B. (1974). Membrane properties underlying spontaneous activity of denervated muscle fibres. *J. Physiol.* 239: 125-153.
- Redfern, P. & Thesleff, S. (1971a). Action potential generation in denervated rat skeletal muscles. I. Quantitative aspects. *Acta Physiol. Scand.* 81: 557-564.
- Redfern, P. & Thesleff, S. (1971b). Action potential generation in denervated rat skeletal muscles. II. The action of tetrodotoxin. *Acta Physiol. Scand.* 82: 70-78.
- Reiser, P.J. & Stokes, B.T. (1982). Development of contractile properties in avian embryonic skeletal muscle. *Am. J. Physiol.* 242: C52-C58.
- Ridge, R.M. (1971). Different types of extrafusal muscle fibres in snake costocutaneous muscles. *J. Physiol.* 217: 393-418.
- Ritchie, A.K. & Fambrough, D.M. (1975). Electrophysiological properties of the membrane and acetylcholine receptor in developing rat and chick myotubes. *J. Gen. Physiol.* 66: 327-355.
- Ritchie, J.M. & Rogart, R.B. (1977). The binding of labeled saxitoxin to the sodium channels in normal and denervated mammalian muscle and in amphibian muscle. *J. Physiol.* 269: 341-354.
- Rudel, R. & Senges, J. (1972). Mammalian skeletal muscle: reduced chloride conductance in drug-induced myotonia and induction of myotonia by low-chloride solution. *Naunyn-Schmiedeberg's Arch. Pharmacol.* 274: 337-347.
- Russell, J.M. (1978). Effects of ammonium and bicarbonate on intracellular chloride levels in *Aplysia* neurons. *Biophys. J.* 22: 131-137.
- Russell, J.M. (1979). Chloride and sodium influx: a coupled uptake mechanism in squid giant axon. *J. Gen. Physiol.* 73: 801-818.
- Russell, J.M. & Brodwick, M.S. (1979). Properties of chloride transport in barnacle muscle fibers. *J. Gen. Physiol.* 73: 343-368.
- Russell, J.M. & Brown, A.M. (1972). Active transport of chloride by the giant neuron of the *Aplysia* abdominal ganglion. *J. Gen. Physiol.* 60: 499-518.

- Sánchez, J.A. & Stefani, E. (1978). Inward calcium current in twitch muscle fibres of the frog. *J. Physiol.* 283: 197-209.
- Sarkadi, B., Mack, E. & Rothstein, A. (1984). Ionic events during the volume response of human peripheral blood lymphocytes to hypotonic media. II. Volume- and time-dependent activation and inactivation of ion transport pathways. *J. Gen. Physiol.* 83: 513-528.
- Sastre, A. & Podleski, T.R. (1976). Pharmacological characterization of Na ionophores in L6 myotubes. *Proc. Natl. Acad. Sci. USA* 73: 1355-1359.
- Schein, S.J., Colombini, M. & Finkelstein, A. (1976). Reconstitution of planar lipid bilayers of a voltage-dependent anion-selective channel obtained from paramecium mitochondria. *J. Membrane Biol.* 30: 99-120.
- Schlichter, L.C. (1983). Spontaneous action potentials produced by Na and Cl channels in maturing *Rana pipiens* oocytes. *Devel. Biol.* 98: 47-59.
- Shami, Y., Rothstein, A. & Knauf, P.A. (1978). Identification of the Cl⁻ transport site of human red blood cells by a kinetic analysis of the inhibitory effects of a chemical probe. *Biochim. Biophys. Acta* 508: 357-363.
- Sherman, S.J. & Catterall, W.A. (1982). Biphasic regulation of development of the high-affinity saxitoxin receptor by innervation in rat skeletal muscle. *J. Gen. Physiol.* 80: 753-768.
- Sigworth, F.J. & Neher, E. (1980). Single Na channel currents observed in cultured rat muscle cells. *Nature* 287: 447-449.
- Singer, J.J. & Walsh, J.V. Jr. (1980). Passive properties of the membrane of single freshly isolated smooth muscle cells. *Am. J. Physiol.* 239(5): C153-C161.
- Spector, I. & Prives, J.M. (1977). Development of electrophysiological and biochemical membrane properties during differentiation of embryonic skeletal muscle in culture. *Proc. Natl. Acad. Sci. USA* 74: 5166-5170.
- Spitzer, N.C. (1979). Ion channels in development. *Ann. Rev. Neurosci.* 2: 363-397.

- Sreter, F.A. & Woo, G. (1963). Cell water, sodium and potassium in red and white mammalian muscles. *Am. J. Physiol.* 205: 1290-1294.
- Standen, N.B. & Stanfield, P.R. (1978). A potential- and time-dependent blockade of inward rectification in frog skeletal muscle fibres by barium and strontium ions. *J. Physiol.* 280: 169-191.
- Standen, N.B. & Stanfield, P.R. (1979). Potassium depletion and sodium block of potassium currents under hyperpolarization in frog sartorius muscle. *J. Physiol.* 294: 497-520.
- Stanfield, P.R. (1970a). The differential effects of tetraethylammonium and zinc ions on the resting conductance of frog skeletal muscle. *J. Physiol.* 209: 231-256.
- Stanfield, P.R. (1970b). The effects of the tetraethylammonium ion on the delayed currents of frog skeletal muscle. *J. Physiol.* 209: 209-229.
- Stanfield, P.R. (1975). The effect of zinc ions on the gating of the delayed potassium conductance of frog sartorius muscle. *J. Physiol.* 251: 711-735.
- Stefani, E. & Chiarandini, D.J. (1982). Ionic channels in skeletal muscle. *Ann. Rev. Physiol.* 44: 357-372.
- Stefani, E. & Steinbach, A.B. (1969). Resting potential and electrical properties of frog slow muscle fibres. Effect of different external solutions. *J. Physiol.* 203: 383-401.
- Stefani, E. & Uchitel, O.D. (1976). Potassium and calcium conductance in slow muscle fibres of the toad. *J. Physiol.* 255: 435-448.
- Strichartz, G., Bar-Sagi, D. & Prives, J. (1983). Differential expression of sodium channel activities during the development of chick skeletal muscle cells in culture. *J. Gen. Physiol.* 82: 365-384.
- Ulbricht, W. (1977). Ionic channels and gating currents in excitable membranes. *Ann. Rev. Biophys. Bioeng.* 6: 7-31.
- Vaughan, P. & Fong, C.N. (1978). Effects of SITS on chloride permeation in *Xenopus* skeletal muscle. *Can. J. Physiol. Pharmac.* 56: 1047-1054.

- Vaughan, P.C., McLarnon, J.G. & Loo, D.D.F. (1980). Voltage dependence of chloride current through *Xenopus* muscle membrane in alkaline solutions. *Can. J. Physiol. Pharmac.* 58(9): 999-1010.
- Vergara, C., Moczydlowski, E. & Latorre, R. (1984). Conduction, blockade and gating in a Ca-activated K channel incorporated into planar bilayers. *Biophys. J.* 45: 73-76.
- Warner, A.E. (1972). Kinetic properties of the chloride conductance of frog muscle. *J. Physiol.* 227: 291-312.
- Weidmann, S. (1952). The electrical constants of Purkinje fibres. *J. Physiol.* 118: 348-360.
- Westgaard, R.H. (1975). Influence of activity on the passive electrical properties of denervated soleus muscle fibres in the rat. *J. Physiol.* 251: 683-697.
- White, M.M. & Miller, C. (1979). A voltage-gated anion channel from the electric organ of *Torpedo californica*. *J. Biol. Chem.* 254(20): 10161-10166.
- White, M.M. & Miller, C. (1981). Probes of the conduction process of a voltage-gated Cl channel from *Torpedo* electroplax. *J. Gen. Physiol.* 78: 1-18.
- Yonemura, K. (1967). Resting and action potentials in red and white muscles of the rat. *Jpn. J. Physiol.* 17: 708-719.

